Dissertation zur Erlangung des Doktorgrades

der Fakultät für Chemie und Pharmazie

der Ludwig-Maximilians-Universität München

Influence of *Ginkgo biloba* extract EGb 761 on signaling pathways in endothelial cells

Anja Koltermann

aus Elsterwerda

2007

Erklärung:

Diese Dissertation wurde im Sinne von §13 Abs. 3 bzw. 4 der Promotionsordnung vom 29. Januar 1998 von Herrn PD Dr. Stefan Zahler betreut.

Ehrenwörtliche Versicherung:

Diese Dissertation wurde selbständig, ohne unerlaubte Hilfe erarbeitet.

München, am

_____

(Anja Koltermann)

Dissertation eingereicht am: 17.12.07

1. Gutachter: PD Dr. Stefan Zahler

2. Gutachter: Prof. Dr. Christian Wahl-Schott

Mündliche Prüfung am: 25.01.08

dedicated to my family

1 CONTENTS

2 INTRODUCTION

2.1 The endothelium

The endothelium is a thin monolayer of cells which line the lumen of all blood vessels, thereby regulating exchanges between the blood and the surrounding tissue. Endothelial cells (ECs) are not inert but rather have metabolic and secreting functions. Moreover, ECs exert significant autocrine, paracrine, and endocrine actions and influence either smooth muscle cells, platelets or peripheral leukocytes.[1, 2]

The endothelium plays an important role in many physiological functions including: the control of vascular tone, blood cell trafficking, hemostatic balance, permeability, inflammation and host defense as well as the formation of new blood vessels (angiogenesis). The loss of proper endothelial function, also referred to as endothelial dysfunction, has been associated with a number of pathological processes that are briefly discussed below.[3, 4]

i. Disturbed endothelial function plays a prominent role in cardiovascular diseases. As the major cause of death in the USA and Europe, cardiovascular diseases are characterized by multiple factors including impaired vasodilation, tissue perfusion, homeostasis, and thrombosis. One of the main mechanisms of a variety of cardiovascular pathological processes, like hypertension and atherosclerosis, is associated with a reduced nitric oxide (NO) bioavailability.[5-9]

ii. Endothelial cells can be the prime target for an infection leading to severe inflammation. As a first line of defense, ECs, besides monocytes and macrophages, recognize invading pathogens. These cells are able to produce different cytokines, adhesion molecules, and enzymes (such as matrix metalloproteinases or NO synthase) and react to a variety of mediator substances, thereby modulating inflammatory processes.[10, 11]

iii. ECs are a target for tumor-induced blood vessel growth (angiogenesis), a process leading to dissemination and implantation of tumor cells, finally leading to metastasis. With the identification of several pro-angiogenic molecules (such as growth factors and the angiopoietins) and anti-angiogenic substances (such as platelet factor-4 and angiostatin), it is recognized that therapeutic interference with vasculature formation offers a tool for clinical applications in various pathological situations.

In addition to the abovementioned diseases, there are numerous other pathopysiological states caused *via* disturbed endothelial function. Therefore, the regulation of endothelial processes represents a valid approach for drug discovery in order to combat these severe disorders. In brief, the endothelium offers enormous, yet largely untapped diagnostic and therapeutic potential.

2.2 *Ginkgo biloba* extract - EGb 761

Ginkgo biloba ("maidenhair tree" in English, "Ginkgobaum" in German) has been described as a "living fossil" that represents the only surviving species of the order *Ginkgoales*. The use of *Ginkgo biloba* fruits for medical purposes dates back to the origins of Traditional Chinese Medicine. However in Europe, the extract of *Ginkgo biloba* leaves was first introduced into medical practice in 1965 by Dr. Willmar Schwabe (Karlsruhe), a German physician and pharmacist. Since that time, the *Ginkgo biloba* leaf extract EGb 761 has been developed and has become commercially available as drops and tablets under the trade-name Tebonin® (Dr. Willmar Schwabe Pharmaceuticals, Karlsruhe, Germany). EGb 761 is a water/acetone extract that has been stringently standardized to ensure the consistency of its composition and reliable safety and efficacy profiles. The standard is a ratio of 35-67:1 (dried *Ginkgo biloba* leaves to final extract) containing approximately 24% flavonoid glycosides (Figure 2.1), 6% terpene trilactones, 7% proanthocyanidins and certain low molecular weight organic acids.[12, 13] Terpene trilactones are unique to *Ginkgo biloba* and can be divided into different subgroups: ginkgolides A, B, C, and J (diterpenoids, Figure 2.2) as well as the bilobalide (sesquiterpene, Figure 2.3). Moreover, EGb 761 is standardized to contain less than 5 ppm ginkgolic acids (Figure 2.4) as these substances can cause allergic reactions, especially dermatitis.[14]

	R1	R2
Kaempherol	H	H
Quercetin	OH	H
Myricetin	OH	OH
Isorhamnetin	OCH_3	H
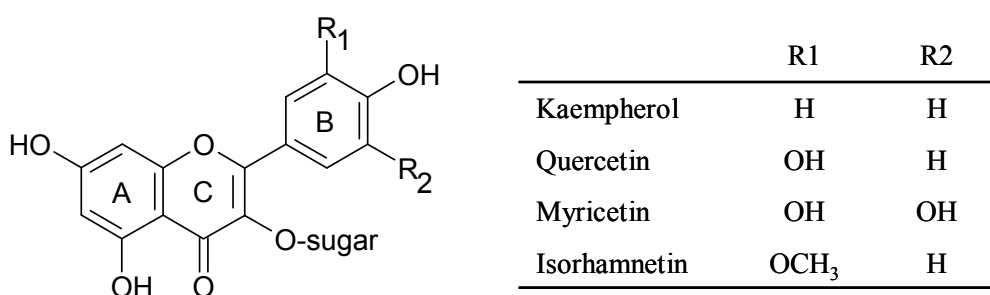
Figure 2.1   Chemical structure of flavonoids in EGb 761.
The 24% flavonoids present in EGb 761 are nearly exclusively flavonol-O-glycosides; i.e., combinations of the phenolic aglycon (kaempherol, quercetin, myricetin or isorhamnetin) with sugars which can be either glucose and/or rhamnose.

Ginkgolide	R1	R2	R3
A	OH	H	H
B	OH	OH	H
C	OH	OH	OH
J	OH	H	OH
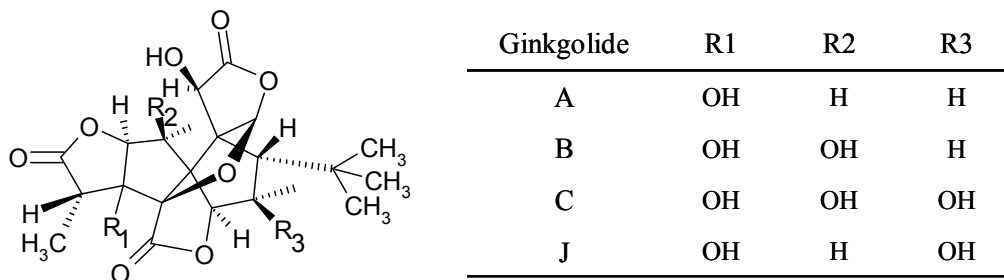
Figure 2.2   *Chemical structure of ginkgolides in EGb 761.*
                      The ginkgolides A, B, C and J are displayed. Taken together ginkgolides A, B and C account
                      for 3.1% of EGb 761. In contrast the ginkgolide J accounts for only ≤0.5%.
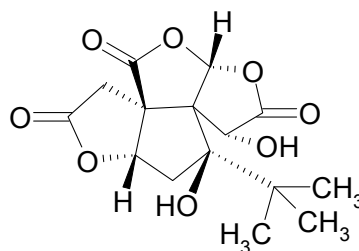
Figure 2.3   *Chemical structure of the bilobalide in EGb 761.*
                      The bilobalide is a sesquiterpen, which accounts for about 2.9% of EGb 761.

n=7-9
ginkgolic acids
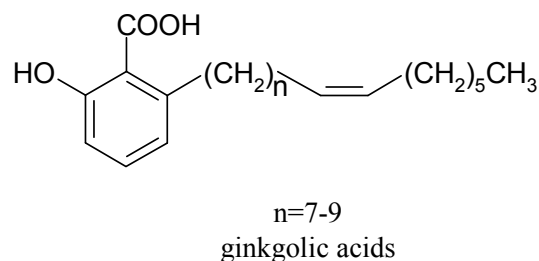
Figure 2.4   *Chemical structure of ginkgolic acids in Ginkgo biloba leaves and fruits.*
                      Ginkgolic acids are chemicals classified as alkylphenols that can cause allergic skin
                      inflammation. Because of this and other undesired side effects, the maximum level of ginkgolic
                      acids in the standardized extract EGb 761 is restricted to an amount of less than 5 ppm.

Current therapeutic strategies

Today, preparations of EGb 761 are among the most widely used herbal remedies in the industrialized world. Since 1995 the extract of *Ginkgo biloba* leaves holds a top-selling position in the USA. Clinical studies conducted during the last 30 years have revealed that EGb 761 is useful in treating a wide range of diseases including:[12, 15, 16]

i.   Disturbances of brain function: EGb 761 exerts cognition-enhancing effects, and is therefore commonly used in treatment of symptoms associated with both cognitive decline and more severe types of senile dementias of primary degenerative nature, such as Alzheimer's disease, and vascular dementia and mixed types.[17-19]

ii. Peripheral arterial disease: EGb 761 improves the pain-free walking distance in Fontaine's Stage II intermittent claudication (peripheral arterial occlusive disease, pAOD), a condition characterized by pain in the legs while walking, indicating tissue ischemia.[20-22]

iii. Dizziness and tinnitus of a vascular and involutional origin.[23]

Therapeutic actions

Different molecular mechanisms of action can be used to explain the therapeutic effects of EGb 761. This may be due to the various active chemical constituents, which act in a complementary manner. Along this line, additive, antagonistic, and synergistic effects may occur in pharmacological experiments as a result of interactions of the different active compounds. This combined activity, or polyvalent action, is responsible for the therapeutic benefits and is discussed very briefly below.[12, 15, 16] An overview of the pharmacological effects of EGb 761 according to the German Federal Health Authority (BGA-Commission E, 1994) is given in Table 2.1.[24]

i.   EGb 761 has vasoregulatory effects. Studies conducted during the past three decades have revealed that several molecular mechanisms contribute to the vasoregulatory activity of EGb 761. The extract elicits a vasorelaxant effect that partly depends on an intact endothelium. Furthermore, EGb 761 has beneficial effects on the rheological properties of the blood, defined as increased fluidity and inhibition of platelet and erythrocyte aggregation. These effects increase the blood supply in the brain and other body organs, thereby improving their oxygen and nutrient supply.[25, 26]

ii. EGb 761 exerts a "stress-alleviating" action. Several rodent models on defined animal behavior revealed the anti-stress activity of EGb 761 that can be considered being anxiolytic and/or antidepressant. Furthermore, the extract partially antagonizes stress-responses *via* reduction of adrenal glucocorticoid synthesis.[27, 28]

iii.   EGb 761 exerts antioxidant and free radical scavenging activities. Numerous studies have shown that EGb 761 can oppose the deleterious effects of oxidative damage caused by free radicals and related ROS. EGb 761 thereby acts directly *via* scavenging free radicals or indirectly *via* either decreasing the formation of free radicals or enhancing the expression of genes that encode antioxidant enzymes.[29, 30]

iv.   EGb 761 has neuroprotective properties and effects on learning, memory and behavior. The neuroprotective action of EGb 761 can be summarized as being the result of improved cerebral energy metabolism, protection against hypoxia and ischemia, decreasing ROS-induced brain damage, preventing brain edema, preserving mitochondrial function, and influences on central cholinergic systems known to be involved in learning and memory.[31, 32]

v.   EGb 761 has gene-regulatory effects. cDNA microarray analyses have shown that exposure of human bladder cancer cells to EGb 761 produced an adaptive transcriptional response and an altered the expression of several genes involved in regulating cell proliferation and apoptosis. These results provide a first hint why most of the clinically beneficial effects require repeated administration.[33]

Table 2.1   Pharmacological effects of EGb 761

−   Improvement of hypoxic tolerance, particularly in the cerebral tissue.
−   Inhibition of the development of traumatically or toxically induced cerebral edema, and acceleration of its regression.
−   Reduction in retinal edema and cellular lesions in the retina.
−   Inhibition in age-related reduction of muscarinergic cholinoceptors and alpha-adrenoceptors as well as stimulation of choline uptake in the hippocampus.
−   Increased memory performance and learning capacity, improvement in the compensation of disturbed equilibrium, improvement of blood flow.
−   Improvement of rheological properties of the blood.
−   Antagonism of the platelet-activating factor (PAF) (ginkgolides).
−   Inactivation of toxic oxygen radicals (flavonoids).
−   Improvement of mitochondrial function (ATP production).
−   Neuroprotective effect (ginkgolides A and B, bilobalide).

2.3 Aim of the study

In recent years, the interest in traditional herbal remedies has grown rapidly in the industrialized world. Despite the knowledge about its properties and current therapeutic applications, there is an increasing need for understanding the molecular mechanisms and signaling pathways. Therefore, aim of the present study was to investigate the influence of the standardized *Ginkgo biloba* extract EGb 761 on signaling pathways in endothelial cells. For this purpose, two different projects were pursued:

1) Effects of EGb 761 on endothelial nitric oxide synthase (eNOS) both in cultivated human endothelial cells and in *in vivo* systems:

Cardiovascular diseases are the major cause of death in the USA and Europe. Moreover, a variety of pathological processes, including hypertension and atherosclerosis, are associated with endothelial dysfunction involving a reduced nitric oxide (NO) bioavailability. Although the efficacy of the standardized *Ginkgo biloba* extract has been well proven, the underlying molecular mechanisms and signaling pathways leading to *Ginkgo's* beneficial cardiovascular effects have as yet remained widely unknown. Thus, aim of the study was to elucidate the molecular basis on which EGb 761 might protect against endothelial dysfunction *in vitro* and *in vivo*. We hypothesized that EGb 761 is able to influence the nitric oxide formation in endothelial cells.

2) Effects of EGb 761 on angiogenic parameters in endothelial cells:

Angiogenesis, the formation of new blood vessels by sprouting from pre-existing capillaries, is a pre-requisite for tumor development and metastasis. Inhibition of angiogenesis, therefore, represents a valid approach for cancer treatment or even prevention and is successfully used in clinical applications. The standardized *Ginkgo biloba* extract EGb 761 is traditionally used for anticancer treatment.[13] However, as seen with most of the widely used herbal remedies, no profound mechanistic studies providing a rational, mechanistic molecular background for the respective therapeutic indications exist. Thus, aim of the study was to provide a rational basis elucidating EGb 761 protective effects on angiogenic parameters in endothelial cells. Along this line, we aimed to clarify the influence of EGb 761 on growth factor-signaling pathways in endothelial cells focusing on the ERK-cascade and the role of phosphatases.

2.4   Endothelial nitric oxide production

In 1980 Furchgott and Zawadzki provided the landmark observation that endothelial cells produce a factor that causes relaxation of the underlying vascular smooth muscle cells.[34] Seven years later this factor, called the endothelium-derived relaxing factor (EDRF), was shown to be identical to the free diffusible gas nitric oxide (NO).[35, 36] NO, a simple diatomic molecule is crucial for maintaining vascular endothelial health and function. In detail, NO is released by endothelial cells and is a major endogenous vasodilator counterbalancing vasoconstriction. It participates as key mediator in the signaling pathway L-arginine/NO/cyclic guanosine monophosphate (cGMP) as displayed in Figure 2.5.
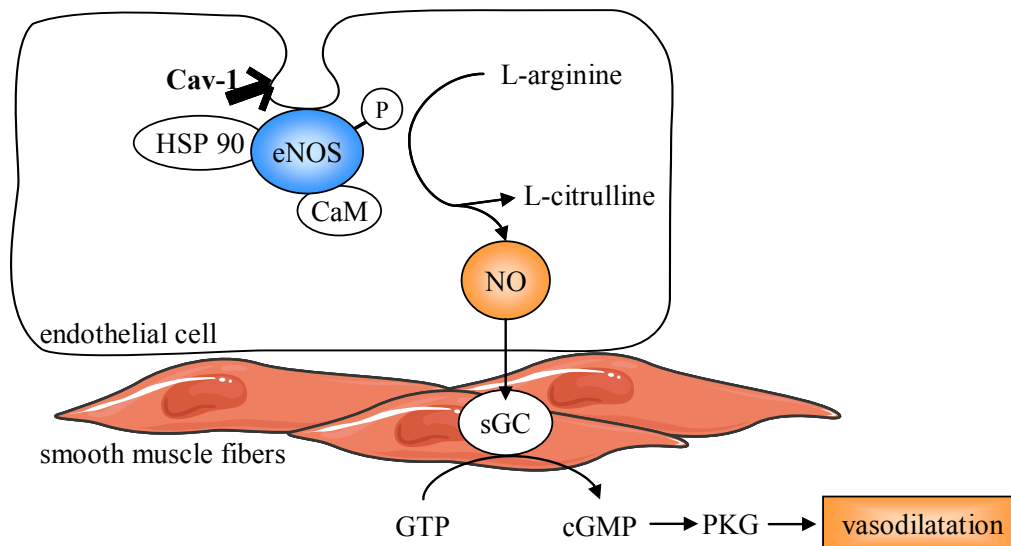
Figure 2.5   *The L-arginine/NO/cyclic GMP pathway leading to vasodilation.*
This signaling cascade starts with the activation of the endothelial nitric oxide synthase (eNOS) in response to receptor-dependent agonists or physicochemical stimuli. The enzyme eNOS generates NO and L-citrulline from L-arginine and oxygen. NO diffuses to the adjacent smooth muscle where it interacts with soluble guanylate cyclase (sGC) leading to an increase in cyclic guanosine monophosphate (cGMP) formation. cGMP elicits different biological effects including vasodilation by activation of cGMP-activated protein kinase (protein kinase G, PKG).

In the endothelium, NO synthesis is controlled by the endothelial form of nitric oxide synthases (NOSs, see section 2.4.2 for detailed description). The small, lipophilic gas NO rapidly diffuses out of the endothelial cells into neighboring smooth muscle cells. In the adjacent smooth muscle NO activates the soluble guanylate cyclase (sGC) by binding of iron in the active site, thereby stimulating the production of the small intracellular mediator cGMP. Once produced, cGMP elicits different biological functions including smooth muscle relaxation through the activation of cGMP-dependent protein kinase (protein kinase G, PKG),

thus dilating the vessel and increasing blood flow. The current chapter summarizes the physiological and pathophysiological role of NO in the endothelium, the cellular regulation of NOS isoforms and gives a short overview about the PI3K/Akt signaling pathway.

2.4.1   Role of NO in the vascular wall

In addition to its vasodilator properties, endothelial NO has numerous vasoprotective and even anti-atherosclerotic effects. The physiological actions of NO include thrombosis protection by inhibition of platelet aggregation and conclusively platelet adhesion to the vessel wall. NO mediates the reduction in endothelial permeability as well as the inhibition of the expression of the chemoattractant protein MCP-1 and surface adhesion molecules like P-selectin and intercellular adhesion molecule-1 (ICAM-1). Furthermore, NO has been shown to inhibit DNA synthesis and, in higher concentrations prevent smooth muscle cell proliferation and migration. It also exerts anti-inflammatory actions and down-regulates the oxidation of low-density lipoproteins (LDLs). Conditions with an absolute or relative NO deficit known as endothelial dysfunction, initiate and accelerate the process of atherosclerosis. Altogether there are four principle causes of diminished NO bio-activity: (I) decreased expression and/or activity of endothelial NO synthase (eNOS), (II) eNOS uncoupling, (III) enhanced scavenging of NO and (IV) impaired transmission of NO-mediated signaling events (failure of effector mechanisms).[37, 38] In fact, eNOS uncoupling, which is the transformation of eNOS from a protective enzyme to a contributor of oxidative stress, is likely to play an important role in the pathological states. Based on these facts, the enhancement of endothelial NO production in an aging or diseased endothelium either by eNOS activation/expression or restoring eNOS functionality is of great therapeutic interest.[9, 39, 40]

2.4.2   Nitric oxide synthases

The biological synthesis of NO from the amino acid L-arginine is catalyzed by a family of nitric oxide synthases (NOSs). It can be found in three distinct isoforms: (i) neuronal NOS (also known as Type I, nNOS or NOS-1) being the isoform first found in neuronal tissue, (ii) inducible NOS (also known as Type II, iNOS or NOS-2) being the isoform which is inducible in a wide range of cells and tissues, and (iii) endothelial NOS (also denoted as Type III, eNOS or NOS-3) being the isoform first found in endothelial cells. These three mammalian NOS isoforms can also be differentiated on the basis of their constitutive (nNOS and eNOS) or

inducible (iNOS) expression, and their calcium-dependence (nNOS and eNOS) or -
independence (iNOS). All NOS isoforms exhibit a bidomain structure composed of an
oxygenase and reductase domain, which are linked by a calmodulin (CaM)-recognition site.
In addition, all three isoforms are hemoproteins and require the following co-factors: the
reduced nicotinamide adenine dinucleotide phosphate (NADPH), flavin adenine dinucleotide
(FAD), flavin mononucleotide (FMN), and (6R)-5,6,7,8-tetrahydro-L-biopterin (BH_4), one of
the most potent naturally occurring reducing agents. The dimerized enzymes transfer
electrons from NADPH *via* FAD and FMN in the reductase domain of one monomer to the
heme iron (Heme-Fe) in the oxygenase domain of a separate monomer (Figure 2.6). To
synthesize NO, the enzymes catalyze two successive oxidation-reduction reactions. In the first
step, NOS hydroxylates L-arginine to N-hydroxy-L-arginine. In the second step, NOS
oxidizes N-hydroxy-L-arginine generating L-citrulline and NO as final products.[41, 42]
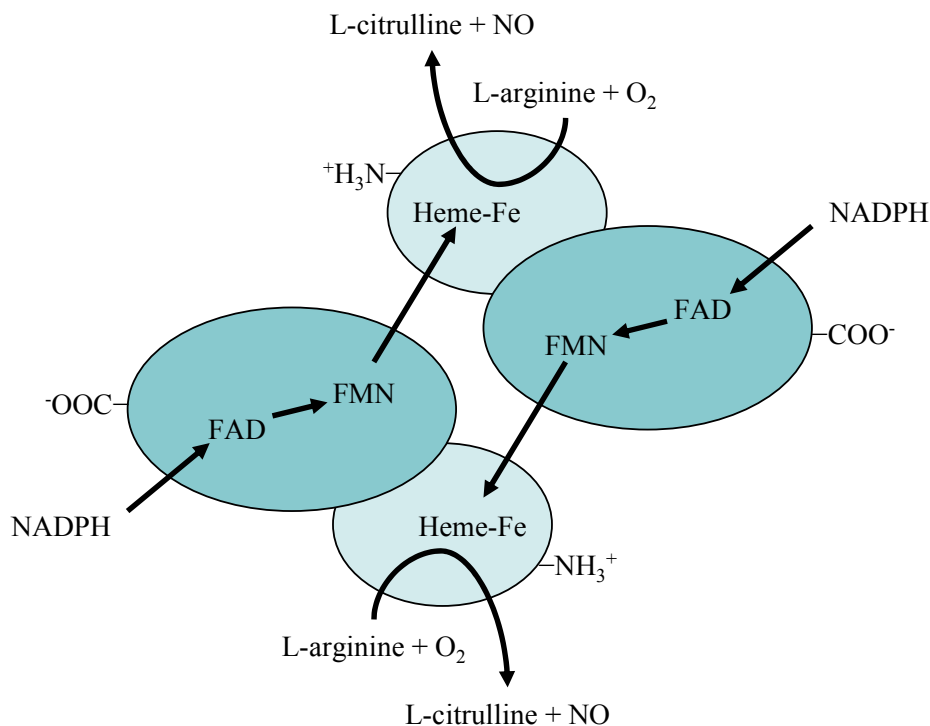
Figure 2.6   *Structure of the eNOS homodimer.*
            The enzyme is composed of two identical monomers, and each monomer contains a carboxy-
            terminal reductase (dark blue unit) and an amino-terminal oxygenase (light blue unit) domain.
            The electron flow in the eNOS dimer goes *via* NADPH → FAD → FMN in the reductase
            domain of one monomer to the heme iron in the oxygenase domain of a separate monomer.
            There the reaction of L-arginine with oxygen is catalyzed generating L-citrulline and NO as
            products. The arrows indicate the direction of the electron flow.

Endothelial nitric oxide synthase (eNOS)

In the vasculature, the endothelial NOS is the predominant and most important isoform and is responsible for most of the NO produced in this tissue. The eNOS synthesizes NO in a Ca^{2+}/calmodulin (CaM)-activated manner in response to a variety of mechanical forces and humoral factors. Moreover, to cope with the continuously changing environment, endothelial cells need to control their nitric oxide production by various mechanisms. Hence, the enzyme eNOS is under complex and tight control, which is afforded by three specific processes: eNOS expression, eNOS localization, and eNOS activation.[43]

i.   eNOS expression: Although the eNOS gene is constitutively expressed in endothelial cells, it is regulated by multiple compounds and conditions. An up-regulation of eNOS expression is controlled by biophysical stimuli (e.g. shear stress and chronic exercise), hormones (e.g. estrogens, insulin, angiotensin II, endothelin 1), and phorbol esters. Cell proliferation as well as growth factors [i.e. transforming growth factor (TGF)-ß, fibroblast growth factors (FGFs), vascular endothelial growth factor (VEGF) and platelet-derived growth factor (PDGF)] are important stimuli for eNOS expression in vascular endothelial cells. In contrast, tumor necrosis factor-α (TNF-α) and bacterial lipopolysaccharide (LPS) down-regulate the expression of this enzyme.[44]

ii.   eNOS localization: Because NO is an extremely reactive and short-lived signaling molecule, its subcellular distribution is mainly determined by the subcellular localization of the eNOS and its local production. Subcellular localization and trafficking of endothelial NO synthase is controlled by co- and post-translational lipid modifications. eNOS is modified by myristoylation of a glycine residue and dual palmitoylation of cysteine residues, which targets the enzyme to the plasma membrane. A major pool of eNOS residues at the cytosolic face of Golgi complex, with smaller pools in caveolae, the plasma membrane cholesterol-rich microdomains, and endothelial junctions, indicating the presence of discrete localization of eNOS.[45-47]

iii. eNOS activation: Multiple mechanisms are involved in regulating NO production following eNOS activation. eNOS activity is regulated firstly by Ca^{2+}/CaM, followed by phosphorylation on multiple residues and finally through protein-protein-interactions. All three aspects are briefly discussed below and summarized in Figure 2.7. First, elevation of the intracellular concentration of free Ca^{2+} plays a crucial role

in eNOS activation and regulation. Free calcium will bind to CaM and the newly formed Ca^{2+}/CaM complex in turn will bind to the CaM binding site. In caveolae of endothelial cells eNOS is held inactive by its association with caveolin-1 (cav-1). The association with cav-1 is counteracted by calcium-activated CaM, which leads to the dissociation of eNOS from caveolin-1 and finally increases eNOS enzymatic activity. Second, the effects of eNOS phosphorylation on specific serine and threonine residues are complex and involve numerous kinases and phosphatases. The two most thoroughly studied sites are the activating phosphorylation site Ser1177 and the inhibitory site Thr495. Several protein kinases including protein kinase B (PKB)/Akt (briefly discussed in section 2.4.3), protein kinase A (PKA) and AMP-activated protein kinase (AMPK) activate eNOS by phosphorylation of Ser1177 in response to various stimuli. In contrast, bradykinin and hydrogen peroxide activate eNOS activity by promoting Thr495 dephosphorylation. Finally, diverse phosphatases have been implicated in the regulation of eNOS dephosphorylation and modulate eNOS activity. As an example, protein phosphatase 2A catalyzes dephosphorylation of the activation site Ser1177. Third, in recent years several proteins have been described that directly associate with endothelial NOS and regulate its activity or spatial distribution in the cell. A positive impact on eNOS function involves the molecular chaperon HSP90 (heat-shock protein 90), which participates in protein folding and signal transduction. On the other hand, eNOS is inhibited by binding to certain G-protein coupled receptors such as angiotensin II type 1 (AT_1) or bradykinin B2. The nitric oxide synthase-interacting protein (NOSIP) and the nitric oxide synthase traffic inducer (NOSTRIN) can negatively regulate eNOS localization in the plasma membrane.[48-52]
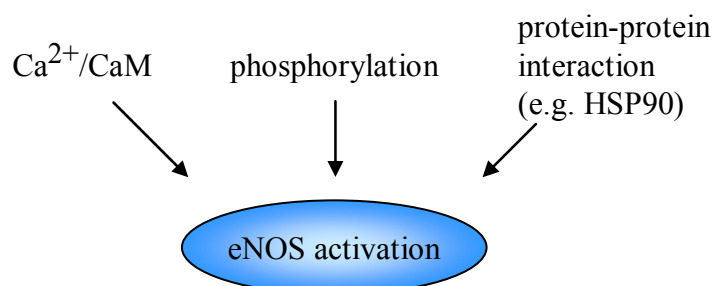
Figure 2.7   *Mechanisms of eNOS activation.*
eNOS activity is regulated by Ca^{2+}/calmodulin (CaM), phosphorylation on multiple residues and/or through protein-protein-interactions [e.g. direct association with heat-shock protein 90 (HSP90)].

Since NO has potent and diverse biological effects and an NO deficiency plays a major role in endothelial dysfunction, the discussed control mechanisms of the enzyme eNOS are of great pathophysiological importance. The focus on an enhanced expression and/or activation of eNOS in response to pharmacological interventions could provide a promising approach to cardiovascular diseases.

2.4.3   Role of the PI3K/Akt pathway in nitric oxide signaling

Phosphoinositide 3-kinases (PI 3-kinases or PI3Ks) are a family of related enzymes, organized into three classes; I, II, and III, which are activated by tyrosine kinase and G-protein-coupled receptors, respectively. The PI3Ks are heterodimeric molecules composed of a regulatory (p85) and a catalytic (p110) subunit. Following its recruitment to these receptors in the plasma membrane, PI3K phosphorylates the 3'-inositol position of the membrane associated phosphoinositide(4,5)bisphosphate (PIP2) generating the second messenger phosphoinositide(3,4,5)trisphosphate (PIP3). PIP3 does not directly activate the protein kinase B, in the following denoted as Akt, but instead appears to recruit Akt to the inner leaflet of the plasma membrane and alters its conformation to allow subsequent phosphorylation by the phosphoinositide-dependent kinase-1 (PDK-1).

The serine/threonine kinase Akt contains two regulatory phosphorylation sites, Thr308 in the activation loop within the kinase domain and Ser473 in the C-terminal regulatory domain. Thr308 is phosphorylated by PDK-1 leading to a partial activation of Akt. In order to obtain full activation of the kinase, the phosphorylation on the second site (Ser473) is also required. It is suspected that Ser473 is most likely targeted by the mammalian target of rapamycin (mTOR)-Rictor complex, however, the true mechanism remains to be elucidated. Once it has been fully activated by phosphorylation of both sites, Akt regulates several cellular functions including nutrient metabolism, cell growth, angiogenesis, apoptosis, and survival. Moreover, Akt mediates direct eNOS phosphorylation at Ser1177 (in human eNOS, equivalent to Ser1179 in bovine eNOS) and increases eNOS activity leading to NO release and vasodilation. The described signaling pathway is displayed in Figure 2.8 and can be inhibited by wortmannin. Wortmannin is a product of the fungus *Penicillium fumiculosum* that specifically inhibits PI3Ks.[53-57]
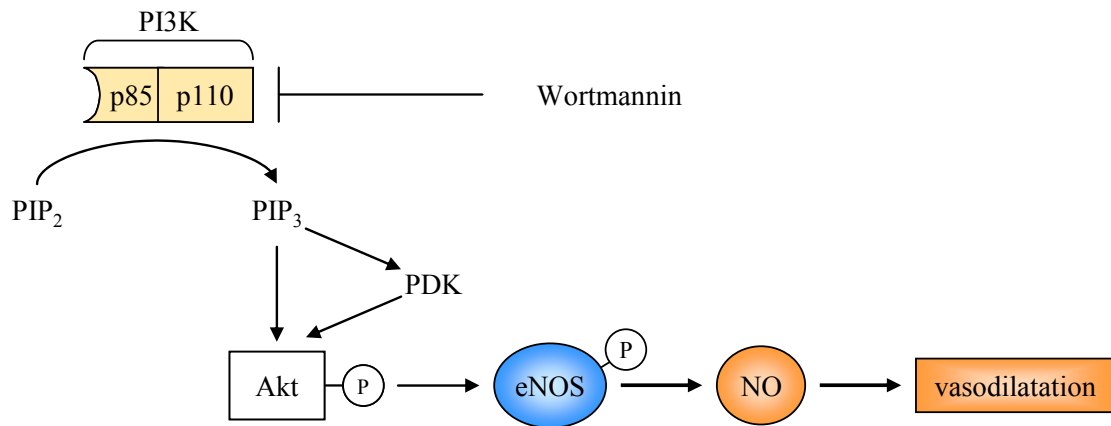
Figure 2.8   *Activation of eNOS and nitric oxide release by PI3K/Akt signaling*
The phosphoinositide 3-kinases (PI3Ks) are heterodimeric molecules composed of a regulatory
(p85) and a catalytic (p110) subunit. They convert the phosphoinositide(4,5)bisphosphate
(PIP2) to phosphoinositide(3,4,5)trisphosphate (PIP3) on the inner leaflet of the plasma
membrane. PIP3 produced by phosphorylation leads to the activation of the PDK/Akt pathway
resulting in eNOS phosphorylation and NO release. All PI 3-kinases are inhibitable by
wortmannin.

2.5 Angiogenesis

Angiogenesis is the process of the development and growth of new blood vessels from pre-existing vasculature. It plays a key role in various physiological and pathological conditions, including embryonic development, normal tissue growth, wound healing, the female reproductive cycle (i.e. ovulation, menstruation and placental development), as well as in the development of numerous types of tumor. Without blood vessels, tumors can not grow beyond a critical size of few mm³ and metastasize to another organ. As early as 1971, Folkman proposed that tumor growth and metastasis are angiogenesis-dependent, and therefore, blocking angiogenesis could be a strategy to arrest tumor growth.[58] The onset of angiogenesis, or the "angiogenic switch", is regulated by both pro-angiogenic and anti-angiogenic molecules that can occur at any stage of tumor progression.[59] Normally, the effect of activator molecules is balanced by that of inhibitor molecules blocking growth. Should a need for new blood vessels arise, the net balance is tipped in favor of angiogenesis. Various signals that trigger the angiogenic switch have been discovered. These include metabolic stress, mechanical stress or genetic mutations. Furthermore, the process of angiogenesis implies complex cellular and molecular interactions between cancerous cells, endothelial cells and the components of the extra-cellular matrix.[60, 61]

2.5.1 Angiogenesis cascade

Angiogenesis is a multi-step process induced by the release of angiogenic signals from diseased tissue or cancer cells into the surrounding area. When angiogenic growth factors encounter endothelial cells, they bind to specific receptors located on the outer surface of the cells. The binding of the growth factor to its appropriate receptor activates a series of relay proteins that transmit a signal into the nucleus of ECs. Activation of ECs leads to the localized degradation of the basal membrane of the parent vessel and of the extra-cellular surrounding. The endothelial cells begin to proliferate and migrate into the perivascular space towards chemotactic angiogenic stimuli from the diseased tissue (tumor). This leads to the formation of solid endothelial cell sprouts into the stromal space. Additional enzymes (e.g. matrix metalloproteinases) are produced from either tumor or endothelial cells to dissolve the tissue in front of the sprouting vessel tip in order to accommodate it. Then, vascular loops are formed and capillary tubes are developed by formation of tight junctions and a deposition of new basement membrane.[62] In contrast to physiological normal vessels, the tumor vasculature significantly differs and is highly disorganized. Differences include an abnormal blood flow, altered endothelial cell-pericyte interactions, increased permeability, delayed maturation and an aberrant vascular structure. The latter means that tumor vessels are irregular shaped, tortuous and dilated, with uneven diameter, excessive branching and shunts.[59, 60]
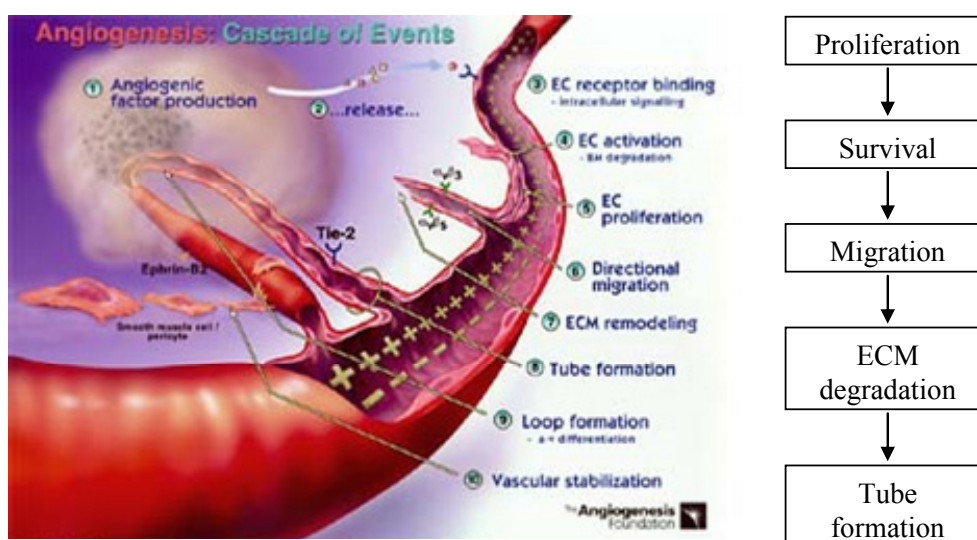
Figure 2.9   *Key steps in angiogenesis.*
The angiogenesis cascade occurs as an orderly series of events. Angiogenic endothelial cells must proliferate, avoid apoptosis, migrate, produce molecules able to degrade the extracellular matrix and, finally, differentiate into new vascular tubes. The image is adapted from http://www.angio.org/understanding/understanding.html.

In summary, angiogenic signals promote endothelial cell proliferation, increase resistance to apoptosis, initiate the degradation of the extracellular matrix (ECM), change endothelial adhesive properties, induce migration, and finally differentiation as well as the formation of a new vascular lumen (Figure 2.9).

During angiogenesis the regulation of endothelial behavior is the result of a very complex network of intracellular signaling systems. The major pathways are:

i.   the mitogen-activated protein kinase pathway, which is very important in the transduction of proliferation signals and detailed described in section 2.5.2;

ii.   the phosphatidylinositol-3-kinase/protein kinase B signaling system, particularly essential for the survival of the angiogenic endothelium;

iii.   the small GTPases involved in cytoskeletal reorganization and migration;

iv.   the kinases associated to focal adhesions which contribute to integrate the pathways from the extracellular matrix and growth factors.[63]

2.5.2   Mitogen activated kinases

As aforementioned, the mitogen-activated protein kinases (MAPKs) pathway presents one signaling system leading to angiogenesis. MAPKs are a family of serine/threonine kinases that respond to a wide variety of stimuli including growth factors, cytokines and environmental stresses.

In mammalian cells, there are more than a dozen MAPK genes. The best known genes are: (i) the extracellular signal-regulated kinases 1 and 2 (ERK1/2); (ii) c-Jun N-terminal kinases (JNK (1-3)); and (iii) the p38 kinase isozyme (p38α, β, γ, and δ) families. These three major MAPK families are implicated in a variety of human diseases and thus prominent targets for drug development. MAPKs regulate critical cellular functions required for homeostasis such as the expression of cytokines and proteases, cell cycle progression, cell adherence, motility and metabolism. In brief, MAPKs influence cell proliferation, differentiation, survival, apoptosis and development.[64]

MAPKs are similar in their activation by dual phosphorylation of conserved threonine and tyrosine residues within the activation loop (known as Thr-X-Tyr motif). Moreover, each MAPK pathway contains a core triple kinase cascade comprising an apical MAP kinase kinase kinase (also denoted as MAPKKK, MAP3K, MEKK or MKKK), a MAP kinase kinase (also known as MAPKK, MAP2K, MEK or MKK) and a downstream MAP kinase.[65] This core module is summarized in Figure 2.10.
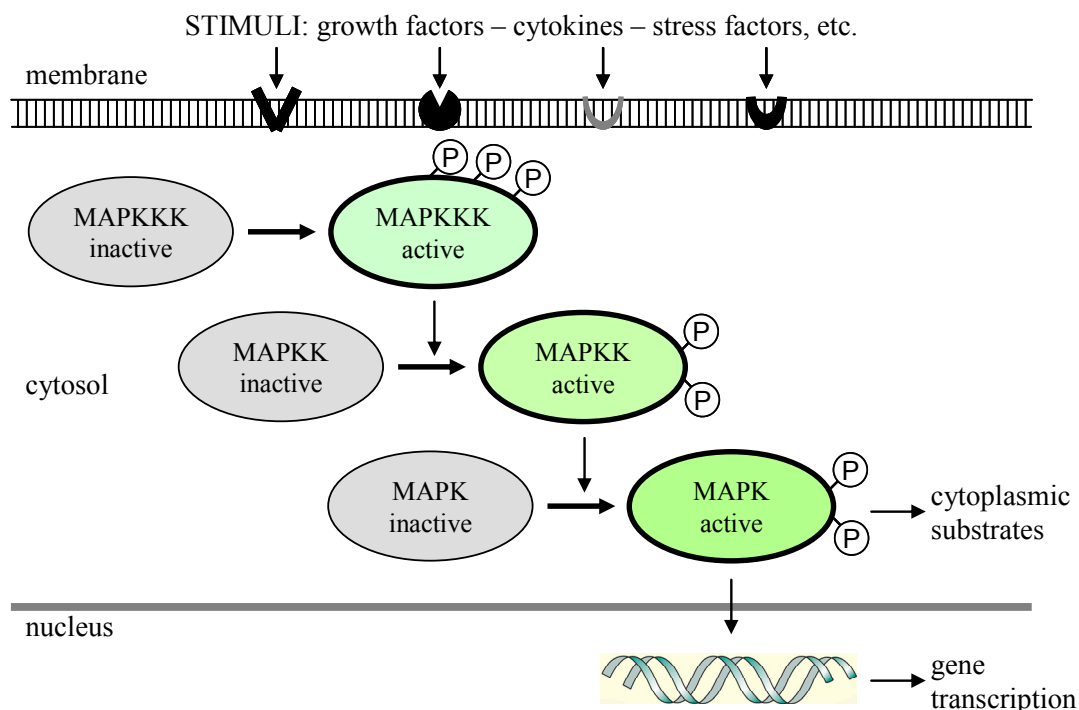
Figure 2.10   *Activation of all MAPKs is regulated by a central three-tiered core signaling module.*
The three-tier module mediates responses to stimuli like growth factors, cytokines or stress factors and activates the apical MAP kinase kinase kinase (MAPKKK). This activation leads to a dual phosphorylation of serine residues of the MAP kinase kinase, which in turn activate MAPKs by phosphorylation on threonine and tyrosine residues. The active MAPKs frequently translocate from the cytoplasm to the nucleus to phosphorylate nuclear targets.

These signal transduction pathways are organized as communication networks that process and integrate information. Their relay stations are formed by multiprotein complexes. Therefore, the pathway specificity is regulated at several levels, including kinase-kinase and kinase-substrate interactions, colocalization of kinases with scaffold proteins and inhibitors. The described dynamic spatial control of MAPK signaling networks contributes to the highly specific physiological responses in cells, organs and organisms.[66, 67]

Extracellular signal-regulated kinase (ERK) cascade

The isoforms ERK1 and ERK2, often referred to as p44 and p42 MAPKs, contain a
Thr-Glu-Tyr motif within the activation loop of the kinase domain and are activated by
mitogenic stimuli such as growth factors (as described in section 2.5.3), serum, cytokines and
phorbol esters, which activate a variety of receptors and G proteins.[68] The ERKs are
expressed in many tissues and form a part of a MAPK module that includes the Raf family
kinases (MAPKKKs) and the MEK 1/2 MAPKK.
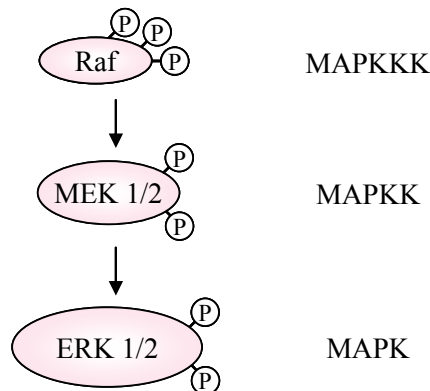
Figure 2.11   The ERK cascade.
                 In the three-tier module the apical MAP kinase kinase kinase (MAPKKK) Raf is activated.
                 This activation leads to a dual phosphorylation of serine residues of the MAP kinase kinase
                 MEK 1/2, which in turn activate ERK 1/2 by phosphorylation on Thr and Tyr.

The critical link that allows signal transduction from RTKs to ERK is the activation of Raf
family kinases (comprised of A-Raf, B-Raf and C-Raf/Raf-1). The serine/threonine kinase
Raf is activated *via* membrane localization, cycles of phosphorylation/dephosphorylation and
protein binding.[69, 70] Once activated, all Raf family members are capable of initiating the
phosphorylation cascade, in which Raf activates the MAPK/ERK kinases 1 and 2 (MEK 1/2)
by phosphorylation of two serine residues within their activation segment.[69] This dualspecific
MEK 1/2 in turn activates ERK *via* phosphorylation of threonine and tyrosine residues in the
ERK activation loop. However, in contrast to the complexity observed in Raf activation,
MEK 1/2 and ERK become fully activated simply through the dual phosphorylation of the
activation segments in their respective kinase domains.[71] A schematic representation of the
MAPK cascade comprised of Raf, MEK 1/2 and ERK kinases (known as the ERK cascade) is
displayed in Figure 2.11.

The ultimate goal in RTK downstream signaling is achieved when active ERK1 and ERK2 phosphorylate crucial targets in the nucleus, cytosol, membranes and cytoskeletal compartments. These targets are required to carry out the cellular response specified by the initiating signal. Identified ERK substrates include:

i.   key transcription factors, such as AP-1, NF-κB, ELK1, cFOS, c-Myc and Ets;

ii.   several protein kinases, such as p90 ribosomal S6 kinase (RSK), mitogen and stress activated kinase (MSK) and MAPK-interacting kinase (MNK);

iii. proteins involved in cell attachment and migration, including myosin light chain kinase (MCLK) and focal adhesion kinase (FAK).[72]

Finally, ERK regulates diverse cellular mechanisms including embryogenesis as well as angiogenesis, proliferation, cell motility, differentiation and apoptosis. These programs are based on signals derived from the cell environment, surface, and the metabolic state of the cell. In particular, aberrant regulation of the ERK pathway contributes to cancer. Additionally, ERK activation is a fundamental step in bFGF- and VEFG-induced angiogenesis. Because of this key role the ERK pathway has been in focus for drug discovery for almost 15 years with Ras, Raf and MEK 1/2 being the main targets.[73, 74] Inhibition of ERK activation, therefore, represents a valid approach for anti-angiogenic therapy and cancer treatment.

2.5.3   Growth factors

In recent years more than a dozen different proteins, as well as several smaller molecules, have been identified as angiogenic factors, meaning that these proteins are released by tumors as angiogenesis-inducing signals. Among these molecules, two proteins appear to be the most important ones: basic fibroblast growth factor (bFGF) and vascular endothelial growth factor (VEGF).[75] Both angiogenic growth factors are produced by various kinds of cancer cells and by certain types of normal cells, too. Currently, bFGF and VEGF are targets of great interest to inhibit deregulated blood vessel formation. Thus, concentrated efforts in this area of research led to development of inhibitors of bFGF and VEGF signaling. Some are already in clinical trials or therapeutically used. Examples of angiogenesis inhibitors which bind to and inhibit the biological activity of human VEGF are bevacizumab (Avastin®, Genentech, Inc., CA, USA, humanized anti-VEGF antibody) and ranibizumab (Lucentis®, Genentech, antibody fragment designed for intraocular use).[76-78]

Basic fibroblast growth factor

Basic fibroblast growth factor (bFGF), also denoted as FGF-2, was the first pro-angiogenic molecule to be identified.[79] bFGF is a prototypic member of a family comprising 22 proteins, which was first purified as a heparin-binding polypeptide from a bovine pituitary. It was subsequently characterized as a 18 kDa (low molecular weight; LMW) basic protein due to its high isoelectric point.[80] The ubiquitous bFGF is one of the most potent angiogenic factors, possesses neuron-protective properties, and is implicated in vascular remodeling and tumor metastasis. The terminus bFGF comprises distinct isoforms that are generated by alternative initiation of translation on a single mRNA. These alternative isoforms of bFGF, collectively referred to as high molecular weight bFGF (HMW), have different subcellular localizations and functions.[81, 82] The LMW-bFGF is primarily located in the cytoplasm, but can also be released from dead or injured cells. In the extracellular matrix it is associated with heparan-sulfate proteoglycans. Along this line, LMW-bFGF functions in an autocrine and paracrine manner, whereas HMW-bFGF isoforms are nuclear and exert activities through an intracrine mechanism. Furthermore, LMW-bFGF exerts its effects *via* specific binding and activation of four different receptor tyrosine kinases (RTKs) designated FGFR1, FGFR2, FGFR3 and FGFR4. Unlike other growth factors, bFGF acts in concert with heparin or heparan sulfate proteoglycan (HSPG) to activate RTKs by forming a ternary complex. Activation of the receptor kinase activity *via* receptor dimerization and intermolecular autophosphorylation of specific tyrosine residues allows coupling to downstream signal transduction pathways that have been associated with multiple biological activities, including proliferation, migration and differentiation of endothelial cells. Several intracellular signaling cascades are known to be activated by binding of bFGF to its receptors, including the phospholipase C-γ (PLC-γ) pathway, the PI3K-Akt pathway and the Ras-MAP kinase pathway. The latter signal transduction cascade is mainly activated by binding of bFGF to the FGFR1 and is briefly described below (Figure 2.12).[83, 84]

The activated FGFR1 becomes a platform for the recognition and recruitment of a specific complement of adaptors, enzymes or docking proteins. One of these adaptor proteins is the growth factor receptor bound protein 2 (Grb2). The recruitment of Grb2 from the cytoplasm to the plasma membrane brings the associated guanine nucleotide exchange factor son of sevenless (SOS) near to the membrane-bound proto-oncogene Ras. Through guanine exchange, SOS enhances GDP release and GTP binding to Ras, converting this small GTPase

into its active conformation. This conformational activation of Ras allows the interaction of various downstream target effectors, including the mitogen activated protein kinase kinase kinases (MAPKKK) Raf. Activated Raf kinases are the point of entry into the three-tiered kinase cascade in which Raf phosphorylates the MAPK/ERK kinases 1 and 2 (MEK 1/2), and MEK 1/2 in turn phosphorylates and activates the extracellular signal-regulated kinases 1 and 2 (ERK 1/2) as described in section 2.5.2. A number of angiogenic inhibitors have been discovered that are able to antagonize bFGF activity, among them platelet factor-4 (PF-4), angiostatin, endostatin and the 16 kDa human prolactin fragment (16 kDa hPRL).
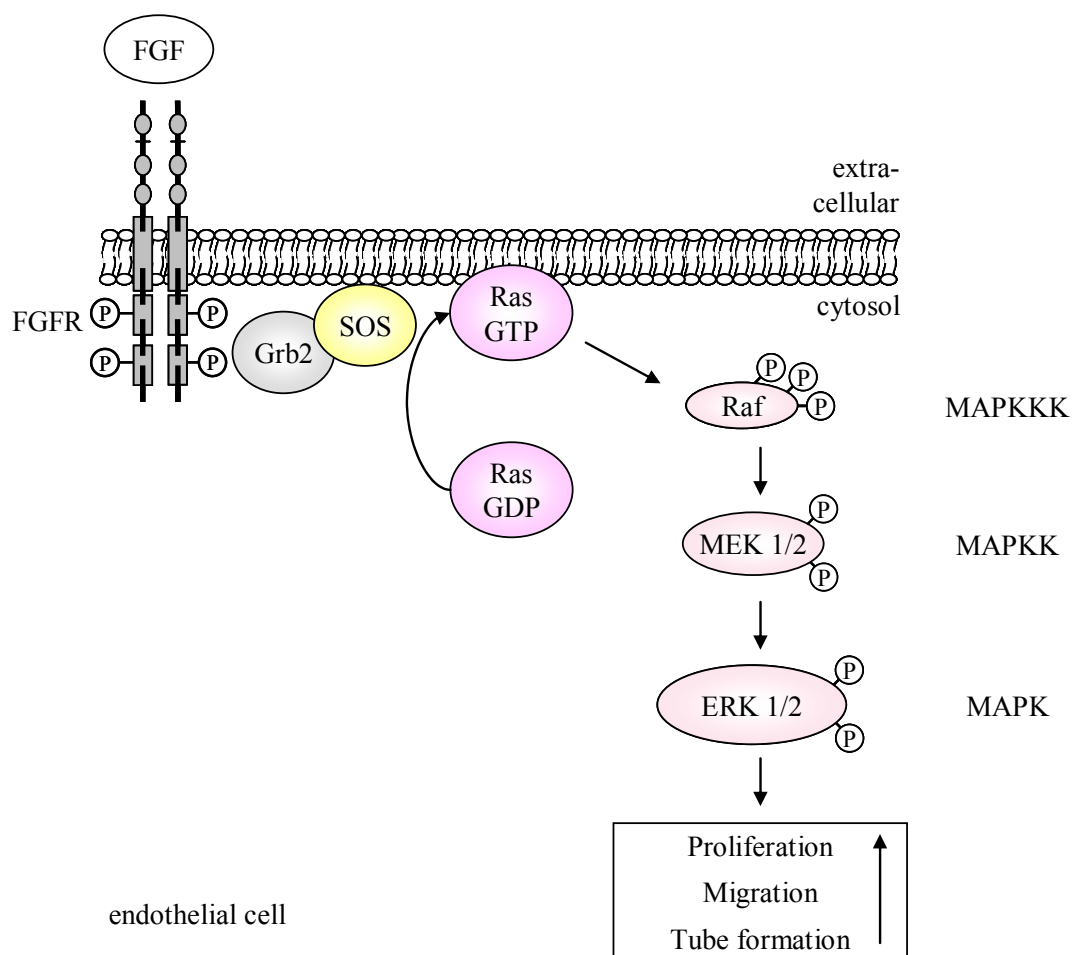
Figure 2.12   *FGF binding to FGFRs activates the Ras-MAP kinase pathway.*
                     Upon ligand binding, receptor dimers are formed and their intrinsic tyrosine kinase is activated
                     causing phosphorylation of multiple tyrosine residues on the receptor. Subsequently, signaling
                     complexes are assembled and recruited to the active receptor leading to activation of the Ras-
                     MAP kinase pathway.

Vascular endothelial growth factor

Vascular endothelial growth factors (VEGFs) are crucial regulators of vascular development during embryogenesis (vasculogenesis) as well as blood-vessel formation (angiogenesis). During the last few years, several members of the vascular endothelial growth factor (VEGF) family have been described including VEGF-A, B, C, D, E and the placenta growth factor (PIGF). All members of the VEGF family are dimeric glycoproteins belonging to the platelet derived growth factor (PDGF) superfamily.[85] Among these proteins VEGF-A, also referred to as vascular permeability factor (VPF), plays an important role in angiogenesis. Consonant with its pivotal role in vascular development, VEGF-A is a multi-tasking cytokine, which stimulates endothelial cell proliferation, migration, survival and differentiation. Moreover, VEGF-A increases vascular permeability, causes vasodilation (partly through stimulation of NO synthase in endothelial cells), induces tubulogenesis and influences gene expression.[86-88] The prominent role of VEGF in angiogenesis has been demonstrated utilizing mice lacking a VEGF allele. These mice die in utero between day 11 and 12, probably due to defective vascularization.[89, 90]

The multifunctionality of VEGF-A at the cellular level results from its ability to initiate a diverse, complex and integrated network of signaling pathways. It either binds to one of the three receptor tyrosine kinases (RTKs), known as VEGF receptor-1, -2 and -3 (VEGFR1-3), and/or co-receptors such as heparan sulfate proteoglycans (HSPGs) and neurophilins (multifunctional transmembrane glycoproteins).[91] Most, if not all, biologically relevant VEGF-A signaling in endothelial cells is mediated *via* VEGFR2, also denoted as the kinase domain region (KDR) or Flk-1. The VEGFR2 is activated through ligand-stimulated receptor dimerization and trans(auto)phosphorylation of multiple tyrosine residues in the cytoplasmic domain. A major mitogenic signaling mechanism for VEGF-A is the phospholipase C-γ (PLC-γ) pathway. VEGF-A induces strong PLC-γ tyrosine phosphorylation and activation leading to hydrolysis of phosphatidylinositol 4,5-bisphosphate, and thereby generation of inositol 1,4,5-trisphosphate (IP$_3$) and diacylglycerol and subsequent activation of the protein kinase C (PKC). PKC mediates direct activation of Raf-1, which in turn leads to the activation of MEK 1/2 (mitogen-activated protein kinase/ERK kinase 1/2) and extracellular-signal-regulated protein kinase 1 and 2 (ERK 1 and ERK 2).[92-94] The described PLC-γ pathway is the main signaling mechanism in VEGF-induced ERK activation (Figure 2.13). However, to a minor extent ERK activity is also enhanced by VEGF through the Ras-dependent pathway.[95]
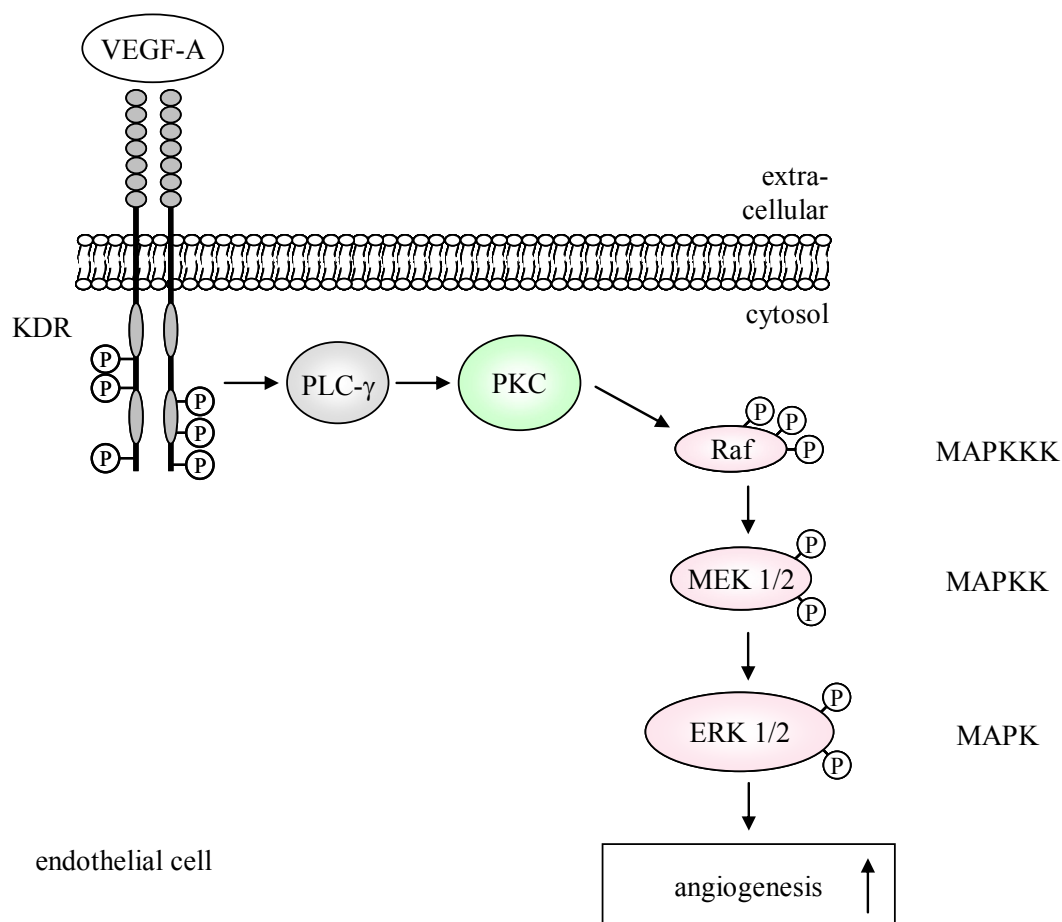
Figure 2.13   *VEGF binding to KDR activates the MAPK pathway.*
Upon VEGF binding, the KDR dimerize and autophosphorylates tyrosine residues.
Subsequently, downstream signaling molecules including the MAP kinases are activated.

2.5.4   Protein phosphatases

Protein phosphorylation plays a crucial role in regulating various cellular processes. Along this line, target proteins are phosphorylated at specific sites by one or more protein kinases, and these previously "attached" phosphate residues are later on removed by specific protein phosphatases (Figure 2.14). Kinases and phosphatases are counterparts that function in a strictly organized and coordinated manner to tightly control signaling pathways. The level of protein phosphorylation reflects the balance between kinase and phosphatase activity. Protein phosphatases can be classified into three groups on the basis of sequences, structures and catalytic mechanisms. The three distinct groups are categorized as follows: serine/threonine phosphatases (PPs), protein tyrosine phosphatase (PTP), and aspartame-based protein phosphatases.

kinases
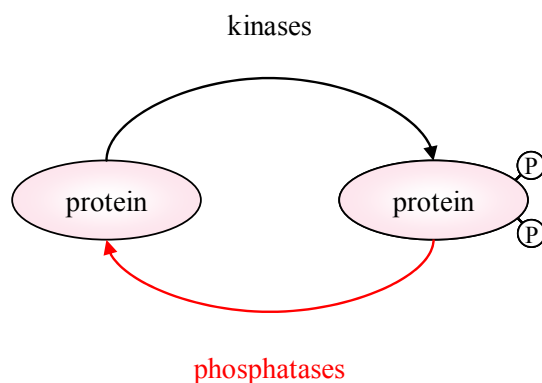
phosphatases

Figure 2.14   *The Yin and Yang of protein phosphorylation*
                      Target proteins are phosphorylated by protein kinases. The phosphate residues are removed by
                      protein phosphatases.

2.5.4.1 Protein serine/threonine phosphatases

Initially the protein serine/threonine phosphatases (PPs) were classified as either type-1 (PP1)

or type-2 (PP2) according to biochemical parameters. Type-1 protein phosphatases (PP1) are

inhibited by heat-stable inhibitor proteins and preferentially dephosphorylate the ß-subunit of

phosphorylase kinase. In contrast, type-2 protein phosphatases (PP2) are insensitive to these

inhibitors and preferentially dephosphorylate the α-subunit of phosphorylase kinase. The

type-2 enzymes were further subdivided into spontaneously active protein phosphatase

(PP2A, does not require metals for activation), Ca^{2+}-stimulated protein phosphatase (PP2B,

also known as calcineurin) and the Mg^{2+}-dependent protein phosphatase (PP2C). Further

experimentation with cDNA cloning revealed that PP1, PP2A and PP2B belong to the same

gene family, whereas PP2C is structurally different.

Today, PPs are subdivided into the phosphoprotein phosphatase (PPP) and Mg^{2+}-dependent

protein phosphatase (PPM) gene families on the basis of metal-ion requirements and substrate

specificity (Figure 2.15). The PPP family includes the most abundant protein phosphatases:

PP1, PP2A and PP2B, whereas the PPM family comprises the PP2C isoforms. PPs catalyze

the direct hydrolysis of phosphosubstrate, a process that is facilitated by two metalions at the

active centre of the enzyme.
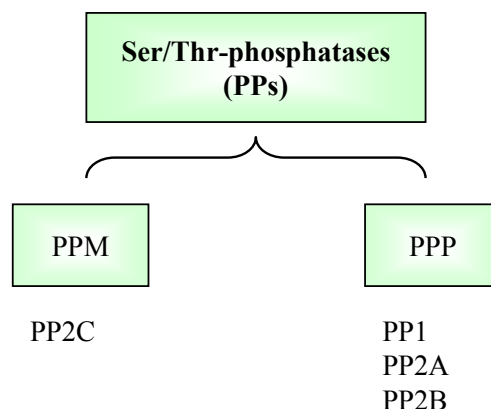
Figure 2.15   *Serine/threonine phosphatases (PPs)*
The family of PPs comprises the large phosphoprotein phosphatase (PPP) family and the protein phosphatase Mg^{2+}-dependent (PPM) family. The active centre of these enzymes contains a metal-ion (Fe^{2+} and Zn^{2+} or Mn^{2+}), which are required for catalysis.

Protein phosphatase 2A (PP2A)

PP2A is a major regulator of growth-regulatory signal transduction pathways and proliferation. The PP2A multi-tasking enzyme system is the cellular target of okadaic acid and exerts positive as well as negative functions due to its distinct subcellular location and diverse substrate specificity. Recent studies have demonstrated that PP2A functions as positive regulator of Raf-1 and kinase suppressor of Ras *via* dephosphorylation of phosphorylated serine and threonine residues that inhibit kinase activity. PP2A activity is required for the membrane translocation of the scaffold protein kinase suppressor of Ras 1 (KSR1), which interacts with kinase components of the ERK cascade and facilitates signal transmission from Raf-1 to MEK 1/2 and ERK.[96-100]

2.5.4.2 Protein tyrosine phosphatases

Protein tyrosine phosphatases (PTPs) encode the largest family of phosphatase genes and are divided into the classical, phosphotyrosine-specific phosphatases and the dual specificity phosphatases (DUSPs) (summarized in Figure 2.16). These enzymes share an identical catalytic mechanism and a common CX_5R sequence motif, in which the thiol group of an active site cysteine residue functions as the attacking nucleophile. The classical PTPs include transmembrane receptor-like proteins (RPTPs) that have the potential to regulate signaling through ligand-controlled protein tyrosine dephosphorylation. Many of the RPTPs, exemplified by DEP-1, LAR and PTPα, generally contain extracellular domains often resembling adhesion receptors and have been implicated in processes that involve cell-cell

and cell-matrix contact.[101, 102] The cytoplasmic PTPs, i.e. SHP-1, SHP-2 and PTP1B, are characterized by regulatory sequences that flank the catalytic domain and control activity either directly or by regulating substrate specificity. Members of dual specificity phosphatases are the MAPK phosphatases (i.e. MKP-1 and MKP-3), the cell cycle regulators Cdc25 phosphatases, and the tumor suppressor PTEN.[103] All PTPs are characterized by their sensitivity to vanadate, the ability to hydrolyze *p*-nitrophenyl phosphate, an insensitivity to okadaic acid and a lack of metal ion requirement for catalysis.[104]
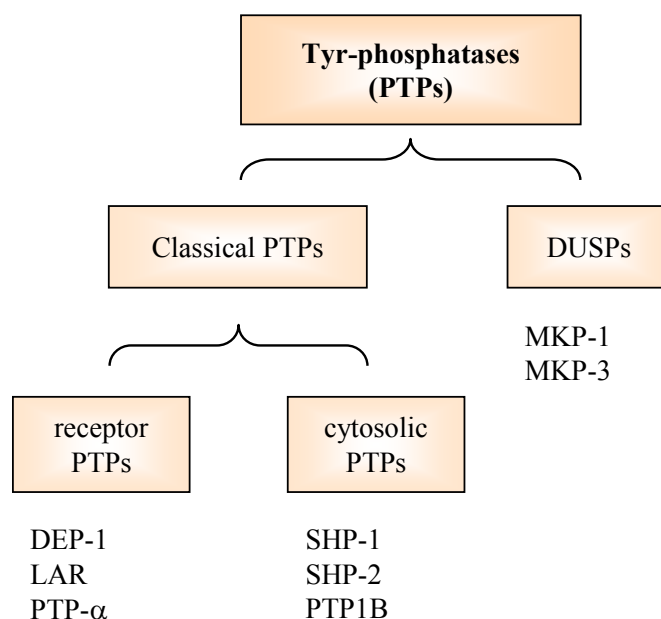
Figure 2.16   *Protein tyrosine phosphatases (PTPs)*
                      The family of PTPs can be divided into the classical, phosphotyrosine-specific phosphatases
                      and the dual specificity phosphatases (DUSPs). Moreover, the first group of PTPs can be
                      categorized as receptor–like or cytosolic phosphatases. The active centre of these enzymes
                      contains a cysteine residue.

In the following two PTPs are briefly discussed, which can inactivate the growth factor-induced ERK phosphorylation working at different steps of the described signaling cascade.

The MAP kinase phosphatase MKP-1

Members of the MAPK family could be rapidly inactivated through dephosphorylation by PTPs known as dual specificity mitogen-activated protein kinase phosphatases (DUSPs, also referred to as MKPs). Among these phosphatases, MKP-1, encoded by an immediate early gene, inactivates ERK by dephosphorylation of the two critical MAPK residues (Thr202/Tyr204) accountable for its activation. It was also shown that MKP-1 dephosphorylates and inactivates the p38 MAPK as well as JNK. MKP-1 is widely

distributed, however, expressed at low levels. Therefore, MKP-1 underlies a rapid and tight transcriptional upregulation in response to numerous stimuli, including mitogens like growth factors, oxidative stress, heat shock or hormones.[105-107]

The src homology-2 (SH2) domain-containing PTPs

The src homology-2 (SH2) domain-containing PTPs (SHPs) are a subfamily of the classical cytosolic PTPs composed of two SH2 domains (one within the NH_2-terminal half and another within the C-terminal half) and the proteintyrosine-binding (PTB) domain (Figure 2.17). There are two vertebrate SHPs: SHP-1 (also denoted as SH-PTP1 or PTP1C) and SHP-2 (also denoted as SH-PTP2 or PTP2C). It is intriguing that despite their close sequence and structurally homology these two phosphatases play quite different and often opposing cellular roles.[108-110]

Figure 2.17   *Structure of Src homology-2 (SH2) domain-containing phosphatase*
A schematic of a typical member of the SHP subfamily is shown, indicating the two SH2 domains (N-SH2 and C-SH2) and the catalytic protein-tyrosine phosphatase domain.

SHP-2 plays a mainly positive signaling role in the Raf-MEK-ERK pathway. In contrast, SHP-1 acts as a largely negative signaling role suppressing cellular activation and ERK phosphorylation. Recent studies have demonstrated that SHP-2 positively regulates signaling downstream of the insulin receptor, epidermal growth factor receptor (EGFR), platelet-derived growth factor receptor (PDGFR) and fibroblast growth factor receptor (FGFR). Contrary to these findings, SHP-1 interacts with activated cytokines, growth factors, and antigen receptors and performs a negative regulatory role in signaling pathways by dephosphorylation of the receptors or receptor substrates to which it binds. Thus, treatment of endothelial cells with TNF-α increases SHP-1 activity and consequently, attenuates growth factor-induced ERK phosphorylation. Activation of VEGF receptor-2 by VEGF has been shown to enhance SHP-1 activity resulting in the dephosphorylation of VEGFR-2 and the

MAP kinase ERK. Finally, elevated SHP-1 activity weakens VEGF-induced endothelial proliferation.[111-113]

SHP-1 has been proposed to be a potential tumor suppressor gene in leukemia, lymphoma and other cancers. It is also believed that its expression might be diminished in some cancers. In contrast to hematopoietic cancers, SHP-1 proteins were reported to be over-expressed in epithelial cancers such as prostate, ovarian and breast cancers. These data suggest that SHP-1 can play either negative or positive roles in regulating signal transduction pathways. In summary, SHP-1 plays a role in the negative regulation of growth factor-induced cellular effects and appears to be a key molecule in the prevention of endothelial dysfunction (i.e. atherogenesis) and in the induction of angiogenesis in ischemic diseases.[114, 115]

3   MATERIALS AND METHODS

3.1 Materials

The following materials were used for cell culture and animal experiments.

3.1.1 *Ginkgo biloba* extract - EGb 761

EGb 761 is a well-defined preparation of *Ginkgo biloba* leaves and was kindly provided by Dr. Willmar Schwabe Pharmaceuticals (Karlsruhe, Germany). The composition, therapeutic uses as well as actions are described in section 2.2. The chemical structures of the main compounds of EGb 761 are displayed in the same section.

For experiments, EGb 761 was freshly dissolved in growth medium at a maximal concentration of 1,000 µg/ml.

3.1.2 Biochemicals and inhibitors

Biochemicals

A23187	Alexis Biochemicals, San Diego, CA, USA
FGF	PeproTech, Rocky Hill, NY, USA
Forskolin	Biotrend Chemikalien GmbH, Cologne, Germany
IBMX	Applichem, Darmstadt, Germany
PDGF	Sigma, Taufkirchen, Germany
PMA	Sigma, Taufkirchen, Germany
VEGF	PeproTech, Rocky Hill, NY, USA

Inhibitors

cAMPS-Rp	Biotrend, Cologne, Germany
L-NAME	Cayman Chemical Company, Michigan, USA
Na_3VO_4	ICN Biomedicals, Aurora, Ohio, USA
NaF	Merck, Darmstadt, Germany
PKA inhibitor fragment (6-22)	Biotrend, Cologne, Germany
U0126	Tocris, MO, USA
Wortmannin	Alexis Biochemicals, San Diego, CA, USA

3.2 Cell culture

3.2.1   Solutions and Reagents

The following solutions and reagents were used for either isolation or culture of ECs.

PBS (pH 7.4)		
NaCl	123.2	mM
Na_2HPO_4	10.4	mM
KH_2PO_4	3.2	mM

PBS Ca^{2+}/Mg^{2+} (pH 7.4)		
NaCl	137	mM
KCl	2.68	mM
Na_2HPO_4	8.10	mM
KH_2PO_4	1.47	mM
$MgCl_2$	0.25	mM
$CaCl_2$	0.50	mM
H_2O		

Trypsin/EDTA (T/E)		
Trypsin	0.05	%
EDTA	0.20	%
PBS		

Collagen G solution		
Collagen G	0.001	%
PBS		

Cell Culture Reagents

Aminopteridine	PAN Biotech, Aidenbach, Germany
Amphotericin B	PAN Biotech, Aidenbach, Germany
Collagen G	BIOCHROME AG, Berlin, Germany
Collagenase A	Roche, Mannheim, Germany
Culture flasks, plates, dishes	TPP, Trasadingen, Switzerland
DMEM without Phenolred	Cambrex, Verviers, Belgium
ECGM with supplement mix	Provitro, Berlin, Germany
FBS	BIOCHROME AG, Berlin, Germany
Glutamine	PAN Biotech, Aidenbach, Germany
Hypoxanthine	PAN Biotech, Aidenbach, Germany
M199	PAN Biotech, Aidenbach, Germany
Penicillin	PAN Biotech, Aidenbach, Germany
Streptomycin	PAN Biotech, Aidenbach, Germany
Thymidine	PAN Biotech, Aidenbach, Germany

Fetal bovine serum (FBS)

FBS 880FF tested for mycoplasm and endotoxin was supplied by Biochrome AG (Berlin, Germany). For heat inactivation, FBS was partially thawed for 30 min at room temperature. Subsequently, it was totally thawed at 37°C using a water bath. Finally, inactivation was performed at 56°C for 30 min. Thereafter, FBS was aliquoted and stored at -20°C.

Charcoal-stripped FBS

FBS contains a significant amount of different steroids like estrogens. These steroids can influence the experiments, e.g. endothelial nitric oxide synthase (eNOS). Therefore, these experiments were performed with charcoal-stripped FBS. Heat-inactivated FBS (100 ml) were gently swirled with 2 g activated charcoal overnight at 4°C. Afterwards, FBS was cleaned from charcoal by repeated centrifugation (2x 5 min, 4,000 U/min and 1x 1 h, 1,000 U/min, respectively). Thereafter, the serum was sterile filtrated (Steritop 0.22 μM, Millipore, Germany), aliquoted and frozen at -20°C.

3.2.2   Endothelial cells

Endothelial cells were cultured in a humidified atmosphere at 37°C and 5% CO_2 in an incubator (Heraeus, Hanau, Germany). Furthermore, the cells were routinely tested for contamination of Mycoplasma with the PCR detection kit VenorGeM (Minerva Biolabs, Berlin, Germany).

3.2.2.1 Cell lines

HMEC-1 – Human microvascular endothelial cells

The cell line CDC/EU.HMEC-1 (commonly termed HMEC-1) was kindly provided from Centers for Disease Control and Prevention (Atlanta, GA, USA). HMEC-1 is an immortalized cell line (human dermal microvascular endothelial cells transfected with a plasmid coding for the transforming SV40 large T-antigen) that has been shown to retain endothelial morphologic, phenotypic, and functional characteristics.[116, 117]

HMECs were used for all experiments regarding the topic angiogenesis including Western blot analysis, angiogenesis Assays except migration, cAMP Assay and serine/threonine phosphatase Assay.

HMEC growth medium

ECGM	500	ml
Supplement	10	ml

EA.hy926

The human cell line EA.hy926 was graciously provided by Dr. C.-J. Edgell, University of North Carolina (Chapel Hill, NC, USA). EA.hy926 cells were derived by fusing human umbilical vein endothelial cells (HUVECs) with the permanent human lung carcinoma cell line A549. They represents a permanent cell line and are characterized as endothelial cells.[117,118] EA.hy926 cells were cultured in EA.hy926 growth medium. All experiments referring to topic nitric oxide were performed using EA.hy926 cells. These are western blot analysis, [^{14}C]L-arginine/[^{14}C]L-citrulline conversion assay as well as immunohistochemistry and confocal laser scanning microscopy.

EA.hy926 growth medium

DMEM	500	ml
Charcoal-stripped FBS	50	ml
Glutamine	2	mM
Hypoxanthine	100	µM
Aminopterine	0.4	µM
Thymidine	16	µM

EA.hy926-heNOS-Luc

EA.hy926 cells stably transfected with a plasmid containing 3,600 base pairs of the human eNOS promoter driving a luciferase gene (pNOSIII-Hu-3500-Luc-neo) were kindly provided by Dr. P. Wohlfart (Sanofi-Aventis, Germany).[119] EA.hy926-heNOS-Luc cells were cultivated with EA.hy926 growth medium supplemented with the antibiotic G418 (400 µg/ml, Sigma, Taufkirchen, Germany) as a selection marker for transfected cells. Confluent cells were stimulated for 24 h with increasing concentrations of EGb 761 and used for luciferase reporter gene assays in order to determine eNOS promoter activity.

3.2.2.2 Primary cells

Human umbilical vein endothelial cells (HUVECs) were prepared by digestion of umbilical veins with 0.1 g/l of collagenase A (37°C, 45 min).[120] HUVECs were cultured in HUVEC growth medium and used for the following experiments: western blot analysis, cell migration and Raf-1 kinase Assay. Furthermore, all experiments referring to tyrosine phosphatase SHP-1 were performed using HUVECs.

HUVEC growth medium

ECGM	500	ml
Supplement	10	ml
FBS	50	ml
Penicillin	100	U/ml
Streptomycin	100	µg/ml
Amphotericin B	2.5	µg/ml

3.2.3   Passaging

After reaching a confluent state, cells were either sub-cultured 1:3 in 75 cm² culture flasks or seeded in plates or dishes for experiments. For passaging, medium was removed and cells were washed twice with phosphate buffered saline (PBS) before they were incubated with trypsin/ethylene diamine tetraacetic acid (EDTA) (T/E) for 1-2 min at 37°C. Thereafter, cells were gradually detached and the digestion was stopped using passaging medium for either HUVECs or HMECs, or growth medium for EA.hy926 cells. After centrifugation at 1,000 rpm for 5 min at room temperature the pellet was resuspended in growth medium.

Passaging medium

M199	500	ml
FBS	50	ml
Penicillin	100	U/ml
Streptomycin	100	µg/ml
Amphotericin B	2.5	µg/ml

All HUVEC-experiments were performed with cells in passage number three. HMECs as well as EA.hy926 cells were used from passage number 3 up to 20 for experiments.

Culture flasks or plates were coated using collagen G solution before seeding HUVECs or HMECs. Therefore, Collagen G solution was added to plates or dishes and incubated for 20 min at 37°C.

3.2.4   Freezing and thawing

For freezing, confluent HMECs or EA.hy926 cells from a 75 cm² flask were trypsinized, spun down (1,000 rpm, 5 min, 24°C) and resuspended in 3 ml ice-cold freezing medium. Aliquots with 1.5 ml were frozen in cryovials. After storage at -80°C for 24 h, aliquots were moved to liquid nitrogen for long term storage.

For thawing, the content of a cryovial was warmed to 37°C and immediately dissolved in pre-warmed growth medium. In order to remove DMSO from the cells, they were centrifuged at 1,000 rpm for 5 min. After centrifugation, cells were resuspended in growth medium and transferred to a 75 cm² culture flask.

HMEC freezing medium		
FBS	50	%
DMSO	8	%
ECGM		

EA.hy926 freezing medium		
FBS	10	%
DMSO	10	%
DMEM		

3.3 Western blot analysis

Western blot analysis is an extensively used technique to identify proteins based on their ability to bind to specific antibodies in a given cell lysate or sample of tissue homogenate. In the first part of this section; the preparation of either *in vitro* or *in vivo* samples is explained. Afterwards, the separation of protein samples using SDS polyacrylamide gel electrophoresis (SDS-PAGE) is described. Thereafter, the transfer of proteins to a membrane is introduced. This step is also denoted as "blotting". Finally, proteins are visualized using monoclonal or polyclonal detection antibodies.

3.3.1   Preparation of samples

In Vitro Samples

Endothelial cells were grown in 6-well plates until confluence, starved in M199 for 4 h and treated as indicated in the respective figure legend. Subsequently, cells were washed with ice-cold PBS and lyzed in Ripa lysis buffer. Immediately, cells were frozen at -85°C. Afterwards, cells were scraped off and transferred to Eppendorf tubes (Peske, Aindling-Arnhofen, Germany) before centrifugation (16,000 rpm, 10 min, 4°C). For adjustment of samples protein content, protein concentration was determined. Laemmli sample buffer (3x) was added to the remaining supernatant and samples were heated at 95°C for 5 min. Samples were kept at -20°C until Western blot analysis.

Ripa lysis buffer		
NaCl	150	mM
Tris	50	mM
Nonidet P-40	1.00	%
Deoxycholat	0.25	%
SDS	0.10	%
H$_2$O		
add before use:		
Complete^{TM}	4	mM
PMSF	1	mM
activated Na$_3$VO$_4$	1	mM
NaF	1	mM

Laemmli sample buffer (3x)		
Tris-HCl	187.5	mM
SDS	6	%
Glycerol	30	%
Bromphenol blue	0.015	%
H$_2$O		
add before use:		
ß-mercaptoethanol	12.5	%

In Vivo Samples

Stimulation of Sprague-Dawley rats and isolation of thoracic aortas was kindly performed by Andreas Hartkorn (Ludwig-Maximilians-University of Munich, Department of Pharmacy – Centre of Drug Research). Briefly, in anesthetized Sprague-Dawley rats, a bolus of EGb 761 (5 mg/animal, n=2) or an equivalent volume of PBS (n=2) was injected *via* a catheter in the carotid artery. Five minutes after bolus administration, lungs thoracic aortas were excised and immediately frozen in liquid nitrogen. The aortas were lyzed at 4°C by homogenization in a Ripa lysis buffer with a homogenizer (Potter S, B. Braun Biotech International, Melsungen, Germany). After sample centrifugation (14,000 rpm, 10 min, 4°C, two-times) 10 µl of the supernatant were further diluted and used for determination of protein content. The remaining

supernatant was diluted with Laemmli sample buffer (3x) and boiled at 95°C for 5 min. Samples were kept at -20°C until Western blot analysis.

3.3.2   SDS-PAGE electrophoresis

Proteins were separated by discontinuous SDS-polyacrylamid gel electrophoresis (SDS-PAGE) according to Laemmli.[121] SDS is a highly negative charged detergent, which binds to the hydrophobic parts of proteins and solubilises them. After denaturizing the proteins by reduction of disulfide bonds with ß-mercaptoethanol and boiling at 95°C for 5 min, the complexes of SDS with the denatured proteins have a large net negative charge that is related to the mass of the protein. Their migration velocity during the electrophoretic separation is now roughly proportional to the mass of the protein. Equal amounts of protein were loaded on gels and separated using the Mini-PROTEAN 3 electrophoresis module (Bio-Rad, Munich, Germany). Therefore, a discontinuous polyacrylamide gel was used consisting of separation and stacking gel. The concentration of Rotiophorese[TM] Gel 30 in the separating gel was adjusted for an optimal protein separation depending on the molecular weight of the proteins as shown in Table 3.1. Electrophoresis was carried out at 100 V for 21 min for stacking and 200 V for 45 min for separation of the protein mixture. The molecular weight of proteins was determined by comparison with the prestained protein ladder (PageRulerTM, Fermentas, St. Leon-Rot, Germany).

Table 3.1: Separation gel concentrations

Protein	Separation gel concentration	
eNOS, p-eNOS	7.5	%
p-Raf, p-MEK 1/2, SH-PTP1	10	%
ERK, p-ERK, Akt, p-Akt, MKP-1	12	%

Separation gel 12%			Stacking gel		
Rotiophorese [TM] Gel 30	40	%	Rotiophorese [TM] Gel 30	17	%
Tris (pH 8.8)	375	mM	Tris (pH 6.8)	125	mM
SDS	0.1	%	SDS	0.1	%
TEMED	0.1	%	TEMED	0.2	%
APS	0.05	%	APS	0.1	%

Electrophoresis buffer

Tris	4.9	mM
Glycine	38	mM
SDS	0.1	%
H_2O		

3.3.3   Electroblotting

After protein separation by SDS-PAGE, proteins were transferred onto either PVDF or nitrocellulose membranes by electroblotting. Electroblotting also denoted as Western blotting is the most commonly used method to transfer proteins from a gel to a membrane.[122] The protein transfer can be achieved either by placing the gel-membrane sandwich between absorbent paper soaked in transfer buffer (semi-dry transfer) or by complete immersion of a gel-membrane sandwich in a buffer (wet transfer). In the present work semi-dry transfer has been used for eNOS, Akt as well as ERK proteins whereas wet transfer has been performed by electroblotting MEK 1/2, Raf-1 and SHP-1.

3.3.3.1 Semi-dry transfer

Using a Transblot SD semidry transfer cell (Bio-Rad, Hercules, USA), the separated proteins were electrophoretically transferred to a PVDF membrane (Immobilon-P, Millipore, Bedford, MA, USA). Prior to blotting, the membrane was washed in methanol for 5 min and then incubated for at least 30 min in Anode buffer on a shaking platform. For semi-dry transfer, the gel-membrane sandwich is placed between carbon plate electrodes. Therefore, one sheet of thick blotting paper (Whatman Schleicher & Schüll, Dassel, Germany) was well soaked with Anode buffer and rolled onto the anode. Subsequently, the PVDF membrane and the gels were added. Finally the stack was covered with another sheet of thick blotting paper soaked with Cathode buffer. The transfer cell was closed and transfer was carried out at 15 V for 1 h.

Anode buffer

Tris	12	mM
CAPS	8	mM
Methanol	15	%
H_2O		

Cathode buffer

Tris	12	mM
CAPS	8	mM
SDS	0.1	%
H_2O		

3.3.3.2 Wet transfer

For the wet transfer, the sandwich assembly is placed in a buffer tank with platinum wire electrodes (Mini Trans-Blot Cell, Bio-Rad, Munich, Germany). A nitrocellulose membrane (Hybond^{TM}-ECL^{TM}, Amersham Biosciences, Freiburg, Germany) was activated by soaking in tank buffer (1x) for at least 20 min. Transfer sandwich was assembled in a box containing tank buffer (1x) starting with a wetted pad. Subsequently, a soaked blotting paper, the gel followed by the membrane, a second blotting paper and a wetted pad were added. The sandwich assembly was mounted in the buffer tank, with the membrane facing the anode. Finally the cubette was filled up with tank buffer (1x) and transfer was performed at either 25 V overnight or 100 V for 1.5 h, respectively.

Tank buffer (5x)		
Tris	125	mM
Glycine	200	mM
H_2O		

Tank buffer (1x)		
Blotting buffer 5x	20	%
Methanol	20	%
H_2O		

3.3.4 Protein detection

3.3.4.1 Specific protein staining

Prior to the immunological detection of the relevant proteins, unspecific protein binding sites were blocked. Therefore, the membrane was incubated in Blotto 5% or BSA 5% for 2 h at room temperature. Afterwards, detection of the proteins was performed by incubating the membrane with the respective primary antibody at 4°C overnight. After four washing steps with PBS-T (each 5 min), the secondary antibody was added to the membrane for 1 h, followed by 4 additional washing steps. All steps regarding the incubation of the membrane were performed under gentle agitation.

In order to visualize the proteins two different methods have been used depending on the labels of secondary antibodies.

On the one hand, for horseradish peroxidase (HRP)-coupled secondary antibodies luminol was used as a substrate. The membrane was incubated in a 1:1 mixture of ECL solution A and B for 1 minute. The enzyme HRP catalyzes the oxidation of luminol in the presence of H_2O_2.

The reaction is displayed in Figure 3.1. The appearing luminescence was detected by exposure of the membrane to an X-ray film (Super RX, Fuji, Düsseldorf, Germany) and subsequently developed with a Curix 60 Developing system (Agfa-Gevaert AG, Cologne, Germany).
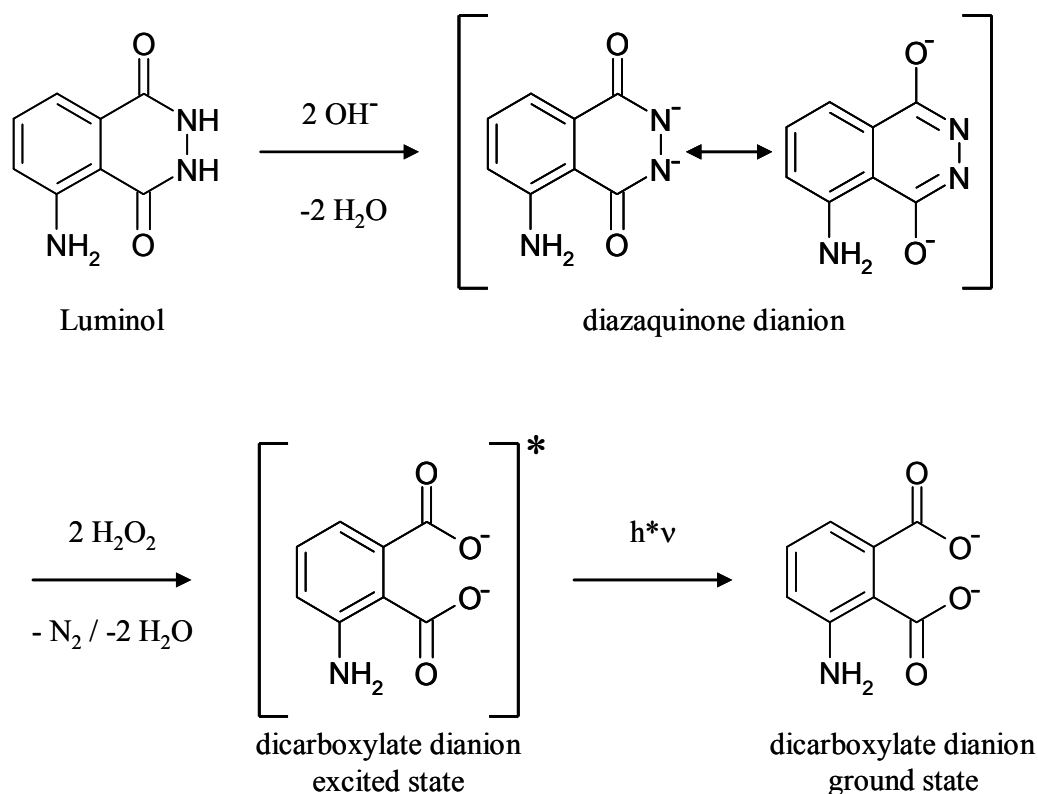
Figure 3.1   HRP-luminol reaction

ECL solution A		
Luminol	25	mM
p-Coumaric acid	0.396	mM
Tris (pH 8.5)	100	mM
H$_2$O		

ECL solution B		
H$_2$O$_2$	0.006	%
Tris (pH 8.5)	100	mM
H$_2$O		

On the other hand, antibodies directly labeled with infrared (IR) fluorophores, e.g. IRDye^{TM}800 and Alexa Fluor$^{®}$ 680 with emission at 800 and 700 nm, were applied. Protein bands of interest were detected using Odyssey imaging system (Li-Cor Biosciences, Lincoln, NE). After scanning the membrane with two-color detection, bands could be quantified using Odyssey software.

3.3.4.2 Antibodies

Primary antibodies used for Western blot analysis are summarized in Table 3.2, while secondary antibodies are listed in Table 3.3.

Table 3.2: Primary antibodies

Antigen	Isotype	Dilution	in	Provider
Actin	mouse monoclonal	1:1,000;	Blotto 1%	Chemicon
eNOS	mouse monoclonal	1:1,000;	BSA 5%	BD Transduction Laboratories
phospho-eNOS	rabbit polyclonal	1:1,000;	BSA 5%	Cell Signaling
Akt	rabbit polyclonal	1:1,000;	Blotto 5%	Cell Signaling
phospho-Akt	mouse monoclonal	1:1,000;	Blotto 5%	Cell Signaling
ERK	rabbit polyclonal	1:1,000;	Blotto 1%	Cell Signaling
phospho-ERK	mouse monoclonal	1:1,000;	Blotto 1%	Cell Signaling
phospho-MEK 1/2	rabbit polyclonal	1:200;	BSA 5%	Cell Signaling
phospho-Raf-1	rabbit polyclonal	1:200;	BSA 5%	SantaCruz
MKP-1	rabbit polyclonal	1:200;	BSA 5%	SantaCruz
SH-PTP1 (SHP-1)	rabbit polyclonal	1:200;	BSA 5%	SantaCruz
phospho-Tyrosine	mouse monoclonal	1:2000;	BSA 5%	Cell Signaling

Table 3.3: Secondary antibodies

Antibody	Dilution	in	Provider
Goat anti-mouse IgG1: HRP	1:1,000;	Blotto 1%	Biozol
Goat anti-rabbit: HRP	1:1,000;	Blotto 1%	Dianova
Alexa Fluor® 680 Goat anti-mouse IgG	1:10,000;	Blotto 1%	Molecular Probes
Alexa Fluor® 680 Goat anti-rabbit IgG	1:10,000;	Blotto 1%	Molecular Probes
IRDye 800CW Goat anti-mouse IgG	1:10,000;	Blotto 1%	LiCor Biosciences
IRDye™ 800 Goat anti-rabbit IgG	1:10,000;	Blotto 1%	Rockland

3.3.4.3 Unspecific protein staining of gels and membranes

In order to ensure equal protein loading and blotting efficiency, gels as well as membranes were stained with Coomassie or Ponceau staining solution, respectively.

After transfer, gels were incubated with Coomassie staining solution for 20 min. The dye penetrates the gel and stains all proteins without any specification. Afterwards, gels were extensively washed with Coomassie destaining solution for 60 min (6x, 10 min) until proteins appeared as blue bands.

Coomassie staining solution		
Coomassie blue G	0.3	%
Glacial acetic acid	10	%
Ethanol	45	%
H_2O		

Coomassie destaining solution		
Glacial acetic acid	10	%
Ethanol	33	%
H_2O		

Moreover, in order to ensure equal protein loading membranes were stained with Ponceau solution by agitation on a shaking platform for 5 min and were washed in water until the background disappeared.

Ponceau solution		
Ponceau S	0.1	%
Glacial acetic acid	5	%
H_2O		

3.3.5   Membrane stripping and reprobing

In order to remove primary and secondary antibodies from the membrane ("stripping"), blots were incubated twice in stripping buffer for 15 min at room temperature. After extensive washing, stripping efficiency was confirmed by scanning the membrane to see if signals have been removed. Subsequently, the blot was re-blocked with Blotto 5% for 2 h and incubated with antibodies.

Stripping buffer (pH 2.0)		
Glycine	25	mM
SDS	1	%

3.4   Protein quantification

In order to employ equal amounts of proteins in all samples, protein concentrations were determined using either Bicinchoninacid Assay (Pierce Assay) or Bradford Assay. After measurement protein concentration was adjusted by adding 1x sample buffer [Laemmli sample buffer (3x):Ripa lysis buffer=1:2].

3.4.1   Bicinchoninic acid (BCA) Protein Assay (Pierce Assay)

Pierce Assay (BC Assay reagents, Interdim, Montulocon, France) was performed as described by Smith *et al.*[123] 10 µl protein samples were incubated with 200 µl BC Assay reagents for 30 min at 37°C. Absorbance of the blue complex was measured photometrically at 550 nm (Tecan Sunrise Absorbance reader, TECAN, Crailsheim, Germany). Protein standards were obtained by diluting a stock solution of Bovine Serum Albumin (BSA, 2 mg/ml). Linear regression was used to determine the actual protein concentration of each sample.

3.4.2   Bradford Assay

Bradford Assay (Bradford solution, Bio-Rad, Munich, Germany) was performed as described by Bradford *et al.*[124] It employes Coomassie Brillant Blue as a dye, which can bind to proteins. 10 µl protein samples were incubated with 190 µl Bradford solution (1:5 dilution in water) for 5 min. Thereafter, absorbance was measured photometrically at 592 nm (Tecan Sunrise Absorbance reader, TECAN, Crailsheim, Germany). Protein standards were achieved as described above (Pierce Assay, 3.4.1).

3.5   Angiogenesis Assays

Angiogenesis is the process of generating new blood vessels from an existing vasculature. Proliferation, migration, and tube formation of endothelial cells are the essential steps in this context. Since each of this steps can be a target for intervention, and each has been tested *in vitro*.[125-127] Furthermore, the Chicken Chorioallantoic Membrane (CAM) Assay was performed. The CAM Assay is well established and widely used as a model to examine angiogenesis and anti-angiogenesis *in vivo*.[126]

3.5.1   Cell proliferation

In order to assess the effects of EGb 761 on proliferation we have carried out two different assays, the Crystal Violet Staining Assay and the Trypan Blue Exclusion Assay.

3.5.1.1 The Crystal Violet Staining Assay

In the Crystal Violet Staining Assay, HMECs were seeded into flat-bottomed 96-well microplates by adding 100 µl of ECGM containing 1.5×10^3 cells. 24 h after incubation, cells in a reference plate were stained with crystal violet solution, serving as baseline (day 0). The cells in the remaining plates were treated with increasing concentrations of EGb 761. After an additional incubation (72 h), the medium was removed and cells were stained with 100 µl crystal violet solution for 10 min at room temperature. After washing five times with distilled water, bound dye was solubilized by addition of 100 µl dissolving buffer to each well. The absorbance was measured at 540 nm in a plate-reading photometer (SPECTRAFluor Plus; Tecan, Crailsheim, Germany).

Crystal violet solution		
Crystal violet	0.5	%
Methanol	20	%
H_2O		

Dissolving buffer		
Sodium citrate 0.1 M	50	%
Ethanol	50	%

3.5.1.2 Direct counting of viable cells

HMECs were seeded at a density of 1×10^5 cells/well in six-well plates. Subsequently, cells were stimulated with increasing concentrations of EGb 761 for 48 or 72 h. Afterwards, cells were trypsinized and the cell concentration as well as percentage of viable cells was determined by a 0.4% trypan blue solution using a Vi-Cell^{TM} cell viability analyzer (Beckman Coulter, Krefeld, Germany).

3.5.2   Cell migration Assay (wound healing Assay)

Confluent HUVEC monolayers were seeded in 24-well microplates and grown as monolayers on collagen G until they reach confluence. Afterwards, cells were scratched in a line across the well with the tip of a micropipette. The wounded monolayers were washed twice with PBS Ca^{2+}/Mg^{2+} to remove floating cellular debris. Immediately, cells were refed with HUVEC growth medium. Endothelial cells were either left untreated, treated with EGb 761

(100 or 500 µg/ml, respectively) or pretreated with Na_3VO_4 (10 µM, 30 min) followed by stimulation with EGb 761. M199 media was used as negative control. After 16 h the area of cell-free wound was recorded using an imaging system (TILL Photonics GmbH, Gräfelfing, Germany) and a CCD-camera connected to an Axiovert 200 microscope (Zeiss, Oberkochen, Germany).

The images were analyzed by a specifically designed software (S.CO LifeScience, Garching, Germany) as displayed in figure 3.2. Migration was expressed as the ratio of pixels covered by cells (yellow) and the number of pixels in the wound area (gray).

A   B   C
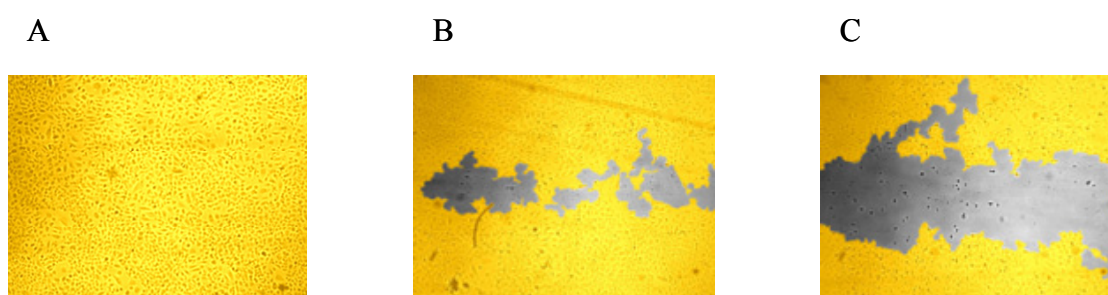
figure 3.2   *Quantitative evaluation of S.CO LifeSciences*
                      A, Cells stimulated with HUVEC growth medium. B, Cells treated with EGb 761 (100 µg/ml, 16 h). C, HUVECs starved with M199 for a periode of 16 h. The uncovered area is displayed in gray, whereas the cell-covered area is highlighted in yellow.

3.5.3   Tube formation

In order to investigate the effects on the formation of capillary-like structures by HMECs, the surface of ibidi µ-slides (18-well, ibidi GmbH, Munich, Germany) was coated with BD Matrigel™ Matrix Growth Factor Reduced (GFR) (BD Biosciences, Heidelberg, Germany). Matrigel[TM] matrix is a solubilised basement membrane preparation extracted from EHS mouse sarcoma. By the time cells are cultured on Matrigel[TM] matrix, they will behave as they do *in vivo*. For this purpose, prior to preparation of gel, the BD Matrigel™ Matrix was thawed at 4°C overnight and kept on ice until use. 19 µl of Matrigel[TM] were added to each well of an ibidi slide using precooled pipettes, and Matrigel[TM] was allowed to polymerize at 37°C for 30 min. Afterwards, the gels were overlaid with 30 µl ECGM containing $1x10^4$ HMECs. Endothelial cells were either left untreated or treated with EGb 761 (100 or 500 µg/ml, respectively) for 16 h. Finally, cells were photographed using an imaging system (TILL Photonics, Gräfelfing, Germany) and a CCD-camera connected to an Axiovert 200 microscope (Zeiss, Oberkochen, Germany).

3.5.4   The chorioallantoic membrane (CAM) Assay

The CAM Assay was kindly performed by Johanna Liebl (Ludwig-Maximilians-University of Munich, Department of Pharmacy – Centre of Drug Research). Briefly, fertilized White Leghorn chicken eggs from Lohmann Tierzucht (Cuxhaven, Germany) were incubated at 37°C at constant humidity for 72 h. Afterwards, fertilized eggs were cleaned with 70% ethanol before transferring the entire egg contents into a plastic culture dish with a size of 100 mm (whole embryo culture). The eggs were returned to the incubator for further 72 h, during that time the CAM develops. CAMs were covered with sterile hydroxyethylcellulose discs loaded with either FGF (1 ng/disc) or combinations of EGb 761 (1.25, 2.5, and 3.75 µg/disc, respectively) and FGF (1 ng/disc). The next day the vascular structure in the CAM was visualized using a stereomicroscope and a CCD camera (Olympus, Munich, Germany).

3.6   Transfection of cells

Transfection describes the introduction of genetic material into cultured mammalian cells. In these experiments genetic material (such as plasmid DNA or siRNA constructs) can be transfected using calcium phosphate, electroporation, lipofection or magnetofection.

In order to silence the expression of SHP-1 genes human umbilical vein endothelial cells (HUVECs) were transiently transfected by electroporation with the Nucleofector™ II device (Amaxa, Cologne, Germany) employing the HUVEC Nucleofector® Kit (Amaxa, Cologne, Germany). Two On-TARGETplus Individual Duplexes were used as SHP-1 siRNA and were purchased from Dharmacon (Lafayette, CO, USA). Sence as well as antisence sequences are displayed in Table 3.4. The receipt siRNA was resuspended in Dharmacon 1x siRNA buffer, aliquoted and stored at -80°C. The concentration of siRNA was verified using a NanoDrop (Wilmington, DE, USA).

<u>Experimental procedure</u>

For each transfection, $2x10^6$ HUVECs from passage three were combined with 100 µl HUVEC Nucleofector Solution and 1.5 µg siRNA Duplex J-009778-09 and 1.5 µg siRNA Duplex J-009778-09, respectively. The mixture of cells and RNA was transferred to an amaxa certified cuvette and transfection was performed using the program A-034. Afterwards, 900 µl of prewarmed culture medium was added to the cuvette. Cells were immediately seeded in

96-well (1×10^4 cells) or 6-well (5×10^5 cells) plates, cultured at 37°C, 5% CO_2. Transiently transfected cells were used for crystal violet staining assays 24 h after transfection. Concurrently, HUVECs were transfected with On-TARGETplus siCONTROL Non-targeting siRNA (Dharmacon, Lafayette, CO, USA) using as transfection control.

Table 3.4 SHP-1 siRNA sequences and Non-targeting siRNA sequence

ON-TARGETplus Duplex SHP-1 siRNA

J-009778-09	Sense Sequence	GGAACAAAUGCGUCCCAUAUU
	Antisense Sequence	5'-PUAUGGGACGCAUUUGUUCCUU
J-009778-10	Sense Sequence	AUACAAACUCCGUACCUUAUU
	Antisense Sequence	5'-PUAAGGUACGGAGUUUGUAUUU

ON-TARGETplus siCONTROL Non-targeting siRNA

D-001810-01	Sequence	5'-UGGUUUACAUGUCGACUAA-3'

3.7 Raf-1 Kinase Assay

In order to determine Raf-1 dependent phosphotransferase activity we used the nonradioactive Raf-1 Kinase Assay Kit (Upstate, Lake Placid, NY, USA) according to the manufacturer's instructions. This kit measures the phosphotransferase activity of Raf-1 *via* phosphorylation of recombinant inactive MEK 1.

The Raf-1 kinase cascade reaction is displayed in figure 3.3. Once phosphorylated by active Raf-1, MEK 1 can be determined by Western blot analysis as a parameter for Raf-1 kinase activity. The recombinant human MEK 1 is a fusion protein expressed in *E. coli* and contains both a N-terminal GST-tag and a C-terminal His_6 tag. Recombinant MEK has a molecular weight of 71 kDa whereas endogen MEK 1 has a molecular weight of 45 kDa.

<div align="center">

Active Raf-1, 30°C, 30 min

MEK1, inactive + ATP ⟶ Active MEK1 + ADP

</div>
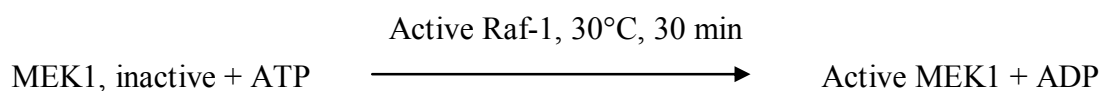
figure 3.3   *Raf-1 Kinase cascade reaction*

Experimental procedure

Briefly, HUVECs were cultured in 100 mm dishes and treated as indicated in the respective figure legend. Subsequently, cells were washed with ice-cold PBS, lyzed with Kinase lysis buffer, homogenized and centrifuged (16,000 rpm, 10 min, 4°C). Supernatants were used for protein determination (Bradford Assay, 3.4.2). Afterwards, 500 µg of protein in each cell lysate were incubated with 1 µg inactive MEK 1 substrate as well as the supplied Mg^{2+}/ATP cocktail (75 mM and 500 mM, respectively) at 30°C for 30 min in a shaking incubator. At the same time 0.1 µg Raf-1 (truncated, active) was incubated with aforementioned reaction mix as positive control. Afterwards, Laemmli sample buffer was added and the samples were heated at 95°C for 5 min. The phosphorylated MEK 1 in the reaction mixture was detected by Western blot analysis with rabbit polyclonal phospho-MEK 1/2 (Ser217/221, Cell Signaling/New England Biolabs, Frankfurt/Main, Germany).

Assay Dilution Buffer I (ADBI, pH 7.2)

MOPS	20	mM
ß-glycerophosphate	25	mM
EGTA	5	mM
add before use:		
activated Na_3VO_4	1	mM
DTT	1	mM

Buffer A

Tris	50	mM
EDTA	1	mM
EGTA	1	mM
ß-mercaptoethanol	0.1	%
Triton X-100	1	%
NaF	50	mM
$Na_4P_2O_7$	5	mM
$C_3H_5(OH)_2PO_4Na_2$	10	mM
add before use:		
Complete^{TM}	4	%
PMSF	0.1	mM
activated Na_3VO_4	0.5	mM

Kinase lysis buffer

M-Per		
add before use:		
Complete^{TM}	8	%
PMSF	2	mM
activated Na_3VO_4	2	mM
NaF	2	mM
$Na_4P_2O_7$	5	mM
$C_3H_5(OH)_2PO_4Na_2$	4	mM

3.8 cAMP Assay

The cAMP Assay consists of two parts: the accumulation of cAMP in intact cells and the determination of cAMP. The latter was studied by an enzyme-linked immunosorbant assay (ELISA) kindly performed by Dr. Hermann Ammer (Professor of Clinical Pharmacology, Department of Veterinary Sciences, University of Munich).

<u>Experimental procedure</u>

Accumulation of cAMP in intact HMECs was determined as follows: HMECs were seeded in 24-well plates and grown as monolayer until 90% confluence. Immediately before stimulation, cells were washed three times with 1 ml/well pre-warmed DMEM containing 10 mM HEPES (pH 7.4) and 0.01% BSA. Subsequently, cells were stimulated in total volume of 250 µl with EGb 761 or a combination of EGb 761 and 10 µM forskolin. Accumulation of cAMP was allowed for 30 min at 37°C and was terminated by the addition of 750 µl of ice-cold HCl 50 mM. The amount of cAMP generated was determined in the supernatants by enzyme-linked immunosorbant assay after acetylation of the samples.

3.9 Phosphatase-Assays

A phosphatase is an enzyme that removes a phosphate group from its substrate. Protein phosphatases can be subdivided based upon their substrate specificity into two main classes: 1) those that remove phosphate from proteins or peptides containing phosphoserine or phosphothreonine, and 2) those that remove phosphate from proteins or peptides containing phosphotyrosine. Members of each group have been investigated. In detail PP2A, PP2B and PP2C which are serine/threonine phosphatases as well as SHP-1 which is a tyrosine phosphatase were evaluated.

3.9.1 Serine/Threonine Phosphatase-Assay

In order to measure serine/threonine phosphatase activity we used the non-radioactive, molybdate dye-based phosphatase Assay kit (Promega, Mannheim, Germany) according to the manufacturer's instructions. This serine/threonine phosphatase Assay system contains the chemically synthesized phosphopeptide, RRA(pT)VA. This peptide substrate is compatible with several serine/threonine phosphatases such as the protein phosphatases 2A, 2B and 2C.

However, the supplied phosphopeptide is a poor substrate for Protein Phosphatase 1 because of its more stringent structural requirements. The system allows the use of a variety of buffer conditions adjusted to the specific phosphatase and determines the amount of free phosphate generated in a reaction by measuring the absorbance of a molybdate:malachite green:phosphate complex.

Experimental procedure

Briefly, HMEC-1 were pre-incubated with EGb 761 (500 µg/ml, 30 min) and subsequently exposed to FGF (5 ng/ml, 30 min). Afterwards, cells were washed with PBS and lyzed with Phosphatase lysis buffer. Cells were scraped off, centrifuged (14,000 rpm, 10 min, 4°C), and supernatants were passed through the supplied Sephadex G-25 Spin column to remove free phosphate. Aliquots of the centrifuged effluent were Assayed for protein content using the Pierce Assay (3.4.1). The standard Assay was performed in PP2A, PP2B, or PP2C Assay buffer, respectively, containing 100 µM phosphoprotein RRA(pT)VA. Reactions were started by the addition of 5 µg samples and conducted for 30 min at 37°C. Reactions were terminated by the addition of 50 µl molybdate dye-additive mixture and color was developed by incubating the mixture for 30 min at room temperature before reading the plate at 600 nm (Tecan Sunrise Absorbance reader, TECAN, Crailsheim, Germany).

Phosphatases lysis buffer (pH 7.4)		
HEPES	20	mM
Glycerol	10	%
Nonidet P-40	0.1	%
EGTA	1	mM
$MgCl_2$	0.1	mM
ß-mercaptoethanol	30	mM
add before use:		
PMSF	1	mM
Complete^{TM}	4	%

PP2A Assay buffer (pH 7.2)		
Imidazole	50	mM
EGTA	0.2	mM
ß-mercaptoethanol	0.02	%
BSA	0.1	mg/ml

PP2B Assay buffer (pH 7.2)		
Imidazole	50	mM
EGTA	0.2	mM
ß-mercaptoethanol	0.02	%
MgCl$_2$	10	mM
NiCl$_2$	1	mM
Calmodulin	50	µg/ml

PP2C Assay buffer (pH 7.2)		
Imidazole	50	mM
EGTA	0.2	mM
ß-mercaptoethanol	0.02	%
MgCl$_2$	5	mM
BSA	0.1	mg/ml

3.9.2   SHP-1 Phosphatase-Assay

SHP-1, also denoted as SH-PTP1 and PTPN6, is a SH2 domain-containing tyrosine phosphatase. This phosphatase plays an essential role in negative regulation of ERK activity and angiogenesis. Its activity was measured by immunoprecipitation of SHP-1 followed by PTP Assay using para-Nitrophenyl phosphate (p-NPP; Sigma, Taufkirchen, Germany) as an artificial substrate. p-NPP is dephosphorylated by SHP-1 to p-Nitrophenol following conversion to p-Nitrophenylene anion (Figure 3.4).
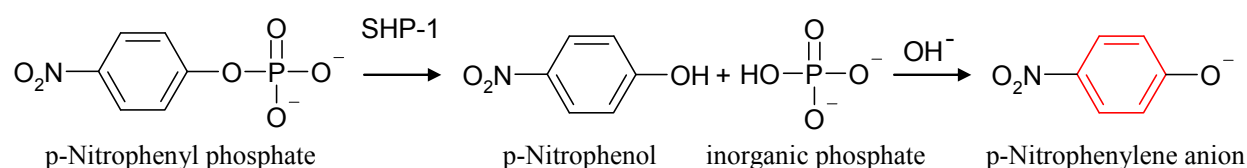
Figure 3.4   Dephosphorylation of p-NPP by SHP-1

Experimental procedure

In brief, HUVECs were cultivated in 100 mm dishes and treated as indicated in the respective figure legend. Thereafter, cells were washed with ice-cold PBS and lyzed with 500 µl SHP-1 lysis buffer. Cells were homogenized and centrifuged (16,000 rpm, 10 min, 4°C). Protein concentrations from supernatants were determined using Pierce Assay (3.4.1). Equal amounts of protein were immunoprecipitated. Therefore, 500 to 1,000 µg of proteins per sample were incubated with 10 µg SHP-1 antibody for 2 h at 4°C under gentle agitation. Subsequently, protein-antibody solution was mixed with 100 µl µMACS protein G microbeads (Miltenyi Biotec; Bergisch Gladbach, Germany) and incubated for 30 min on ice. Immune complexes were transferred to µColumns using a µMACS Separation Unit and washed twice with SHP-1

lysis buffer without Triton X-100 and without deoxycholat. Immune complexes were incubated in the SHP-1 PPase Assay buffer for 1 h at 37°C, and subsequently transferred to 96-well plates. The reaction was stopped by addition of 3 μl NaOH (1 N). The amount of phosphate release was determined by measuring the absorbance at 405 nm (SPECTRAFluor Plus; TECAN, Crailsheim, Germany). In order to verify phosphatase activity immune complexes were incubated with 100 μl Na_3VO_4 (10 mM) for 30 min at 37°C and 100 μl SHP-1 PPase Assay buffer containing Na_3VO_4 (10 mM) for 60 min at 37°C.

SHP-1 lysis buffer (pH 7.35)		
Tris-HCl	20	mM
EDTA	1	mM
add before use:		
Pefabloc® SC	1	mM
Leupeptin* ½ H_2SO_4	1	μM
Pepstatin A	1	μM
Aprotinin	1	μM
Triton X-100	1.0	%
Deoxycholat	0.5	%

SHP-1 PPase Assay buffer (pH 5)		
HEPES	20	mM
NaCl	100	mM
$MgCl_2$	5	mM
add before use:		
p-NPP	100	mM

3.10 Immunocytochemistry and confocal laser scanning microscopy

Immunocytochemistry was performed to determine changes in localization of phospho-eNOS protein levels. Confocal Laser Scanning Microscopy (CLSM) has been used as an optical imaging technique.

Experimental procedure

EA.hy926 cells were cultured on collagen A-coated glass cover slips (diameter: 12 mm) until confluence and treated as indicated. After treatment, cells were washed with PBS Ca^{2+}/Mg^{2+} and fixed with 3% formaldehyde (Sigma, Taufkirchen, Germany) for 15 min. Subsequently, cells were permeabilized with 0.2% Triton X-100 (Sigma, Taufkirchen, Germany) for 2 min. Following further washing steps with PBS Ca^{2+}/Mg^{2+}, unspecific binding was blocked by incubation with 0.2 % bovine serum albumin (BSA) solution for 60 min. Cells were incubated with the primary antibody [anti-phospho eNOS (Ser 1177), Cell Signaling, 1:100 in 0.2% BSA solution] for 1 h. As secondary antibody, AlexaFluor® 633 Goat anti-rabbit antibody

(Molecular Probes, Karlsruhe, Germany) was used at a dilution of 1:400 for 45 min. Finally, the cover slips were embedded in PermaFluor® Aqueous Mounting Medium (Beckman Coulter, Krefeld, Germany) and put onto glass objective slides. Images were obtained with a Zeiss LSM 510 Meta confocal laser scanning microscope (Zeiss, Oberkochen, Germany).

Fixation solution			**Permeabilisation buffer**		
Formalin	3	%	Triton X-100	0.2	%
PBS Ca^{2+}/Mg^{2+}			PBS		

Blocking buffer		
BSA	0.2	%
PBS		

3.11 Luciferase Reporter Gene Assay

Firefly luciferase is widely used as a reporter to study gene expression. Light is produced by converting the chemical energy of luciferin oxidation through an electron transition, forming the product molecule oxyluciferin. The enzyme catalyzes the luciferin oxidation using ATP and Mg^{2+} as co-substrates. The generated flash of light can be conveniently measured on a luminometer. Figure 3.5 displays the bioluminescent reaction.

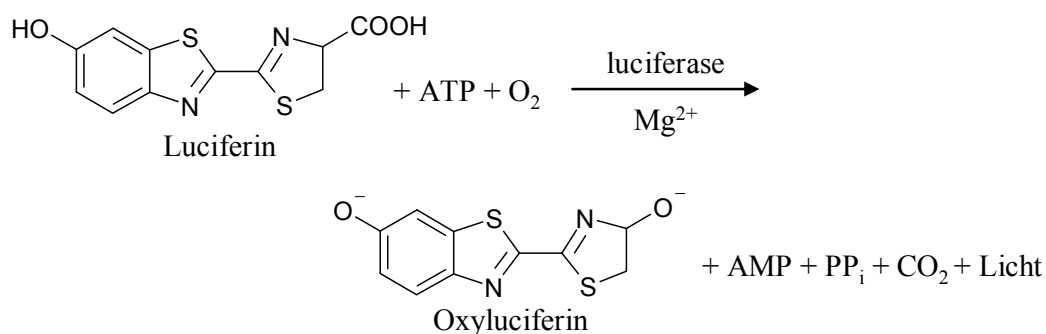*Figure 3.5   Bioluminescent reaction catalyzed by firefly luciferase.*

eNOS promoter activity

Luciferase Reporter Gene Assay (Luciferase Assay system, Promega, Mannheim, Germany) was used to measure the regulatory potential of human eNOS promoter. This has been done by linking the human eNOS promoter sequence to the comfortably detectable reporter gene encoding for firefly luciferase.

Experimental procedure

For Luciferase Reporter Gene Assay experiments stably transfected EA.hy926 cells were used. Endothelial cells were seeded in 24-well plates at a density of 75×10^4 cells per well. Confluent cells were stimulated with increasing concentrations of EGb 761 (10 to 500 µg/ml) for 24 h. Subsequently, cells were washed once with ice-cold PBS and lyzed with 150 µl Luciferase Cell Culture Lysis Reagent (Luciferase Assay System, Promega, Mannheim, Germany). Following 10 min of incubation, cell lysates were centrifuged (6,000 g, 4°C, 5 min). 20 µl of supernatant were recovered in luminometer tubes and adjusted to room temperature. Afterwards, the luminometer (AutoLumatPlus, Berthold Technologies, Bad Wildbad Germany) was programmed to perform a 2-second measurement delay followed by a 8-second measurement read for luciferase activity. The luminometer injector was primed at least three times with Luciferase Assay Reagent (Luciferase Assay System, Promega, Mannheim, Germany). Luminometer tubes were placed in the luminometer and reaction was initiated by injecting 70 µl of Luciferase Assay Reagent into each tube.

3.12   [^{14}C]L-arginine/[^{14}C]L-citrulline conversion Assay

The arginine-citrulline conversion Assay detects the conversion of radio-labelled [^{14}C]L-arginine to radio-labelled [^{14}C]L-citrulline. This reaction, as displayed in Figure 3.6, is catalyzed by endothelial nitric oxide synthase (eNOS). The conversion of L-arginine leads to equimolar amounts of NO as well as L-citrullin. The amount of [^{14}C]L-citrulline can be used indirectly as a parameter of NO production.
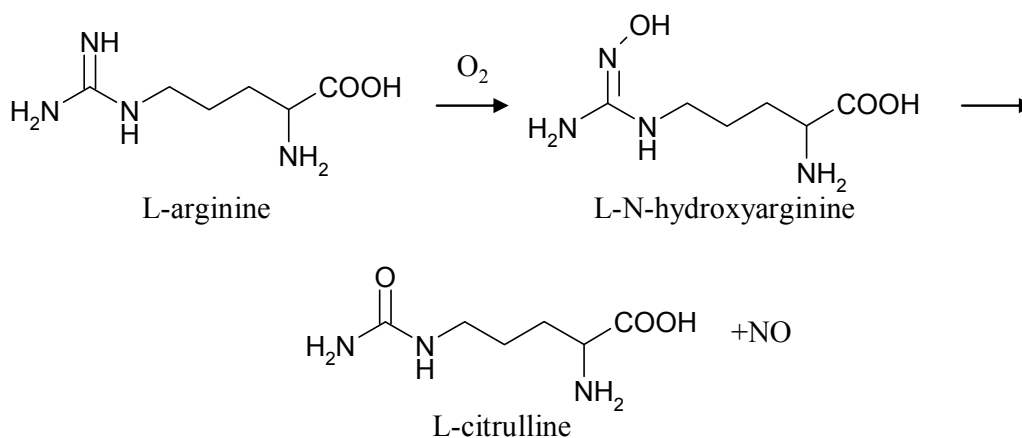

Figure 3.6   Conversion of L-arginine to L-citrulline

Experimental procedure

EA.hy926 cells were seeded in 6-well plates with a concentration of 0.5×10^6 cells/well. Confluent cells were stimulated with increasing concentrations of EGb 761 (10 to 100 µg/ml) for 48 h. Cells were washed and kept in 1 ml HEPES buffer for 45 min at 37°C before addition of 0.32 µM [^{14}C]L-arginine (313 mCi/mM, Perkin Elmer, Massachusetts, USA) and 1 µM A23187. After incubation for 25 min at 37°C cells were lyzed with ice-cold ethanol (96%). Lysates were extracted with water. The supernatants were dried under vacuum. The extract was resolved in water/methanol mixture (1:1) and spotted on a thin layer chromatography plate (Polygram® Sil N-HR, Macherey-Nagel, Düren, Germany). [^{14}C]L-arginine was separated from [^{14}C]L-citrulline using the mobil solvent system water/chloroform/methanol/ammonium hydroxide. The chromatography plates were dried and analyzed using a phosphorimager (Fujifilm BAS-1500).

HEPES buffer (pH 7.4)		
HEPES	2	mM
NaCl	29	mM
KCl	1	mM
$MgSO_4$	0.2	mM
Glucose	2	mM
CaCl	0.3	mM
H_2O		

Mobile phase		
Methanol	45	%
Ammonia 25%	20	%
Chloroform	5	%
H_2O	10	%

3.13 Rat Thoracic Aortic Ring Assay

Rat Thoracic Aortic Ring Assay was kindly performed by Dr. Egon Koch (Preclinical Research, Dr. Willmar Schwabe Pharmaceuticals, Karlsruhe, Germany). Briefly, thoracic aortas from male Sprague-Dawley rats (Janvier, Le Genest, France) were immediately removed after decapitation and placed in Tyrode salt solution (mM: NaCl 118.2; $NaHCO_3$ 24.8; KCl 4.6; $CaCl_2$ 2.5; $MgSO_4$, 1.2; KH_2PO_4 1.2; glucose 10). After removal of fat and connective tissue, vessels were cut into 4 mm long rings. The rings were mounted on stainless steel hooks in an organ chamber (Hugo Sachs, Hugstetten, Germany) and maintained at 37°C equilibrated with 95% O_2 and 5% CO_2. Isometric tension studies were performed using force transducers (Statham UC2, Hugo Sachs, Hugstetten, Germany) connected to a four-channel recorder (Lineacorder, Graphtec). Integrity of vasomotion was tested by repetitive

pre-contraction with phenylephrine (PE, 0.15 µg/ml). Endothelial function was evaluated by vascular relaxation to acetylcholine (ACh, 0.25 µg/ml) after PE-induced contraction. Vasodilatory effects of EGb 761 were studied by cumulative addition of extract concentrations from 6.4 up to 200 µg/ml (n=12) at the plateau of the PE-induced contraction. Finally, endothelial-dependent and -independent relaxation was tested by subsequent application of ACh (0.25 µg/ml) and papaverine (Pap; 37.6 µg/ml), respectively. As a solvent control, respective cumulative concentrations of DMSO were applied (n=4). Endothelial-independent relaxation was studied by using endothelium-denuded aortic rings (n=8).

3.14 *In Vivo* Blood Pressure Measurement

In vivo Blood Pressure Measurement was kindly performed by Andreas Hartkorn (Ludwig-Maximilians-University of Munich, Department of Pharmacy – Centre of Drug Research). In brief, male Sprague-Dawley rats (180–220 g) were purchased from Charles River Wiga GmbH (Sulzfeld, Germany). The animals had free access to chow (Sniff, Soest, Germany) and water up to the time of experiments. All animals received human care according to the criteria outlined in the "Guide for the Care and Use of Laboratory Animals" published by the National Institute of Health (NIH publication 86-23 revised 1985). Studies were performed with the permission of the government authorities. Animals were anesthetized with a mixture of midazolam/fentanyl solution (2.0/0.005 mg/kg, i.p.) and kept continuously anesthetized by inhalation of isoflurane (1.3%). Blood pressure was continuously monitored by a catheter in the carotid artery. One group of animals served as solvent control. Another group received an i.v. injection of EGb 761 (5 mg/animal), whereas a third group received an additional i.v. injection of L-NAME (4 mg/animal, Cayman Chemical Company, Michigan, USA) 30 min prior to the EGb 761 application.

3.15 Flow cytometry (FACS)

Flow cytometry is a technique for counting, examining, and sorting microscopic particles suspended in a stream of fluid. It allows simultaneous multiparametric analysis of the physical and/or chemical characteristics of single cells flowing through a focused laser beam. Each suspended particle passing through the beam scatters the light in some way, and fluorescent chemicals found in the particle or attached to the particle may be excited into emitting light at a lower frequency than the light source. This combination of scattered and fluorescent light is

picked up by the detectors and gives information about size, granularity and stain intensity of each individual particle. Flow cytometry has been used for the analysis of cell cycle and apoptosis. All measurements were performed on a FACSCalibur (Becton Dickinson, Heidelberg, Germany), where cells were illuminated by a blue argon laser (488 nm).

Cell cycle analysis and quantification of apoptosis rate

One of the most widely used techniques for cell cycle analysis and quantification of apoptosis rate is the method described by Nicoletti *et al.*[128] In this technique propidium iodide (PI) is used as a red fluorescent dye which binds to DNA and RNA by intercalating between the bases. When bound to nucleic acids, its absorption and emission wavelengths are 535 and 617 nm, respectively. Cells with an intact membrane are impermeable to PI. Therefore, cells are permeabilised in a hypotonic buffer that contains PI. The whole DNA content of cells is stained and the red fluorescence is measured by flow cytometry giving information about cell cycle phase and apoptosis.

The cell cycle consists of four distinct phases: G_1/G_0 phase, S phase, G_2 phase (collectively known as interphase) and M phase. Most cells of normal untreated cell populations are in G_1/G_0 phase with single DNA content and emit a homogenous fluorescence after binding of PI to DNA. Cells in G_2/M phase with a double DNA content peak at higher fluorescence intensity whereas cells in S phase appear between the G_1/G_0 and G_2/M peaks. Apoptotic cells with DNA fragments containing hypodiploid DNA have lower fluorescence intensity, and thus appear "left" to the G_1/G_0 peak in the histogram. The four distinct phases of the cell cycle and their histogram plot are displayed in Figure 3.7.
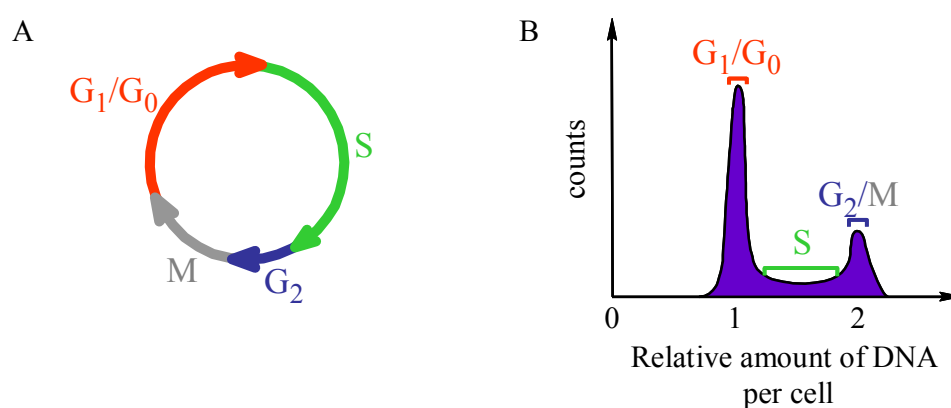
Figure 3.7   *The cell cycle.*
A: The cell cycle with its four distinct phases. B: A histogram plot of the cell cycle phases.

Experimental procedure

HMECs were seeded in 6-well plates and either left untreated or stimulated with increasing concentrations of EGb 761 (10 to 500 µg/ml). After 48 h cells were harvested by trypsination. Cells were washed three-times with PBS and centrifugated at 600 g and 4°C for 10 min. Subsequently, cells were incubated in assay buffer [hypotonic fluorochrome solution (HFS) buffer] containing PI at 4°C overnight and analyzed by flow cytometry on a FACSCalibur. The logarithmic mode of FL2 detector (585 nm) was recorded and the instruments settings were adjusted in each experiment. A histogram plot of untreated cells (control) and EGb 761 treated cells (500 µg/ml) is displayed in Figure 3.8.

FACS buffer (pH 7.37)		
NaCl	138.95	mM
K_2HPO_4	1.91	mM
NaH_2PO_4	16.55	mM
KCl	3.76	mM
LiCl	10.14	mM
NaN_3	3.08	mM
Na_2EDTA	0.97	mM
H_2O		

HFS buffer		
Propidium iodide	75	nM
Sodium citrate	0.1	%
Triton X-100	0.1	%
PBS		
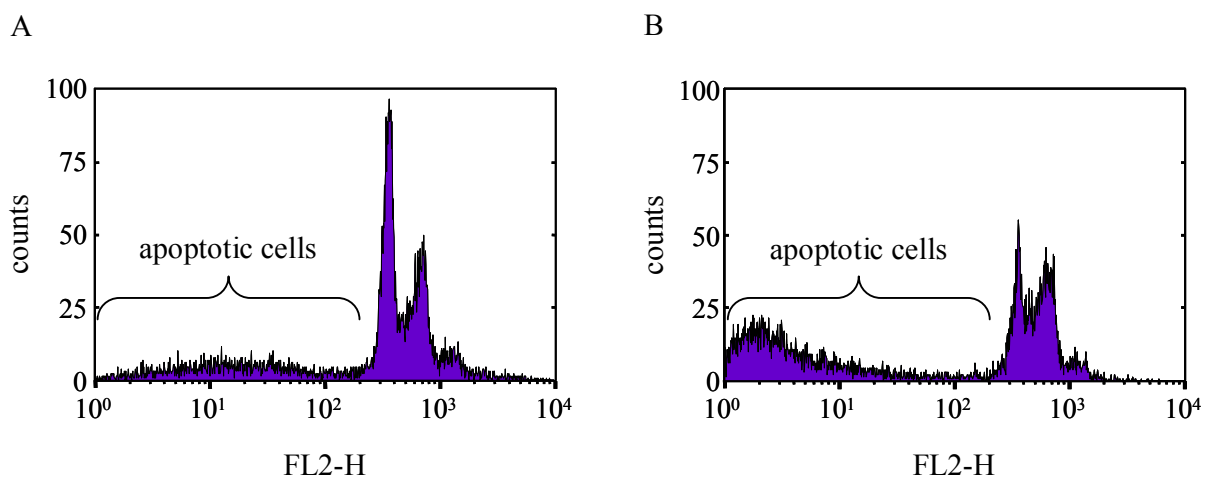
Figure 3.8   *The Histogramm Plot.*
Representative examples of either control cells (A) or EGb 761-treated cells (B) are displayed.

3.16 Real-time RT-PCR

Real-time RT-PCR is a technique used to quantify different mRNA amounts of certain genes. Previous to this technique are two steps: the RNA isolation as well as the translation of RNA into cDNA also denoted as Reverse Transcription. Following these two steps the amplification of cDNA with continuous measurement of DNA amount was performed using a 7500 Real-time PCR System (Applied Biosystems, Foster City, CA, USA). Data are collected throughout the entire process. For this reason, fluorophore-containing DNA probes, such as TaqMan[®] probes, are used to measure the amount of amplified product in real time. TaqMan[®] probe contains a reporter dye at the 5' end of the probe and a quencher dye at the 3' end of the probe. During the PCR reaction the 5' nuclease activity of AmpliTaq Gold[®] DNA Polymerase cleaves the TaqMan[®] probe. This cleavage of the probe separates the reporter dye and the quencher dye, which results in increased fluorescence of the reporter (Figure 3.9). Accumulation of PCR products is detected directly by monitoring the increase in fluorescence intensity of the reporter dye.
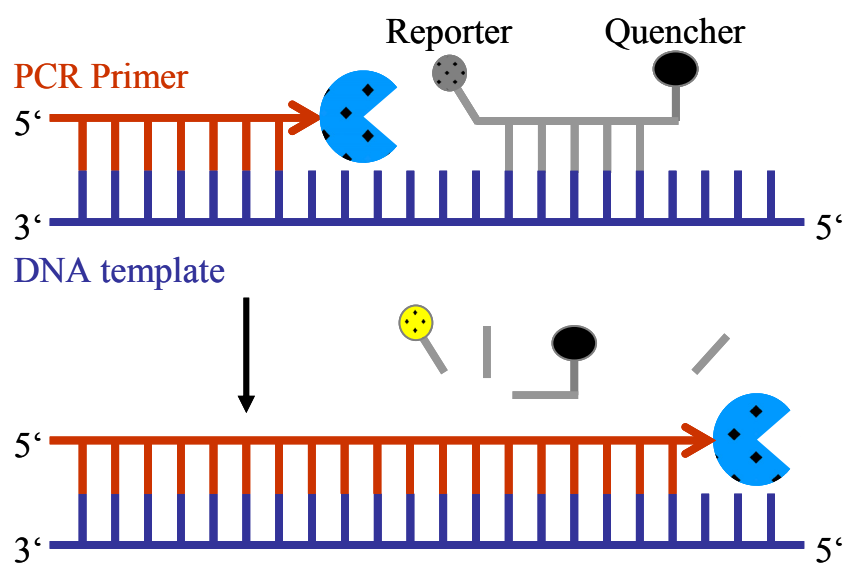
Figure 3.9   *Cleavage of TaqMan[®]-Probe by AmpliTaq Gold[®] DNA Polymerase.*

3.16.1   Isolation of RNA

Total RNA was extracted using the RNeasy mini Kit (Qiagen GmbH, Hilden, Germany) according to the instruction manual. Cells were cultured in 6-well plates and were treated as indicated. Thereafter, cells were lyzed and homogenized in the presence of a highly

denaturating guanidine isothiocyanate (GITC)-containing buffer (Buffer RLT). This buffer immediately inactivates ribonucleases (RNases) to ensure isolation of intact RNA. Samples were loaded onto a QIAshredder Spin Column and spun down (14,000 rpm, 2 min, RT). Samples were mixed with ethanol to provide appropriate binding conditions for RNA and transferred onto RNeasy mini Spin Columns. All other cellular components were removed by washing with two different washing buffers (Buffer RW1 and RPE). Since the method of real-time PCR is accident-sensitive to very small amounts of DNA-contamination, DNA-digestion was performed during the isolation procedure (RNase Free DNase Set, Qiagen, Hilden, Germany). The purified RNA was eluted from the column with 50 µl of RNase free water under low salt conditions. Samples were taken for quantification of total RNA, verification of RNA integrity and stored at -85°C until used for reverse transcription.

RNA concentration was determined by measuring the absorption at 260 nm (A260) and 280 nm (A280) (NanoDrop, Wilmington, DE, USA). Integrity of isolated RNA was checked subjecting 1 µg of total RNA to agarose gel electrophoresis, ethidium bromide staining and densitometric analysis (Kodak Image Station, Kodak, Rochester, USA). The intensity ratio of ribosomal 28S and 18S RNA was used for evaluation of RNA integrity.

3.16.2   Reverse Transcription

Reverse transcription was performed with the High Capacity cDNA Reverse Transcription Kit (Applied Biosystems, Foster City, DA, USA) according to the users' manual. This Reverse Transcription Kit allows the quantitative conversion of up to 2 µg (for a 20-µl reaction) of total RNA to single-stranded cDNA. Reverse transcription was carried out in a Primus 25 advanced[®] (Peqlab Biotechnologie GmbH, Erlangen Germany) using the cycling protocol displayed in Table 3.5. cDNA was aliquoted and stored at -20°C until used for real-time RT-PCR.

Table 3.5 Reverse transcription cycling protocol

Step	Primer extension	cDNA synthesis	Termination
Time	10 min	120 min	5 sec
Temperature	95°C	95°C	60°C

3.16.3   Real-time PCR with TaqMan® probes

<u>Primer and Probe</u>

All Primers and probes were designed with Primer Express 2.0 software (Applied Biosystems) and obtained from Invitrogen™ (Karlsruhe, Germany) or biomers.net (Ulm, Germany), respectively. The probe oligonucleotide sequence is labeled with the reporter dye 6-carboxyfluorescein (FAM) at the 5' end and the quencher dye tetramethyl-6-carboxyrhodamine (TAMRA) at the 3' end. Sequences of forward as well as reverse primers and probe are displayed in Table 3.6.

Table 3.6 Primer and Probe sequences

MKP-1 (DUSP-6)

forward	human	5'-GACGCTCCTCTCTCAGTCCAA-3'
reverse	human	5'-GGCGCTTTTCGAGGAAAAG-3'
probe	human	6-Fam-TTCGGCGCAGAGAGACCCGG-Tamra

GAPDH

forward	human	5'-GGGAAGGTGAAGGTCGGAGT-3'
reverse	human	5'-TCCACTTTACCAGAGTTAAAAGCAG-3'
probe	human	6-Fam-ACCAGGCGCCCAATACGACCAA-Tamra

<u>Experimental procedure</u>

Real-time RT-PCR was performed using the TaqMan® Universal PCR Master Mix, No AmpErase Ung (Applied Biosystems, Foster City, CA, USA) according to the manufactures instructions. In this method thermal cycling conditions as displayed in Table 3.7 have been used. In brief, 45% of the final mixture (20 µl) was provided by the cDNA sample, which contained between 10 and 100 ng cDNA. All samples were run in duplicates. Real time RT-PCR was accomplished with 100 nM probe and 400 nM of each forward and reverse primer. Standard curves were constructed on a 1:5, 1:10, 1:50 and 1:100 dilution of total RNA. The glyceraldehyde 3-phosphate dehydrogenase (GAPDH) gene was used as an internal housekeeping gene to normalize the MKP-1 data sets. Calculation of the mRNA content was performed with the new mathematical model for relative quantification of real time PCR products developed by Pfaffl et al.[129]

Table 3.7 Real-time RT-PCR thermal cycling conditions

Step	AmpliTaq Gold® Enzyme activation	PCR Cycle (40-45 cycles)	
	Hold	Denature	Anneal/Extend
Time	10 min	15 sec	1 min
Temperature	95°C	95°C	60°C

Product determination

In order to check for primer dimers and secondary PCR products, all samples were separated by agarose gel electrophoresis. Therefore, ethidiumbromide agarose gels have been prepared. PCR products were supplemented with 6x blue/orange loading dye and loaded onto an agarose gel. Subsequently, electrophoresis has been performed with TBE buffer for 2 h at 100 V. Fluorescence of intercalated ethidiumbromide into the PCR products was visualized with a Kodak Image Station (Kodak, Rochester, USA) at 254 nm.

TBE buffer		
Tris	89	mM
Boric acid	89	mM
EDTA	0.5	mM
H_2O		

Agarose gel		
Agarose	1.2	%
Ethidiumbromide	0.01	%
TBE buffer		

3.17 Statistical analysis

All experiments were performed at least three times in duplicates unless otherwise noted in the respective figure legend. Data are expressed as mean ± SEM. Statistical analysis was performed with SigmaStat software version 3.1 (Aspire Software International). Samples were analyzed by Kryskal-Wallis One-Way Analysis of Variance on Ranks followed by Dunn's Method or Student-Newman-Keuls post-hoc test, as appropriate (indicated in the figure legend). Differences between groups were considered significant if p≤0.05.

4   RESULTS

4.1   Endothelial nitric oxide production

The standardized *Ginkgo biloba* extract EGb 761 exerts a beneficial role in the treatment of cardiovascular diseases.[130-132] However, the underlying molecular mechanisms and signaling pathways have as yet remained widely unknown. Thus, we were interested in the modulation of nitric oxide (NO) generation by *Ginkgo biloba* extract.

In principle there are two ways to increase NO production: induction of endothelial nitric oxide synthase (eNOS) expression and posttranscriptional activation of eNOS. The effects of EGb 761 on both ways were investigated.

4.1.1   EGb 761 up-regulates eNOS promoter activity, eNOS protein expression, and eNOS activity

In order to investigate the effects of EGb 761 on transcriptional regulation of NO generation, we performed an eNOS promoter activity assay. EA.hy926 cells, stably transfected with a 3.6-kb human eNOS promoter fragment, were stimulated with increasing concentrations of EGb 761 (10 to 500 µg/ml). After the stimulation for 24 h eNOS promoter activity was concentration-dependently enhanced up to 1.4-fold (100 µg/ml, Figure 4.1).
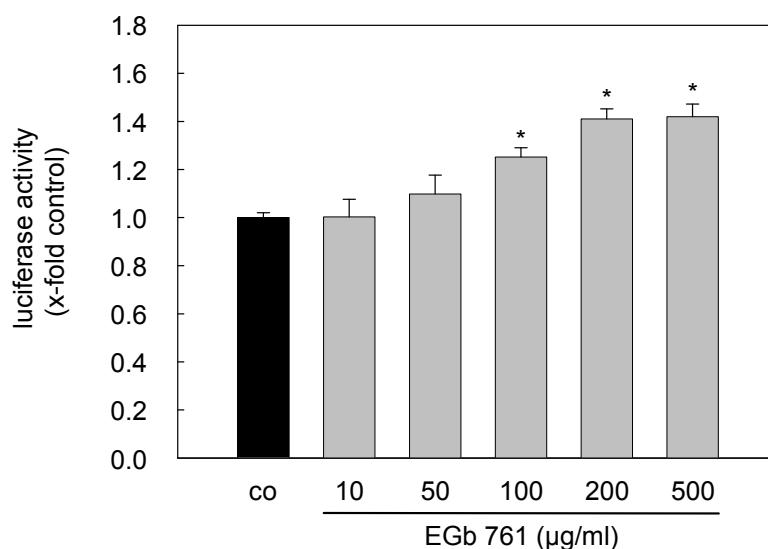
Figure 4.1   *EGb 761 increases eNOS promoter activity.*
Stably transfected EA.hy926 cells containing a 3.6-kb eNOS promoter driving a luciferase reporter gene were either kept untreated (co) or stimulated with increasing concentrations of EGb 761 (10 to 500 µg/ml) for 24 h. Cells were lyzed and analyzed for luciferase activity. Data are presented as mean ± SEM of 3 independent experiments. *≤0.05 vs. control, Kruskal-Wallis One Way Analysis of Variance on Ranks (Dunn's Method).

Furthermore, the influence of EGb 761 on eNOS protein expression was assessed by Western blot analysis. Stimulation with 500 μg/ml EGb 761 induced eNOS protein expression in EA.hy926 cells after 48 h (Figure 4.2).
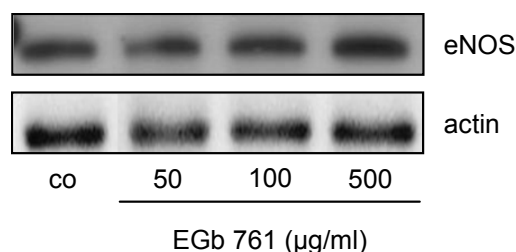
Figure 4.2   *EGb 761 enhances eNOS protein expression.*
EA.hy926 cells were either left untreated (co) or were treated with EGb 761 (50 to 500 μg/ml) for 48 h. Levels of eNOS (upper panel) and actin (lower panel) protein were determined by Western blot analysis. One representative blot out of 3 independent experiments is shown.

After the same period of time (48 h), when eNOS expression was increased, NO production was measured indirectly using the $[^{14}C]$L-arginine/$[^{14}C]$L-citrulline conversion assay. As displayed in Figure 4.3 we detected an increase in $[^{14}C]$L-citrulline production of approximately 1.5-fold after incubation with EGb 761 concentrations ranging between 10 to 100 μg/ml.
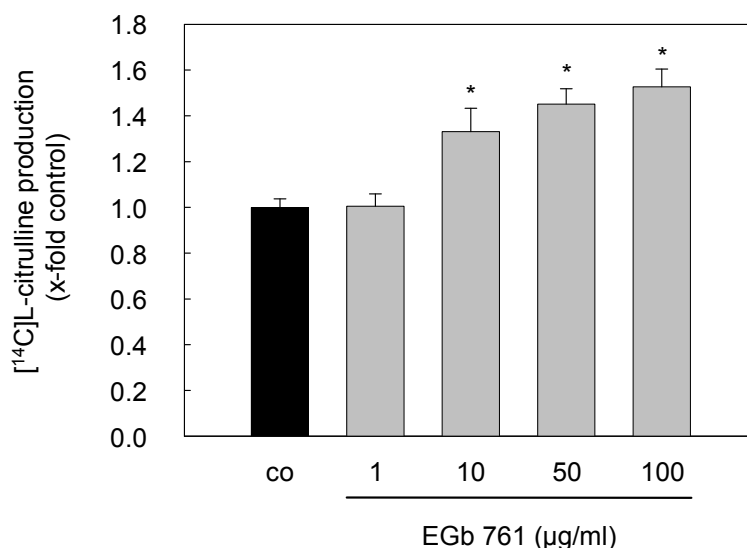
Figure 4.3   *EGb 761 up-regulates eNOS activity/$[^{14}C]$L-citrulline production.*
eNOS activity was determined by $[^{14}C]$L-arginine/$[^{14}C]$L-citrulline conversion assay. Cells were either left untreated (co) or were treated with increasing concentrations (1 to 100 μg/ml) of EGb 761 for 48 h. A, Data are presented as mean ± SEM of 3 independent experiments. $* \leq 0.05$ vs. control, Kruskal-Wallis One Way Analysis of Variance on Ranks (Dunn's Method).

4.1.2   EGb 761 promotes eNOS phosphorylation at Ser1177

In addition to the long-term influence of EGb 761 on transcriptional regulation of eNOS, we evaluated whether eNOS is acutely activated in EA.hy926 cells. As displayed in Figure 4.4 a time course for eNOS phosphorylation at Ser1177 was performed. Ser1177 is a phosphorylation site important for eNOS activation.[43] Indeed, EGb 761 (100 µg/ml) induced an eNOS phosphorylation reaching a maximum at 60 min.

Figure 4.4   *EGb 761 increases eNOS phosphorylation at Ser1177.*
                EA.hy926 cells were either left untreated (co) or were treated with EGb 761 (100 µg/ml) for
                indicated times. Levels of phospho-eNOS (Ser1177, upper panel) and total eNOS (lower panel)
                protein were determined by Western blot analysis. One representative blot out of 3 independent
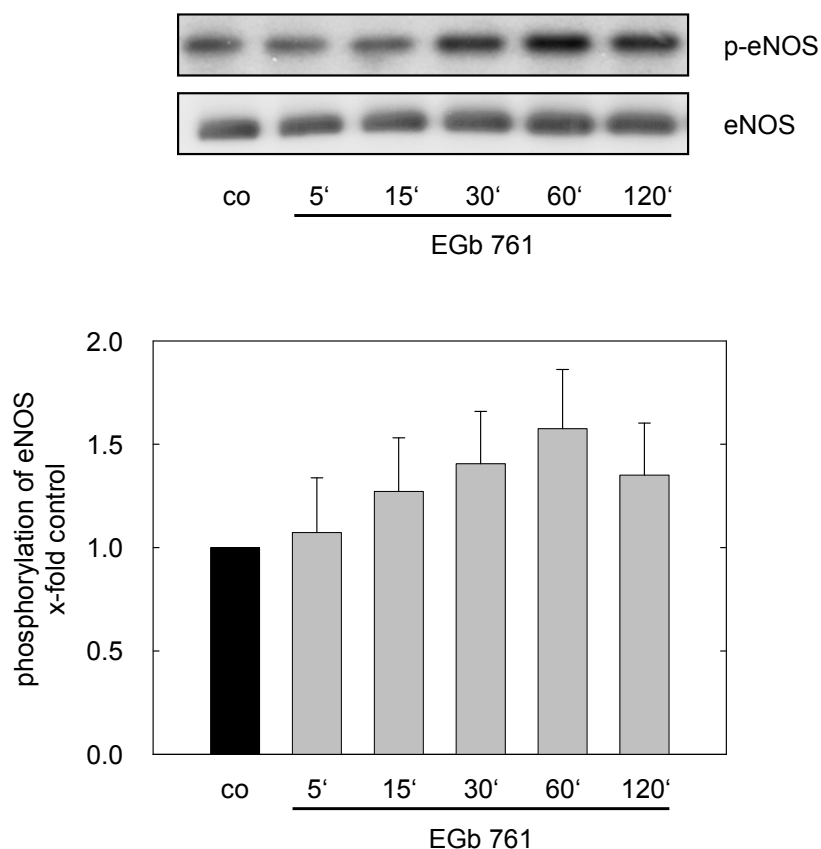   experiments is shown. The graph displays the signal intensities obtained by
                chemiluminescence evaluation. Bars represent the mean ± SEM of phospho-eNOS signals
                normalized by total eNOS signals.

Furthermore, we investigated whether EGb 761 influences the intracellular distribution of phosphorylated eNOS by means of confocal microscopy. As seen in Figure 4.5, phosphorylated eNOS was rapidly translocated to the plasma membrane upon treatment with 100 mg/ml EGb 761 for 15 min.

(1)   control

(2)   EGb 761

(3)   EGb 761
      enlarged detail from
      panel (2)
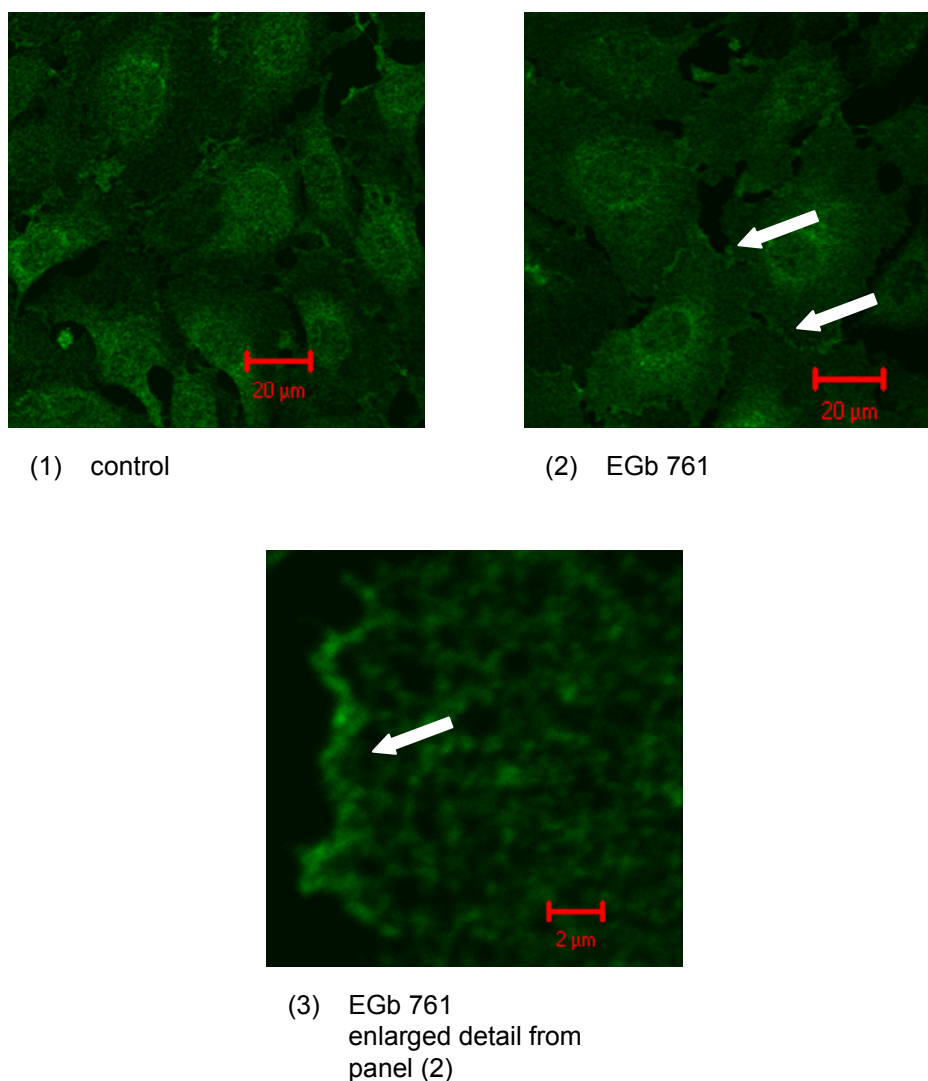
Figure 4.5   *EGb 761 leads to a rapid translocation of phosphorylated eNOS to the plasma membrane.*
                    Representative photomicrographs are shown after immunofluorescent staining of EA.hy926
                    cells. Fluorescence indicates phosphorylated eNOS protein. In contrast to untreated cells (1),
                    cells receiving 100 µg/ml EGb 761 for 15 min (2 and 3) showed translocation of
                    phosphorylated eNOS to the plasma membrane (arrows).

4.1.3   Activation of eNOS *via* the PI3K/Akt pathway

In order to analyze an involvement of protein kinase B/Akt in the phosphorylation of eNOS at
Ser1177, we examined whether EGb 761 activates Akt by phosphorylation (Ser473). Akt
phosphorylation was indeed found to be increased after EGb 761 exposure and occurred in a
time-dependent manner (Figure 4.6). Maximum activation was achieved 60 min after
treatment with EGb 100 µg/ml, closely approximating the time course of eNOS
phosphorylation at Ser1177 (Figure 4.6).
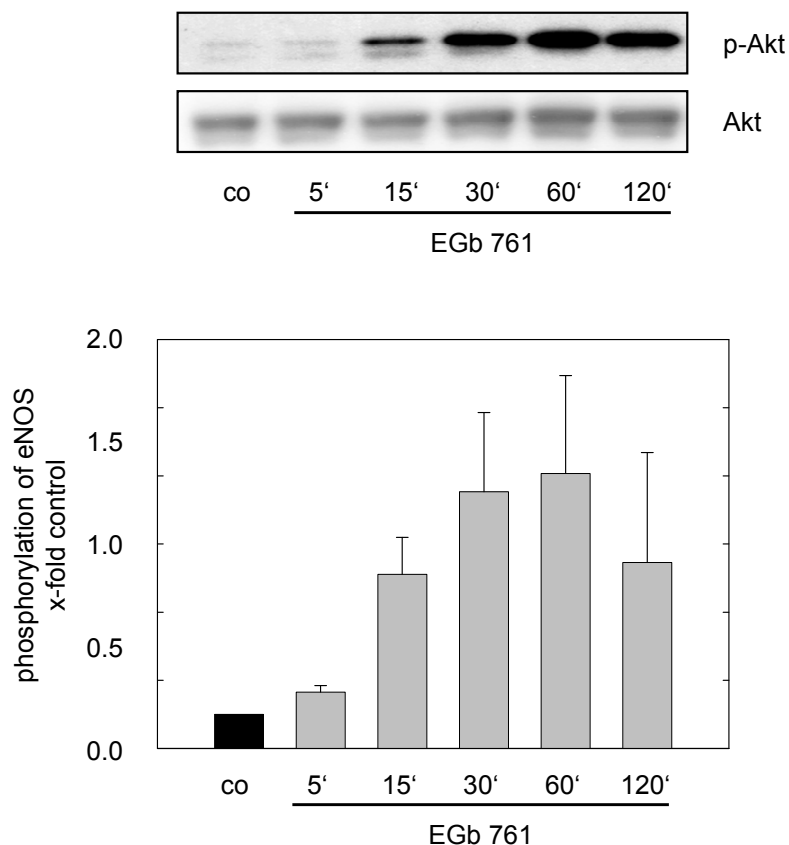
Figure 4.6   *EGb 761 increases Akt phosphorylation at Ser473.*
                     EA.hy926 cells were either left untreated (co) or were treated with EGb 761 (100 µg/ml) for
                     indicated times. Levels of phospho-Akt (Ser473, upper panel) and total Akt (lower panel)
                     protein were determined by Western blot analysis. One representative blot out of 3 independent
                     experiments is shown. The graph displays the signal intensities obtained by
                     chemiluminescence evaluation. Bars represent the mean ± SEM of phospho-Akt signals
                     normalized by total Akt signals.

To further investigate whether PI3K is involved in the EGb-mediated phosphorylation of
eNOS, we incubated EA.hy926 cells with the PI3K-inhibitor wortmannin before exposure to
EGb 761 (100 µg/ml). EGb 761-induced Akt phosphorylation was inhibited by wortmannin
(Figure 4.7).
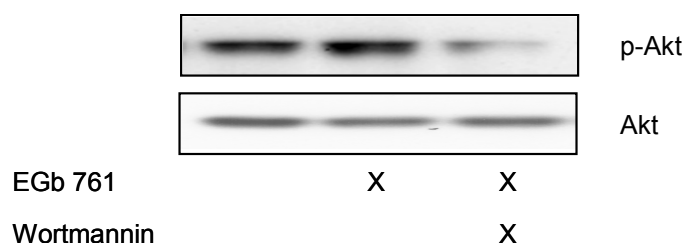
Figure 4.7   *Wortmannin completely abolished EGb 761-induced phosphorylation of Akt.*
                     EA.hy926 cells were pre-treated with wortmannin (50 nM) for 30 min before EGb 761
                     (100 µg/ml, 60 min). Levels of phospho-Akt and Akt protein level were determined by
                     Western blot analysis. One representative blot out of 3 independent experiments is shown

Moreover, the inhibitor completely abolished EGb 761-induced phosphorylation of eNOS (Figure 4.8). These results demonstrate that the EGb 761-induced phosphorylation of eNOS at Ser1177 might be Akt-dependent. An alternative explanation would be the phosphorylation of eNOS by a different kinase downstream of PI3K.

			p-eNOS
			eNOS
EGb 761		X	X
Wortmannin			X
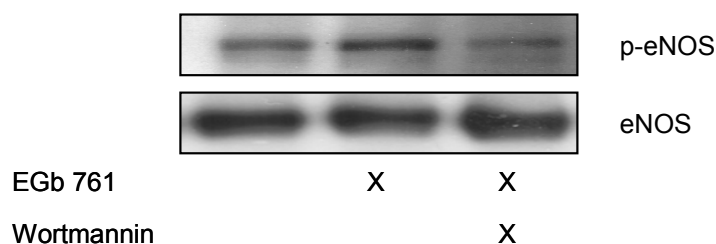
Figure 4.8   *EGb 761-induced phosphorylation of eNOS at Ser1177 is mediated by the PI3K/Akt pathway.* EA.hy926 cells were pre-treated with wortmannin (50 nM) for 30 min before EGb 761 (100 µg/ml, 60 min). Levels of phospho-Akt, Akt, phospho-eNOS, and eNOS protein were determined by Western blot analysis. One representative blot out of 3 independent experiments is shown.

4.1.4   Vasorelaxant effect of EGb 761 on rat thoracic aortic rings

EGb 761 (6.4 to 200 µg/ml) elicited dose-dependent relaxation of rat thoracic aortic rings with intact endothelium. Figure 4.9 A shows the reduced contraction of ring segments of rat thoracic aortas by EGb 761 at the plateau of the phenylephrine (PE)-induced contraction. Moreover, the subsequent application of acetylcholine (ACh) and papaverine (Pap) is displayed controlling endothelial-dependent and -independent vasorelaxation. The maximal relaxation of 50% was reached at a concentration of 200 µg/ml EGb 761 (Figure 4.9 B). In order to exclude any effects of cumulative concentrations of the solvent dimethyl sulfoxide (DMSO), pre-contracted rat thoracic aortic rings were exposed to DMSO (0.3 to 8.0 µl/20 ml). The result, displayed in Figure 4.9 C, assessed no effect of various DMSO concentrations on aortic ring relaxation. Furthermore, the vasorelaxant effect of EGb 761 was analyzed on aortic rings without any functional endothelium. Importantly, EGb 761 failed to produce relaxation in aortas without functional endothelium (Figure 4.9 D). This fact points to an involvement of NO in the endothelium-dependent vasorelaxation induced by EGb 761.
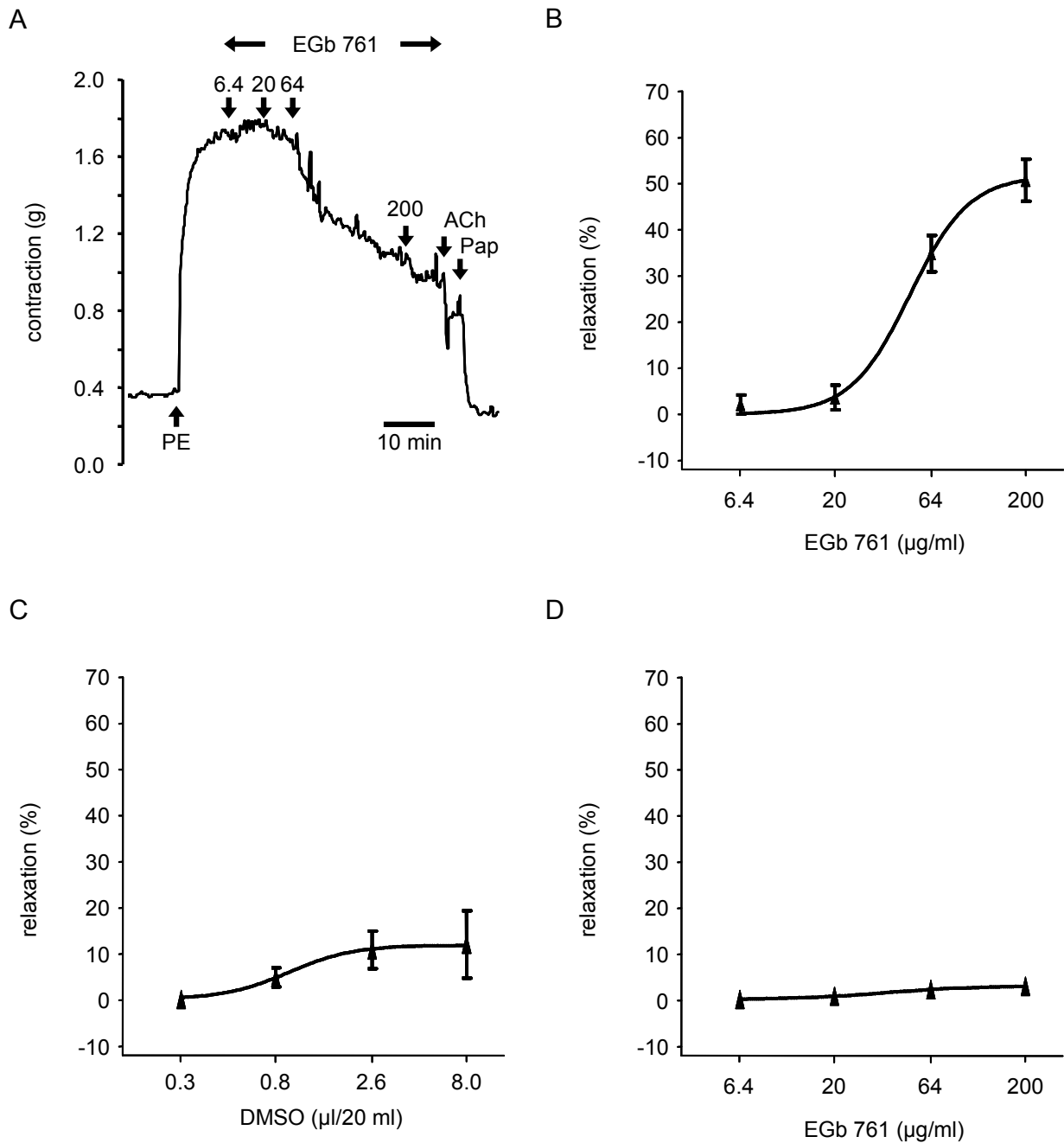
Figure 4.9   *EGb 761 concentration-dependently induces relaxation of pre-contracted thoracic aortic rings.*
A, Relaxation of ring segments of rat thoracic aorta by cumulative addition from 6.4 up to
200 μg/ml EGb 761 (n=12) at the plateau of the phenylephrine (PE)-induced contraction
(0.15 μg/ml), followed by application of acetylcholine (ACh) (0.25 μg/ml) and papaverine
(Pap; 37.6 μg/ml) to control endothelial-dependent and -independent vasorelaxation.
B, Sigmoidal dose-response curve of aortic ring relaxation by EGb 761 expressed as
percentage of the phenylephrine-induced contraction. Values are presented as mean ± SEM
(n=12). C, Sigmoidal dose-response curve of aortic ring relaxation by DMSO expressed as
percentage of the phenylephrine-induced contraction. Values are presented as mean ± SEM
(n=4). D, Concentration-response curve of endothelium-denuded aortic rings to EGb 761
expressed as percentage of the phenylephrine-induced contraction. Values are presented as
mean ± SEM (n=8). The experiment was performed by Egon Koch (Preclinical Research, Dr.
Willmar Schwabe Pharmaceuticals, Karlsruhe, Germany).

4.1.5   EGb 761 reduces systolic blood pressure in rats *via* NO release

In order to analyze the effect of EGb 761 on blood pressure, invasive blood pressure measurements were performed as shown in Figure 4.10. EGb 761 (5 mg/animal) significantly decreased systolic blood pressure. After 5 min the systolic blood pressure decreased from 120 mmHg to 65 mmHg. In order to causally link the blood pressure alterations to an enhanced NO release, animals were pretreated with the eNOS inhibitor L-NAME (4 mg/animal; 30 min). Pre-treatment of animals with L-NAME completely prevented the reduction of blood pressure by EGb 761 (Figure 4.10).
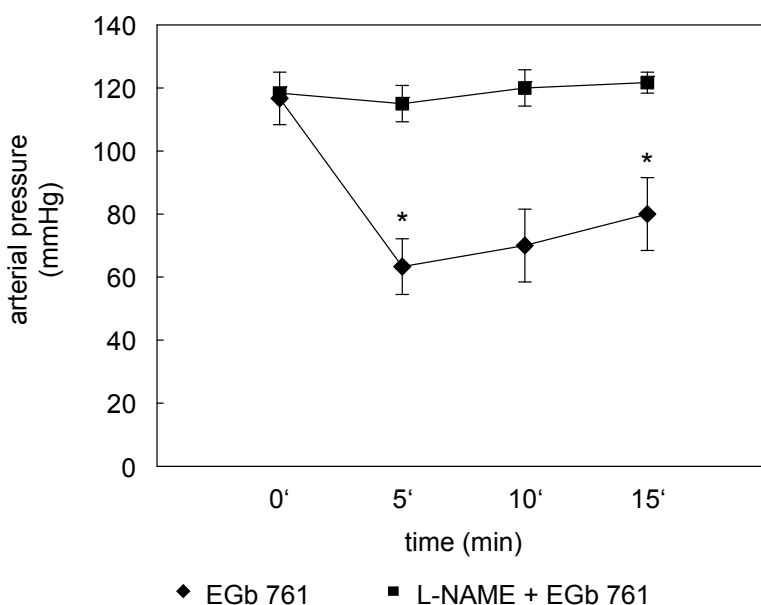
Figure 4.10   *EGb 761 rapidly decreases systolic blood pressure in Spargue-Dawley rats via NO release.*
A time course of systolic blood pressure is displayed. Blood pressure is measured *via* catheterization of the carotid artery after i.v. injection of EGb 761 (5 mg/animal) or i.v. injection of L-NAME (4 mg/animal) 30 min prior to EGb 761 application. Data are presented as mean ± SEM (n=3). *≤0.05 vs. L-NAME/EGb 761 treated animals, Student's t-test. *In Vivo* Blood Pressure Measurement was kindly performed by Andreas Hartkorn (Ludwig-Maximilians-University of Munich, Department of Pharmacy – Centre of Drug Research).

4.1.6   EGb 761 augments eNOS phosphorylation in thoracic aortas

The observed *in vivo* effects, regarding EGb 761-induced reduction of blood pressure were further confirmed by Western blot analysis. Therefore, Sprague-Dawley rats were treated with a bolus injection of EGb 761 (5 mg/animal) and protein samples of lung thoracic aortas were gained as described in materials and methods. The results, displayed in Figure 4.11, show a

significant increase (> 2-fold) in eNOS phosphorylation at Ser1177 in thoracic aortas obtained from EGb 761-treated animals compared to untreated controls.
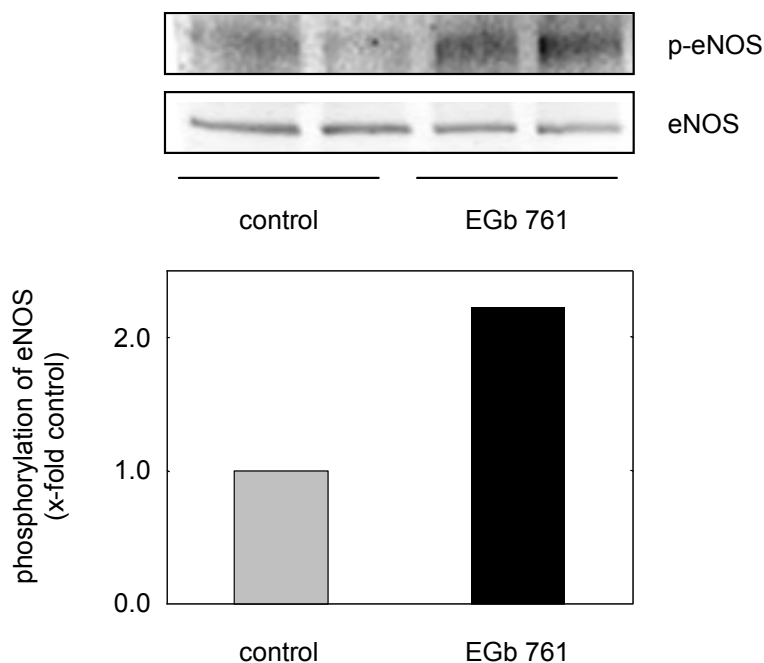
Figure 4.11   *EGb 761 induces phosphorylation of eNOS at Ser1177 in rat thoracic aortas.*
Western blot analysis showing phospho-eNOS (Ser1177, upper panel) and total eNOS protein levels (lower panel) of thoracic aorta in untreated controls or following EGb 761 treatment (5 mg/animal for 5 min). The graph displays the signal intensity obtained by fluorimetric evaluation. Bars represent the mean of phospho-eNOS signals normalized to total eNOS signals (n=2). Stimulation of Sprague-Dawley rats and isolation of lungs thoracic aortas was kindly performed by Andreas Hartkorn (Ludwig-Maximilians-University of Munich, Department of Pharmacy – Centre of Drug Research).

4.2 Angiogenesis

The onset of angiogenesis, i.e. the "angiogenic switch", is responsible for tumor progression beyond a size of 2 to 3 mm³ as well as for tumor metastasis. Inhibition of angiogenesis, therefore, represents a valid approach for cancer treatment or even prevention. Since *Ginkgo biloba* extract is traditionally used for anticancer treatment, we were interested in the anti-angiogenic effect of EGb 761. Furthermore, we investigated the influence of EGb 761 on growth factor-signaling pathways in endothelial cells focusing on the ERK-cascade and the role of phosphatases.

4.2.1   EGb 761 has anti-proliferative properties

Endothelial cell proliferation is one of the first major steps in angiogenesis. Therefore, the effects of EGb 761 on endothelial cell proliferation were assessed using either Crystal Violet Staining or direct counting of viable cells. As demonstrated in Figure 4.12, we were able to show a dose-dependent reduction of endothelial cell proliferation by EGb 761 (50 to 500 µg/ml) after 72 h.
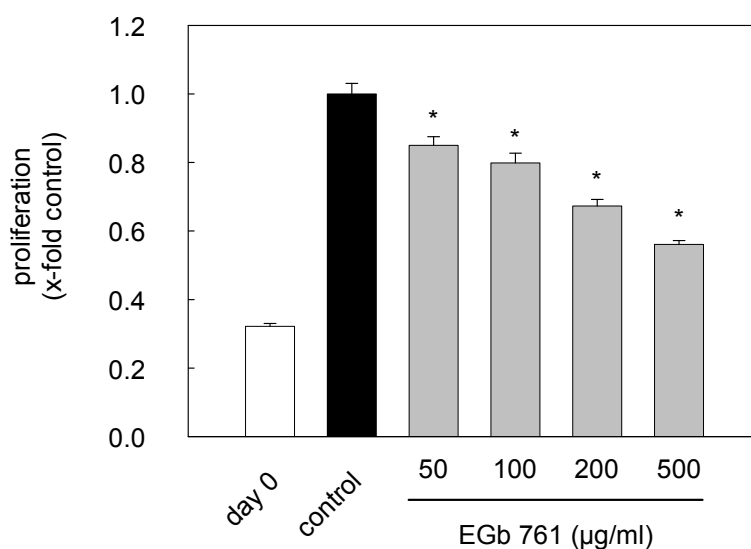
Figure 4.12   *EGb 761 significantly inhibits endothelial cell proliferation after 72 h.*
Crystal Violet Staining Assay: HMECs in a reference plate were stained after 24 h serving as baseline (day 0). HMECs in the remaining plates were either kept untreated (control) or stimulated with different concentrations of EGb 761 for 72 h. *$p \leq 0.05$ vs. control, Kryskal-Wallis One-Way Analysis of Variance on Ranks followed by Student-Newman-Keuls post-hoc test.

Furthermore, the direct counting of viable cells revealed that EGb 761 significantly diminished endothelial proliferation after 48 h down to 54% (EGb 761 500 µg/ml) in comparison to untreated controls (Figure 4.13).
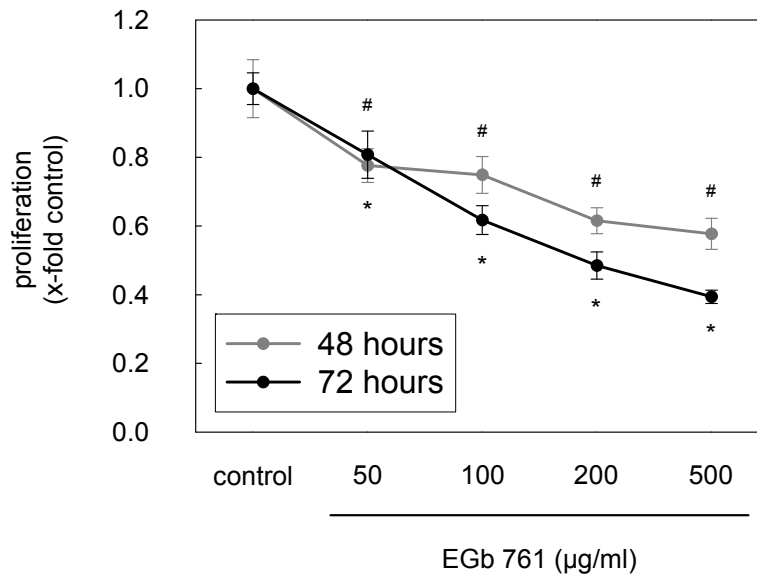
Figure 4.13   *EGb 761 diminishes endothelial cell proliferation after 48 and 72 h.*
Direct counting of viable cells: Cells were either kept untreated (control) or were stimulated with different concentrations of EGb 761 for 48 or 72 h. Data are presented as mean ± SEM of 3 independent experiments. *$p \leq 0.05$ vs. control (72 h), #$p \leq 0.05$ vs. control (48 h), Kryskal-Wallis One-Way Analysis of Variance on Ranks followed by Student-Newman-Keuls post-hoc test.

4.2.2   Effects of EGb 761 on cell cycle and apoptosis

In order to understand the mechanism by which EGb 761 inhibits endothelial cell proliferation, we investigated its effect on cell cycle and apoptosis by flow cytometry. The cell cycle is a series of events during a cell replication period. It comprises the interphase and mitosis. The latter subdivides into G_1/G_0, S and G_2 phase, depending on the DNA amount per cell. Characteristic for G_1/G_0 phase is a single, for G_2 phase a double DNA content. Treatment of HMECs with increasing concentrations of EGb 761 (50 to 500 µg/ml) resulted in S/G_2 cell cycle arrest (Figure 4.14). In detail, the number of cells in G_1/G_0 phase significantly decreased, whereas in contrast the number of cells in S and G_2 phase clearly increased.
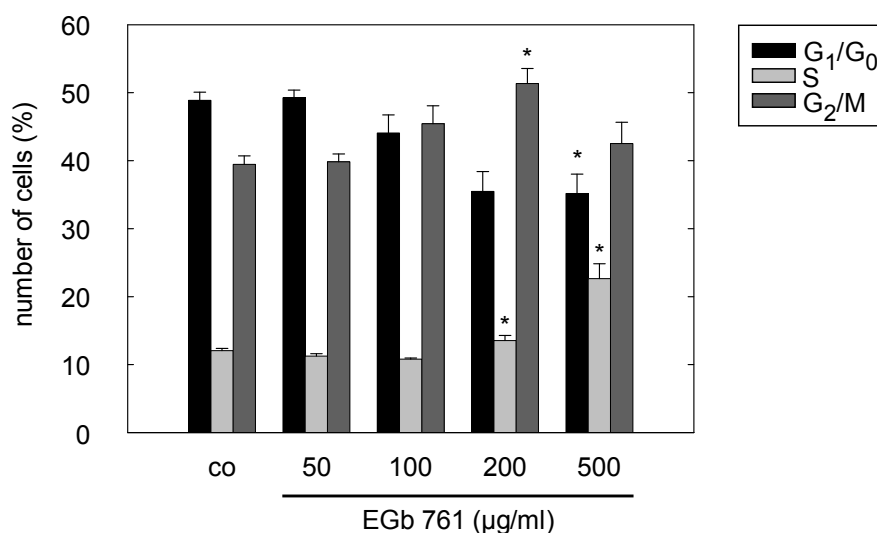
Figure 4.14   *EGb 761 causes cell cycle arrest in S/G$_2$-phase.*
Proliferating endothelial cells were either kept untreated (control) or were treated with increasing amounts of EGb 761 for 48 h. For each stimulation three bars are shown corresponding to G$_1$/G$_0$ (black), S (light gray) and G$_2$ (dark gray) phase. Data are presented as mean ± SEM of 3 independent experiments. *p≤0.05 vs. control, Kryskal-Wallis One-Way Analysis of Variance on Ranks followed by Student-Newman-Keuls post-hoc test.

Moreover, the effects of EGb 761 referring to an induction of apoptosis were assessed in either proliferating or confluent cells. In proliferating cells only the highest concentration of EGb 761 (500 µg/ml) enhances apoptosis up to 3.6 fold (Figure 4.15).
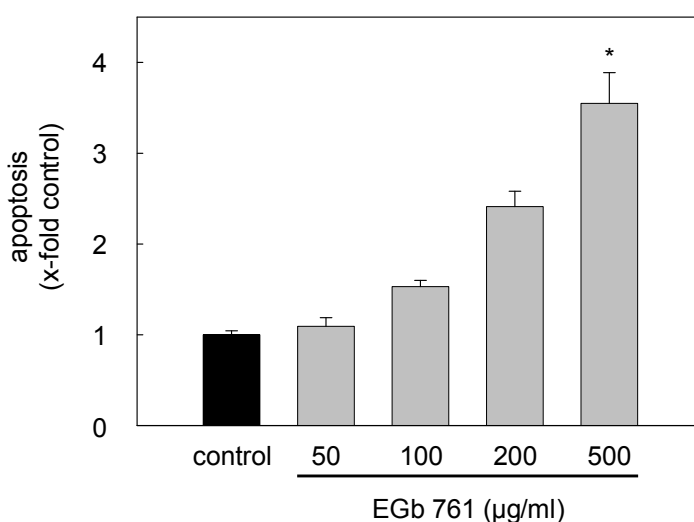
Figure 4.15   *EGb 761 enhances apoptosis in proliferating endothelial cells.*
Proliferating endothelial cells were either left untreated (control) or were exposed to EGb 761 (50 to 500 µg/ml) for 48 h. Data are presented as mean ± SEM of 3 independent experiments. *p≤0.05 vs. control, Kryskal-Wallis One-Way Analysis of Variance on Ranks followed by Dunn's Method.

In contrast apoptosis rate is not influenced by EGb 761 in confluent endothelial cells (Figure 4.16). These findings indicate that the anti-proliferative action of EGb 761 is due to a strong anti-proliferative effect, rather than to an induction of apoptosis.
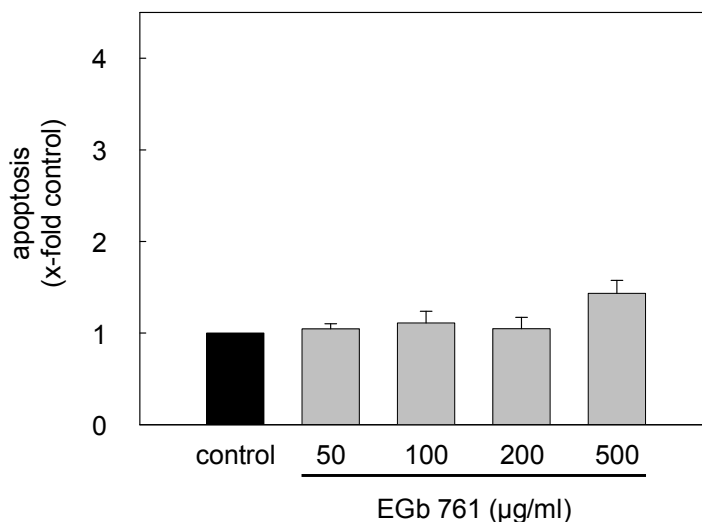
Figure 4.16   *Effects of EGb 761 on apoptosis in endothelial cells.*
Confluent cells were either left untreated (control) or were exposed to EGb 761 (50 to 500 µg/ml) for 48 h. Data are presented as mean ± SEM of 3 independent experiments. *p≤0.05 vs. control, Kryskal-Wallis One-Way Analysis of Variance on Ranks followed by Dunn's Method.

4.2.3   EGb 761 inhibits endothelial cell migration and tube formation

In addition to endothelial proliferation, cell migration and tube formation are targets for intervention in the angiogenesis cascade. Migration of HUVECs, as examined in the wound healing assay, was significantly inhibited by EGb 761. In comparison to untreated controls (HUVEC growth medium) the percentage of cell-covered area in relation to the total image area was reduced to 77% and 72% with EGb 100 and 500 µg/ml, respectively (Figure 4.17 A and B).

Tube formation is a process, which measures the ability of endothelial cells to form three-dimensional structures. The incubation of HMECs with EGb 761 (100 and 500 µg/ml, respectively) on Matrigel^{TM} led to a significant reduction in tube formation (Figure 4.17 C).

A   Migration

control   EGb 761 (100 µg/ml)   EGb 761 (500 µg/ml)

B   Migration

C   Tube formation

control   EGb 761 (100 µg/ml)   EGb 761 (500 µg/ml)
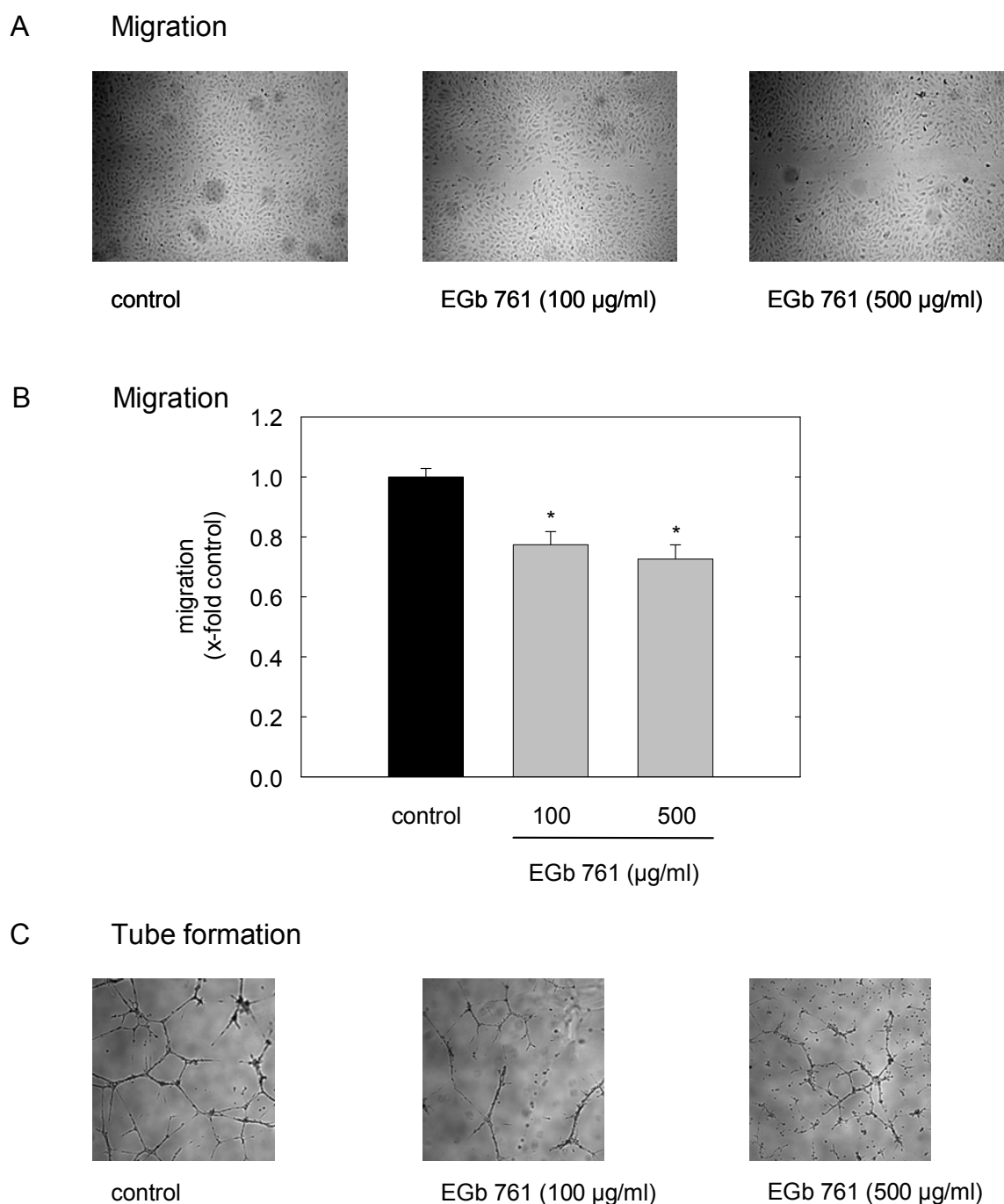
Figure 4.17   *Ginkgo biloba extract abrogates endothelial migration and tube formation.*
A, a confluent HUVEC monolayer was scratched and then exposed to fresh HUVEC growth medium (control) or medium containing EGb 761 (100 and 500 µg/ml, respectively) for 16 h. One representative image out of 3 independent experiments is shown. B, The graph displays the ratio of pixels covered by cells and pixels in the wound area. Data are presented as mean ± SEM of 3 independent experiments. *$p \leq 0.05$ vs. control, Kryskal-Wallis One-Way Analysis of Variance on Ranks followed by Student-Newman-Keuls post-hoc test. C, HMECs were seeded on Matrigel[TM]. Subsequently, cells were either left untreated (control) or were treated with EGb 761 (100 and 500 µg/ml, respectively) for 16 h. Representative images out of 3 independent experiments are shown.

4.2.4   EGb 761 abrogates *in vivo* angiogenesis

The observed anti-angiogenic properties were confirmed *in vivo* using the Chicken Chorioallantoic Membrane (CAM) Assay. Most importantly, the CAM assay, which is a widely used *in vivo* method, revealed a strong induction of angiogenesis with FGF and an inhibition of this effect by EGb 761 showing for the first time an anti-angiogenic effect of EGb 761 *in vivo* (Figure 4.18).

FGF

FGF
EGb 2.5 µg

FGF
EGb 3.75 µg
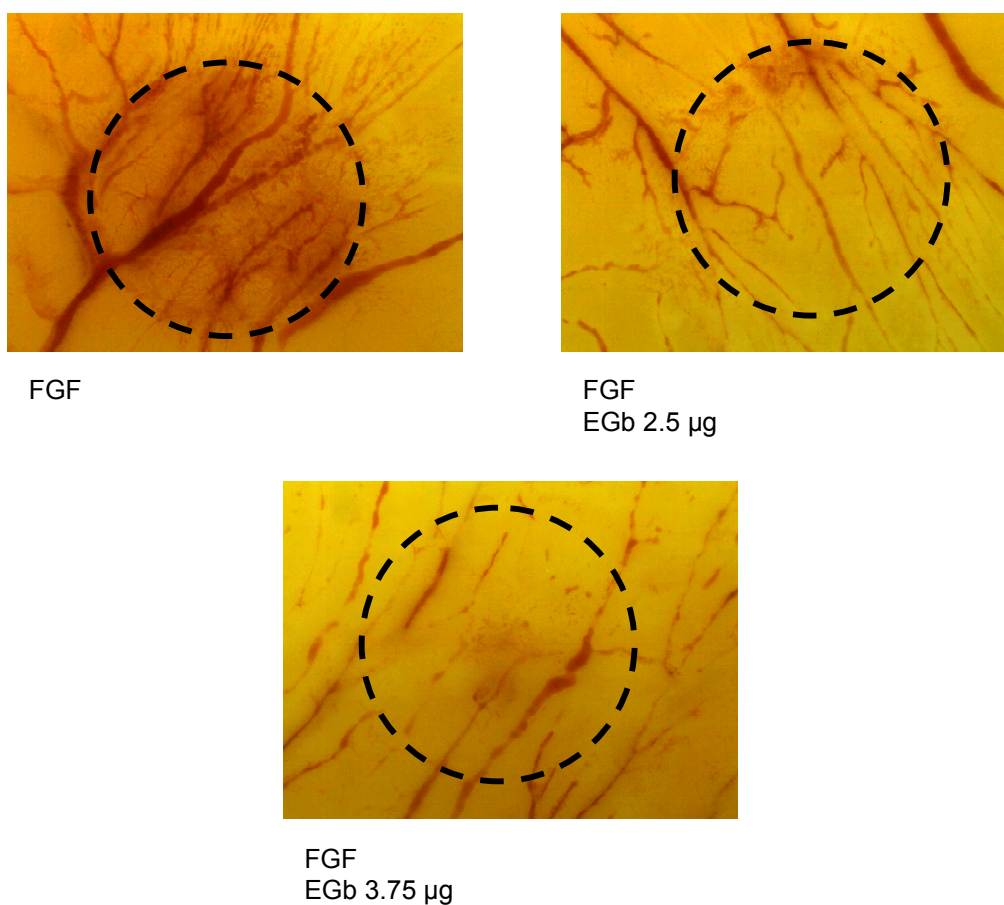
Figure 4.18   *EGb 761 exerts anti-angiogenic effects in vivo.*
Fertilized eggs were stimulated with either FGF (1 ng/disk) alone or FGF and EGb 761 for 16 h. The dotted circles indicate the position of the disk carrying the growth factor and EGb 761. One representative image of the chicken CAM out of 3 independent experiments is shown. The CAM Assay was kindly performed by Johanna Liebl (Ludwig-Maximilians-University of Munich, Department of Pharmacy – Centre of Drug Research).

4.2.5   ERK inhibition exerts anti-angiogenic effects *in vitro* and *in vivo*

Recent studies demonstrate the requirement for the extracellular signal-regulated kinase (ERK) on growth factor induced angiogenesis. In order to confirm the influence of ERK on angiogenic parameters in our setting, we investigated whether U0126, a specific MEK 1/2 inhibitor, shows an anti-angiogenic profile. Indeed, U0126 (10 µM, 72 h) inhibits endothelial cell proliferation in HMECs by 32% (Figure 4.19).
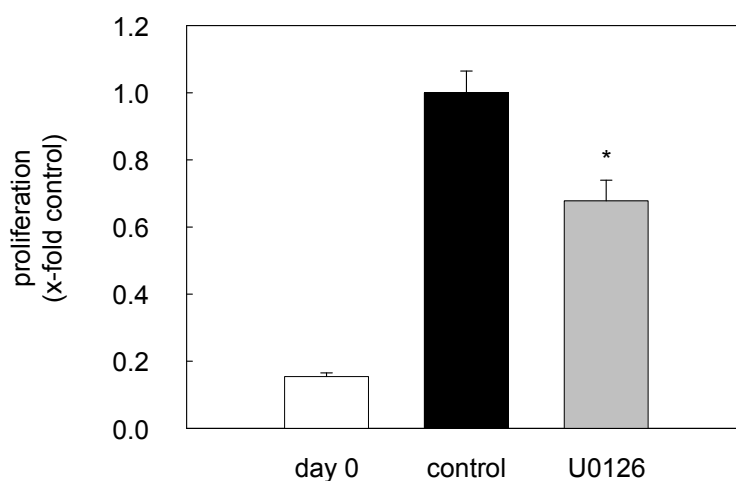
Figure 4.19   *ERK inhibition clearly diminishes endothelial cell proliferation.*
Crystal Violet Staining Assay: HMECs in a reference plate were stained after 24 h serving as baseline (day 0). HMECs in the remaining plates were either kept untreated (control) or stimulated with U0126 (10 µM) for 72 h. Data are presented as mean ± SEM of 3 independent experiments. *p≤0.05 vs. control, Kryskal-Wallis One-Way Analysis of Variance on Ranks followed by Student-Newman-Keuls post-hoc test.

Furthermore, U0126 (10 µM, 16 h) showed a reduction in both angiogenic parameters: cell migration (Figure 4.20 A and B) and tube formation (Figure 4.20 C). In detail, endothelial migration expressed as the ratio of pixels covered by cells and the total number of pixels in the wound area was diminished to 75% by U0126. Moreover, the two panels in Figure 4.20 C clearly illustrate the down-regulation of capillary tubes by U0126 compared with untreated controls.

A   Migration

control   U0126

B   Migration

C   Tube formation
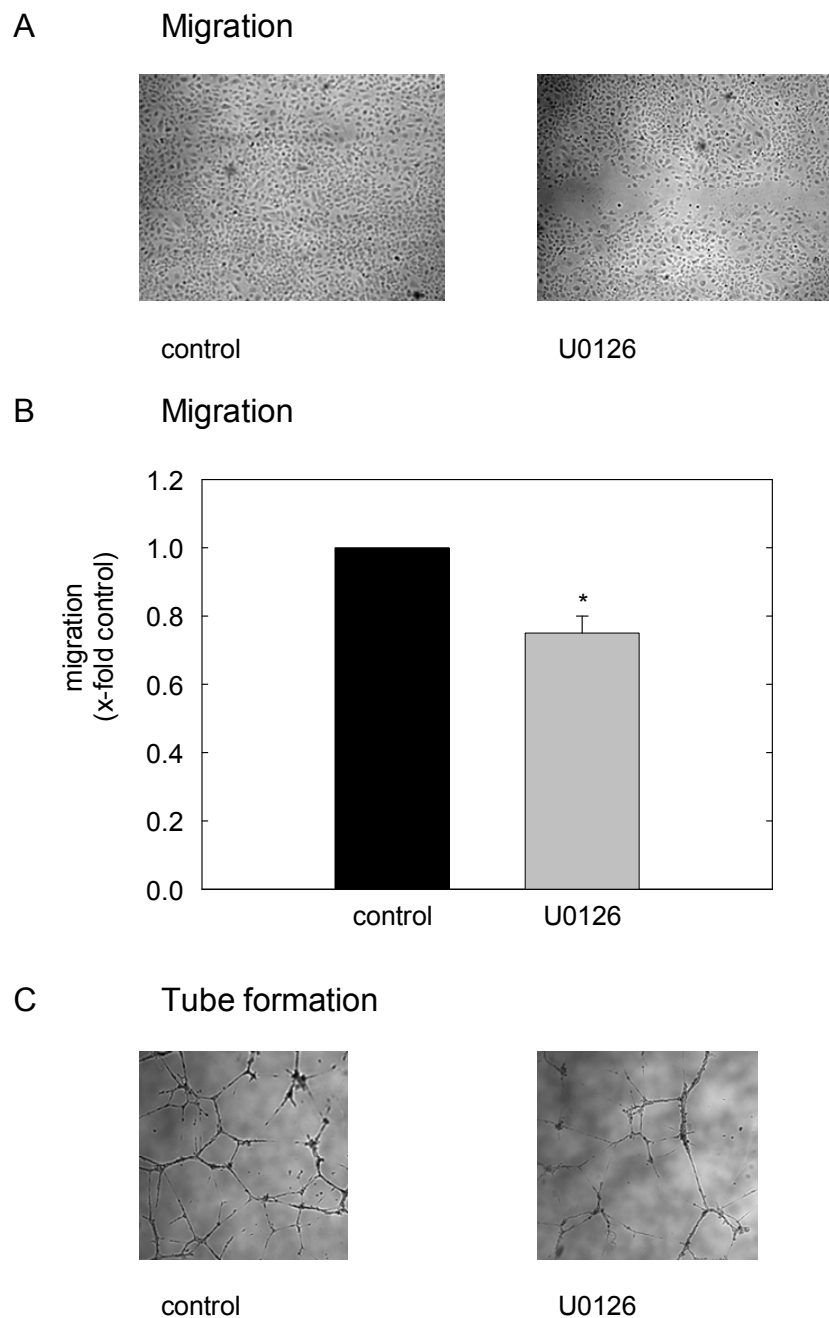
control   U0126

Figure 4.20   ERK inhibition reduces endothelial cell migration and tube formation.
                 A, Confluent HUVEC monolayers were wounded and stimulated with HUVEC growth
                 medium (control) alone or medium containing U0126 (10 μM) for 16 h. One representative
                 image out of 3 independent experiments is shown. B The graph displays the ratio of pixels
                 covered by cells and pixels in the wound area. Data are presented as mean ± SEM of 3
                 independent experiments. *p≤0.05 vs. control, Kryskal-Wallis One-Way Analysis of Variance
                 on Ranks followed by Dunn's Method. C, HMECs were seeded on Matrigel^{TM}. Subsequently,
                 cells were incubated with U0126 (10 μM, 16 h). One representative image out of 3 independent
                 experiments is shown.

In addition to these *ex vitro* experiments, the Chicken Chorioallantoic Membrane (CAM)

Assay was performed. ERK inhibition by U0126 led to a diminished number of vascular

structures in the CAM Assay (Figure 4.21). These data support the hypothesis that ERK indeed plays a crucial role in angiogenesis.

FGF

FGF
U0126 (5 mM)

FGF
U0126 (50 mM)
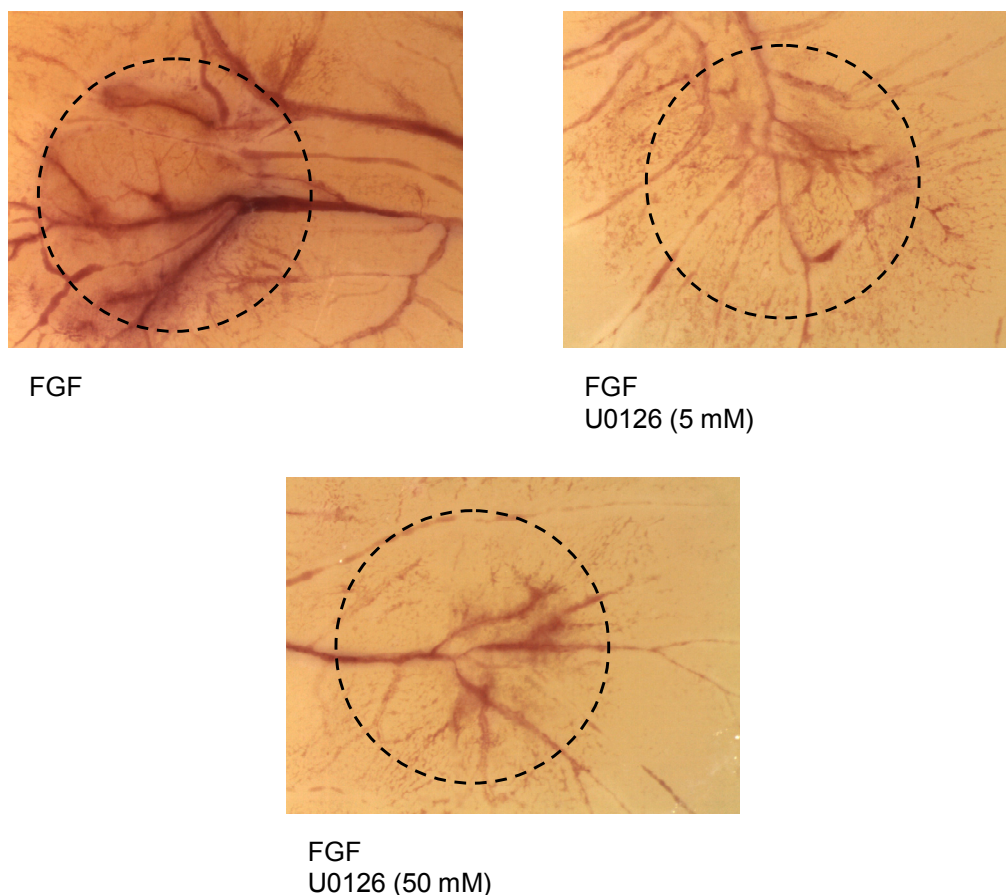
Figure 4.21   *ERK inhibition clearly diminishes the number of vascular structures in the CAM Assay.*
Fertilized eggs were stimulated with either FGF (1 ng/disk) alone or FGF and U0126 for 16 h. The dotted circles indicate the position of the disk carrying the growth factor and U0126. One representative image of the chicken CAM out of 3 independent experiments is shown. The CAM Assay was kindly performed by Johanna Liebl (Ludwig-Maximilians-University of Munich, Department of Pharmacy – Centre of Drug Research).

4.2.6   Effects of EGb 761 on ERK phosphorylation

As described in the previous section, the mitogen activated protein kinase ERK is crucially involved in the angiogenic process. In order to investigate the influence of EGb 761 on ERK phosphorylation induced by growth factors, endothelial cells were pre-treated with EGb 761 (500 µg/ml, 30 min) previous to FGF exposure (5 ng/ml, 30 min). Interestingly, EGb 761 completely abolished FGF-induced ERK phosphorylation both in HMECs and HUVECs

(Figure 4.22 A and B, respectively). Moreover, EGb 761 also suppressed VEGF-induced ERK phosphorylation (Figure 4.22 C and D, respectively).

These results clearly show that EGb 761 abrogates ERK phosphorylation induced by different growth factors leading to the suggestion that EGb 761 inhibits angiogenesis *via* ERK inhibition.
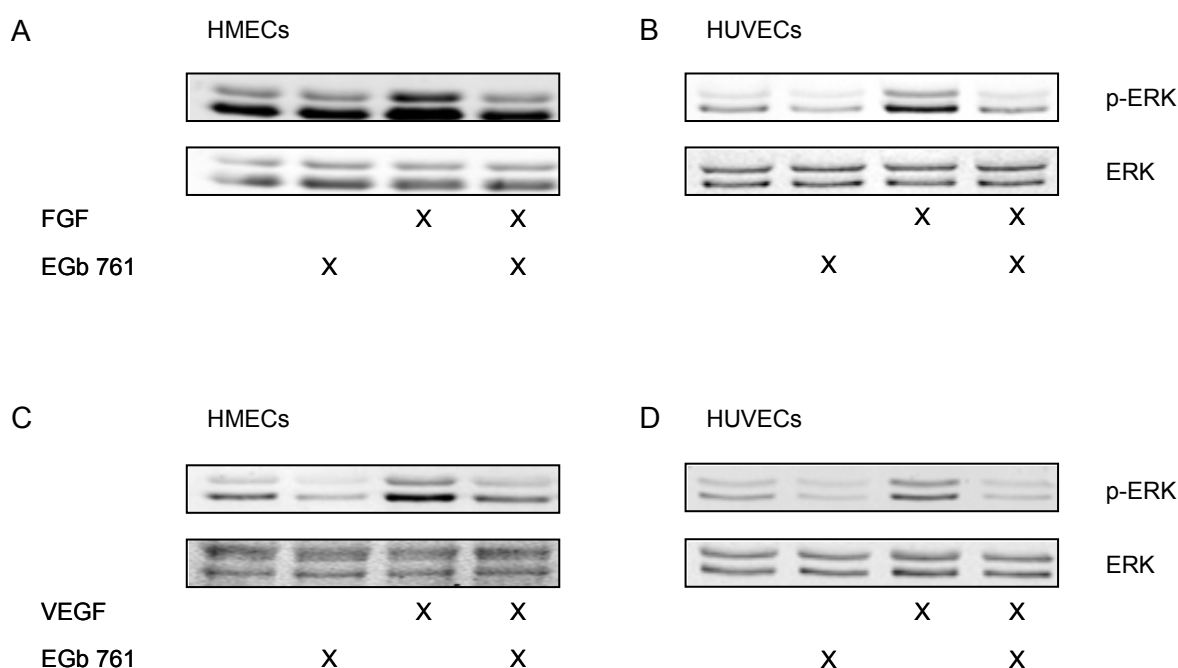
Figure 4.22   *EGb 761 abrogates growth factor-induced ERK phosphorylation in endothelial cells.*
HMECs (A) or HUVECs (B) were pre-treated with EGb 761 (500 µg/ml, 30 min) and subsequently exposed to FGF (5 ng/ml, 30 min). HMECs (C) or HUVECs (D) were pre-treated with EGb 761 (500 µg/ml, 30 min) before VEGF (50 ng/ml, 10 min) stimulation. Levels of phospho-ERK and total ERK protein were determined by Western blot analysis. One representative image out of 3 independent experiments is shown.

4.2.7   EGb 761 short-term treatment exerts anti-proliferative actions

As revealed in the previous experiment, the inhibitory effect of EGb 761 on growth factor-induced ERK phosphorylation was observed after only 1 h treatment. In order to analyze if short-time stimulation also reveals an anti-proliferative action, a Crystal Violet Staining Assay was performed. Importantly, the short-time stimulation with EGb 761 (500 µg/ml, 1 h) significantly reduced endothelial proliferation to 74% of untreated controls (Figure 4.23).

This anti-proliferative effect was weaker compared to treatment over a period of 72 h (down-regulation up to 51%). Conclusively, these findings indicate that the anti-proliferative effects of EGb 761 are in part exerted by a rapid influence of signaling molecules.
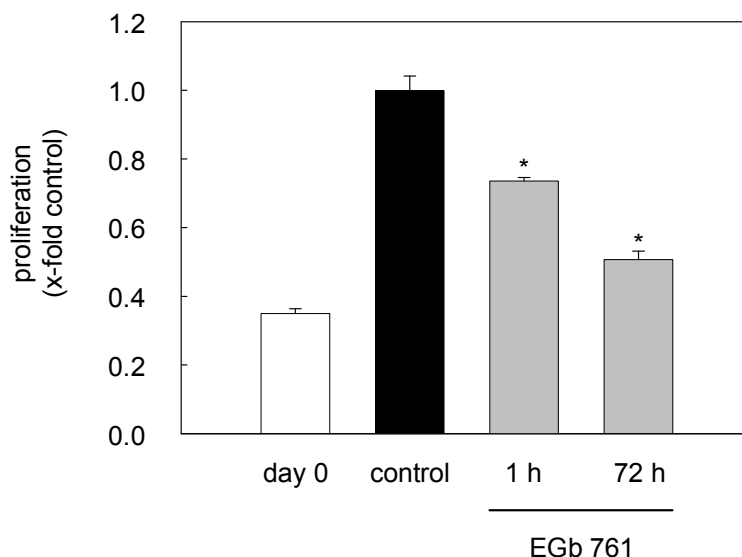
Figure 4.23   *EGb 761 rapidly inhibits endothelial cell proliferation (≤ 1 h treatment).*
Crystal Violet Staining Assay: HMECs in a reference plate were stained after 24 h serving as baseline (day 0). HMECs in the remaining plates were either kept untreated (control) or stimulated with EGb 761 (500 µg/ml) for either 1 or 72 h. Following 1 h of incubation, supernatants containing EGb 761were removed and cells were refed with HMEC growth medium. Data are presented as mean ± SEM of 3 independent experiments. *p≤0.05, Kryskal-Wallis One-Way Analysis of Variance on Ranks followed by Dunn's Method.

4.2.8   Activation of NO/PKG and PI3K/Akt signaling pathways by EGb 761 has no influence on the reduction of ERK phosphorylation

As abovementioned, we have shown that EGb 761 causes an up-regulation and activation of eNOS protein in endothelial cells, thus leading to an enhanced production of nitric oxide (NO). Furthermore, the phosphorylation of protein kinase B/Akt (Ser473) was found to be increased after EGb 761 exposure in EA.hy926 cells. Both signaling pathways, NO/PKG and Akt, were communicated to suppress ERK phosphorylation mainly *via* inhibition of Raf-1. Since EGb 761 activates both signaling molecules, the influence of these mediators on the reduction of ERK phosphorylation was examined. Neither NO synthase inhibitor L-NAME nor PI3K-inhibitor wortmannin affected the inhibitory effect of EGb 761 on ERK phosphorylation (Figure 4.24). These results exclude an involvement of either NO/PKG or PI3K/Akt pathways on the inhibitory effect on ERK phosphorylation.

A

					p-ERK
					ERK
L-NAME					X
EGb 761		X		X	X
FGF			X	X	X

B

					p-ERK
					ERK
Wortmannin					X
EGb 761		X		X	X
FGF			X	X	X
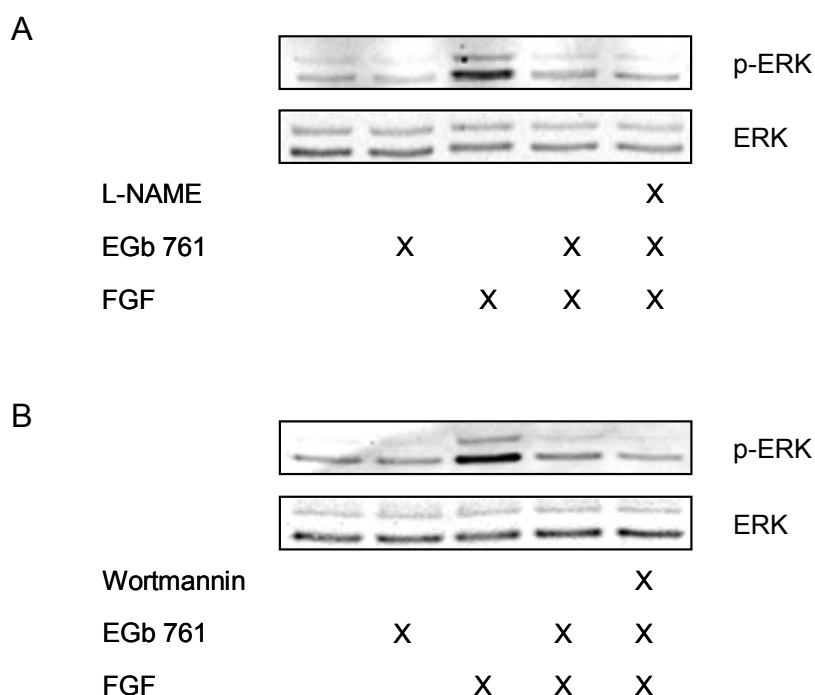
Figure 4.24   *Activation of NO/PKG and PI3K/Akt signaling pathways by EGb 761 did not influence the*
                 effects on ERK phosphorylation.
                 A, HMECs were either left untreated or treated with L-NAME (NOS inhibitor, 100 μM,
                 30 min), EGb 761 (500 μg/ml, 30 min) and FGF (5 ng/ml, 30 min) alone or pre-treated with
                 L-NAME before EGb 761 and FGF. B, Cells were pre-treated with wortmannin (PI3K
                 inhibitor, 50 nM, 30 min) and subsequently exposed to EGb 761 and FGF. Levels of phospho-
                 ERK (Thr202/Tyr204, upper panel) and total ERK (lower panel) protein were determined by
                 Western blot analysis. One representative blot out of 3 independent experiments is shown.

4.2.9   Effects of EGb 761 on cyclic adenosine monophosphate

Cyclic adenosine monophosphate (cAMP, cyclic AMP or 3'-5'-cyclic adenosine
monophosphate), derived from adenosine triphosphate (ATP), is an important second
messenger. cAMP transfers the effects of hormones like glucagon and adrenaline and has an
impact on intracellular signal transduction. Moreover, cAMP is considered to be a potential
regulator of ERK inhibition. Since cAMP activates protein kinase A (PKA), which has also
been shown to inhibit the Raf-MEK-ERK pathway, we examined whether EGb 761 increases
cAMP levels. Indeed, 30 min of EGb 761 treatment increased intracellular levels of cAMP to
approximately 1.6-fold (Figure 4.25).
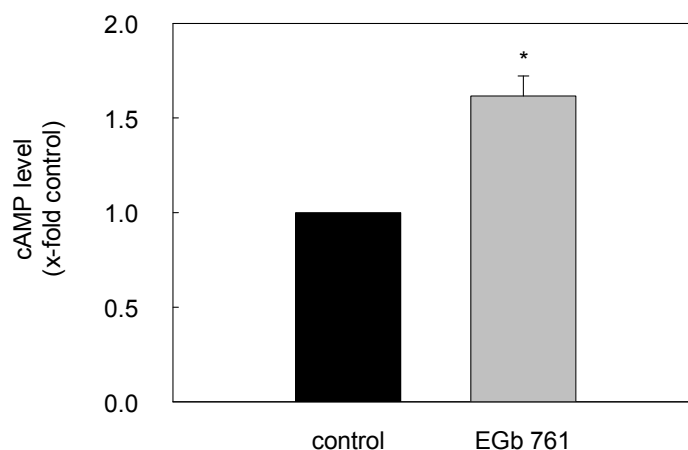
Figure 4.25   *EGb 761 up-regulates adenylat cyclase activity.*
Adenylate cyclase activity was determined by cAMP radioimmunoassay and measured either in absence of any stimulatory agent (control) or in the presence of EGb 761 (500 µg/ml, 30 min). Data are presented as mean ± SEM of 3 independent experiments. *$p \leq 0.05$ vs. control, Kryskal-Wallis One-Way Analysis of Variance on Ranks followed by Student-Newman-Keuls post-hoc test. The second part of this experiment is an enzyme-linked immunosorbant assay (ELISA) which was kindly performed by Dr. Hermann Ammer (Professor of Clinical Pharmacology, Department of Veterinary Sciences, University of Munich).

In order to verify if these increased cAMP levels are able to influence ERK phosphorylation, forskolin as well as 3-isobutyl-1-methylxanthine (IBMX) were used. Forskolin is commonly used to raise levels of cAMP in cell physiology assays by resensitizing cell receptors and activating the enzyme adenylate cyclase. IMBX is a potent cyclic nucleotide phosphodiesterase inhibitor. Due to this action, the compound increases cAMP levels thereby activating cAMP-dependent protein kinase A (PKA). Interestingly, enhanced cAMP levels caused either by forskolin alone or in combination with IBMX reduced FGF-induced ERK phosphorylation in HMECs (Figure 4.26).
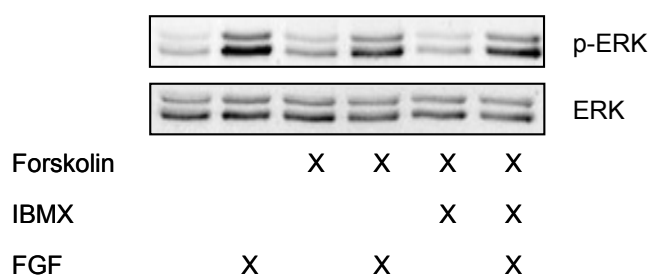
Figure 4.26   *Influence of increased cAMP level on ERK phosphorylation.*
HMECs were pre-treated with either forskolin alone (10 µM, 30 min) or a combination of forskolin and IBMX (10 µM, 30 min). Afterwards, cells were stimulated with FGF (5 ng/ml, 30 min). ERK phosphorylation was investigated by Western blot analysis. One representative blot out of two independent experiments is shown.

To clarify whether the elevated cAMP levels influence the effect of EGb 761 on ERK phosphorylation, cells were pre-treated with two specific inhibitors of PKA, cAMPS-Rp (100 µM, 30 min) and PKI (50 µM, 30 min) (Figure 4.27).

Importantly, the inhibitory effect of EGb 761 on ERK phosphorylation was not influenced by cAMP, since inhibition of PKA did not reverse the effect of EGb 761. In summary, these results clearly demonstrate that the signaling pathway of cAMP/PKA is not involved in the inhibitory effects of EGb 761 on ERK phosphorylation.
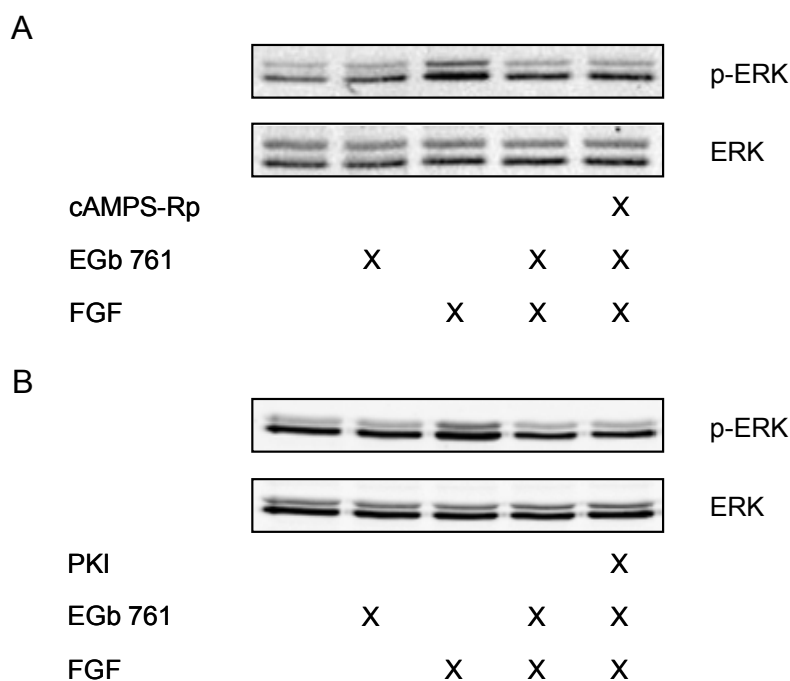
Figure 4.27   *PKA inhibitors do not reverse the decreased ERK phosphorylation by EGb 761.*
          A, HMECs were either left untreated or treated with cAMPS-Rp (PKA inhibitor, 100 µM, 30 min), EGb 761 (500 µg/ml, 30 min) and FGF (5 ng/ml, 30 min) alone or pre-treated with cAMPS-Rp before EGb 761 and FGF. B, endothelial cells were pre-treated with PKI (PKA inhibitor, 50 µM, 30 min) and subsequently exposed to EGb 761 and FGF. Levels of phospho-ERK (Thr202/Tyr204, upper panel) and total ERK (lower panel) protein were determined by Western blot analysis. One representative blot out of two independent experiments is shown.

4.2.10   Serine/threonine phosphatase inhibition does not affect the inhibitory effect of EGb 761 on ERK phosphorylation

Protein phosphorylation is regulated by a balance between kinases and phosphatases. The latter can be subdivided based upon their substrate specificity into two groups: the serine/threonine and tyrosine phosphatases, respectively. In order to investigate an activation of phosphatases by EGb 761, phosphatase inhibitors were used. Pre-treatment of HMECs with

NaF (serine/threonine phosphatase inhibitor) did not reverse the inhibitory effect of EGb 761 on ERK phosphorylation (Figure 4.28).

NaF				X
EGb 761	X		X	X
FGF		X	X	X
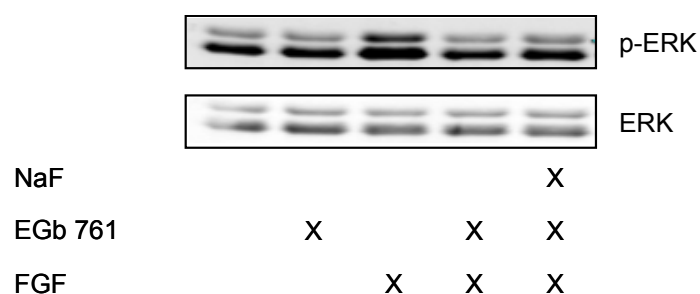
Figure 4.28   *Influence of the serine/threonine phosphatase inhibitor NaF on the diminished ERK phosphorylation by EGb 761.*
HMECs were pre-treated with NaF (1 mM, 30 min). Afterwards, cells were treated with EGb 761 (500 μg/ml, 30 min) and FGF (5 ng/ml, 30 min). Levels of phospho-ERK (Thr202/Tyr204, upper panel) and total ERK (lower panel) protein were determined. One representative blot out of 3 independent experiments is shown.

In order to verify the lack of effects on serine/threonine phosphatases, a phosphatase assay for PP2A, PP2B, and PP2C activities, was performed. Indeed, EGb 761 does not induce, but instead clearly inhibits PP2A (Figure 4.29), PP2B, and PP2C activity (Figure 4.30).

EGb 761	X		X	
FGF		X	X	
NaF				X
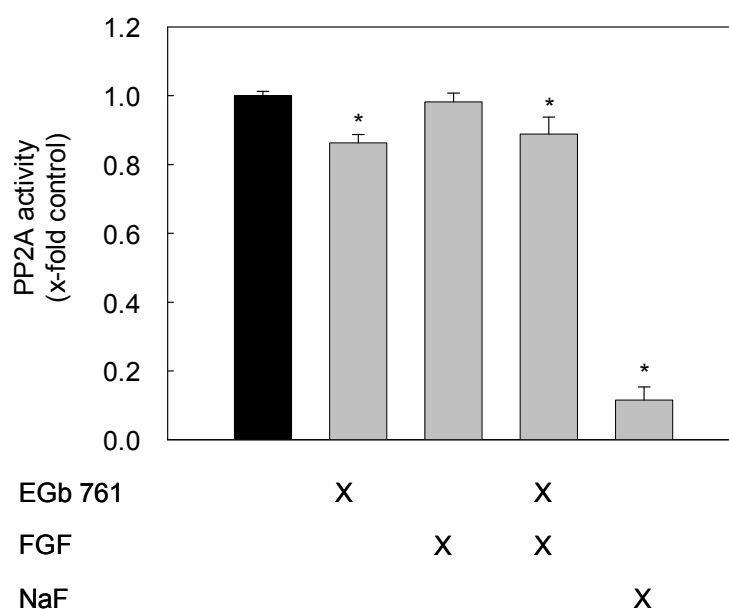
Figure 4.29   *EGb 761 diminishes the activity of PP2A.*
HMECs were either left untreated or treated with NaF (1 mM, 30 min), EGb 761 (500 μg/ml, 30 min) and FGF (5 ng/ml, 30 min) alone or pre-treated with NaF before EGb 761 and FGF. Data are presented as mean ± SEM of 3 independent experiments. *$p \leq 0.05$ vs. control, Kryskal-Wallis One-Way Analysis of Variance on Ranks followed by Student-Newman-Keuls post-hoc test.

A

B
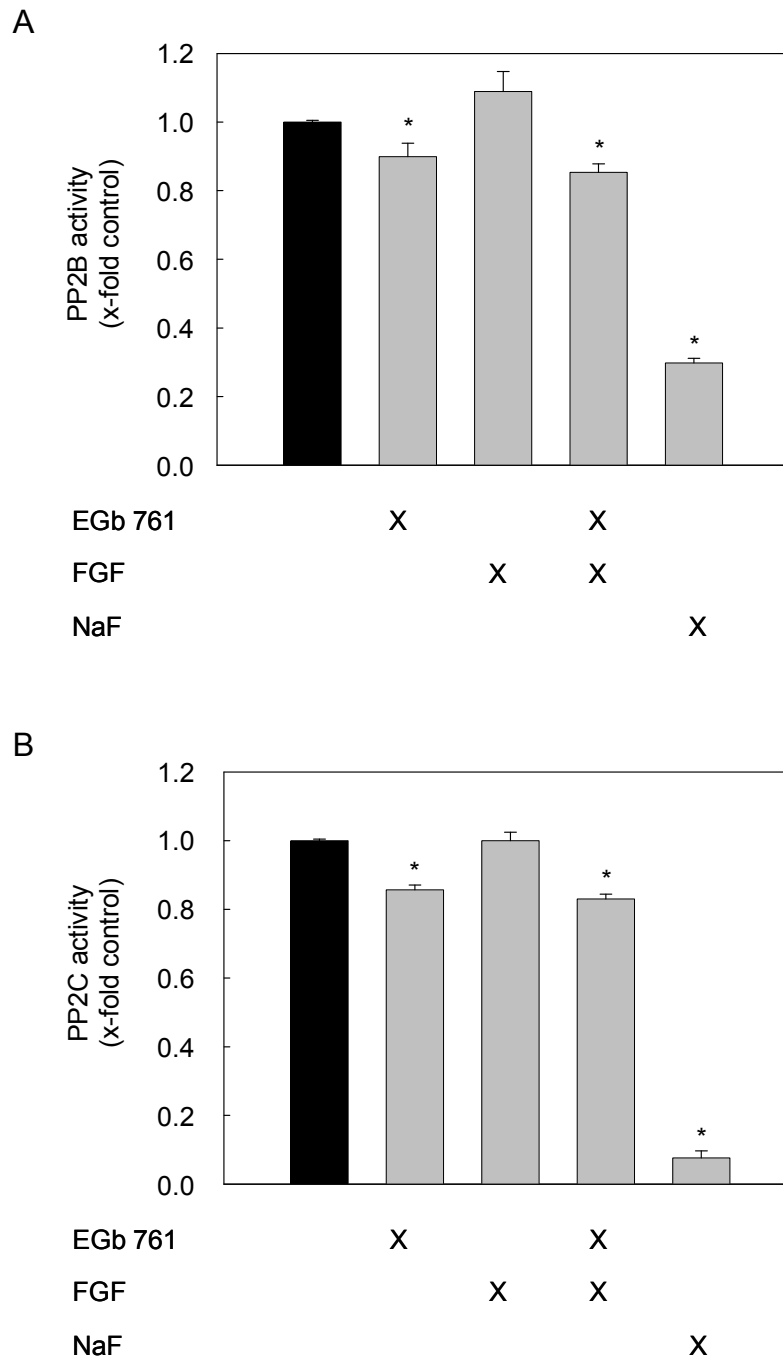
Figure 4.30   *EGb 761 diminishes the activity of PP2B (A) and PP2C (B).*
HMECs were either left untreated or treated with NaF (1 mM, 30 min), EGb 761 (500 µg/ml, 30 min) and FGF (5 ng/ml, 30 min) alone or pre-treated with NaF before EGb 761 and FGF. PP2B and PP2C activity was assessed. Data are presented as mean ± SEM of 3 independent experiments. *p≤0.05 vs. control, Kryskal-Wallis One-Way Analysis of Variance on Ranks followed by Student-Newman-Keuls post-hoc test.

4.2.11 EGb 761 blocks the Raf-MEK-ERK-pathway *via* activation of tyrosine phosphatases

Stimulation with Na_3VO_4 (tyrosine phosphatase inhibitor) previous to EGb 761 and FGF exposure blocked the effect of *Ginkgo biloba* extract on ERK inhibition (Figure 4.31). Conclusively, EGb 761 abolished growth factor-induced ERK phosphorylation in endothelial cells *via* induction of tyrosine phosphatase activity.

A

					p-ERK
					ERK
Na_3VO_4				X	
EGb 761	X		X	X	
FGF		X	X	X	

B

					p-ERK
					ERK
Na_3VO_4				X	
EGb 761	X		X	X	
VEGF		X	X	X	
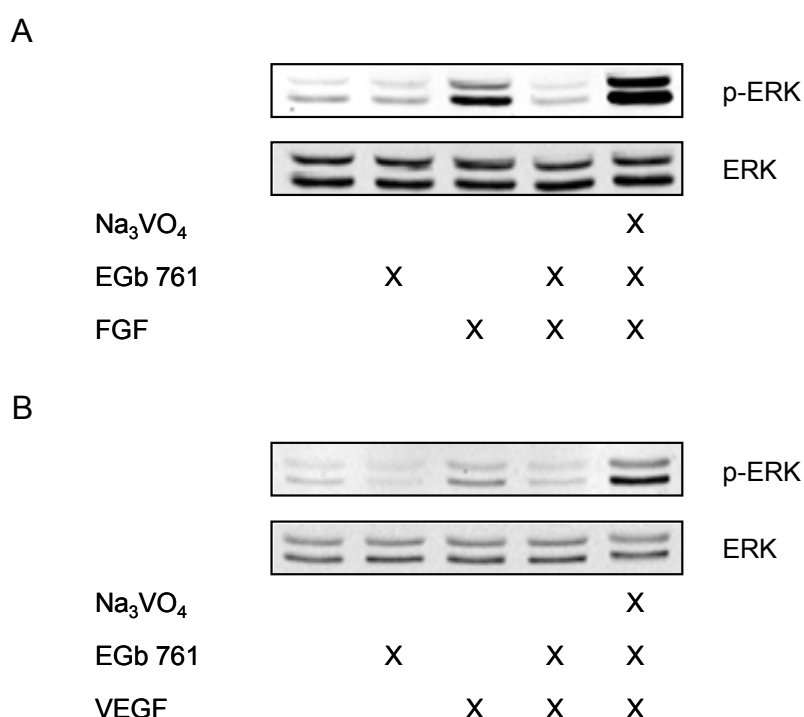
Figure 4.31 *Pre-treatment with sodium vanadate blocks the inhibitory effect of EGb 761 on ERK phosphorylation.*
A, HMECs were pre-treated with Na_3VO_4 (tyrosine phosphatase inhibitor, 100 µM, 30 min). Subsequently, cells were exposed to EGb 761 (500 µg/ml, 30 min) and FGF (5 ng/ml, 30 min). B, HMECs were pre-treated with Na_3VO_4 before EGb 761 and VEGF (50 ng/ml, 10 min). Levels of phospho-ERK (Thr202/Tyr204, upper panel) and total ERK (lower panel) protein were determined. One representative blot out of 3 (A) and 2 (B) independent experiments is shown.

Before we have seen that tyrosine phosphorylation plays a key role in cellular signaling of *Ginkgo biloba* extract. Therefore, overall tyrosine phosphorylation was assessed performing Western blot analysis. EGb 761 diminished tyrosine phosphorylation in comparison to untreated controls and FGF-stimulated HMECs (Figure 4.32).

FGF			X	X
EGb 761		X		X
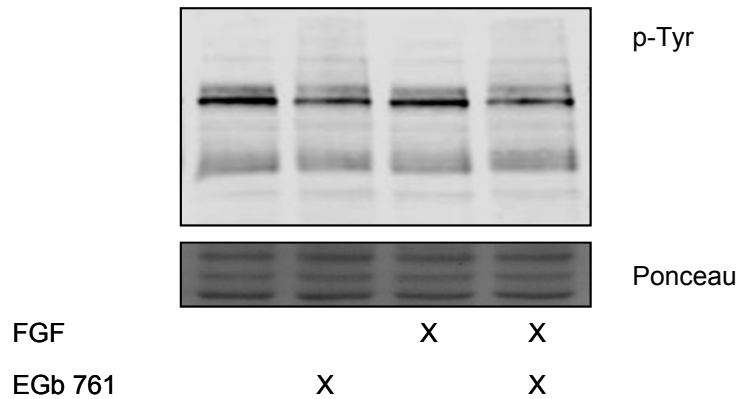
Figure 4.32   *EGb 761 diminishes total tyrosine phosphorylation.*
HMECs were either left untreated or were treated with FGF (5 ng/ml, 30 min) with or without pre-treatment with EGb 761 (500 µg/ml, 30 min). Tyrosine phosphorylation was assessed by Western blot analysis. Equal protein loading was controlled by staining the membrane with Ponceau (a representative fragment of the stained membrane is shown). One representative Western blot out of 3 independent experiments is displayed.

In order to get information on targets of phosphatases in ERK signaling, we examined the activation of upstream kinases MEK 1/2 and Raf-1 using Western blot analysis and kinase assay, respectively. EGb 761 completely abolished FGF-induced MEK 1/2 phosphorylation at Ser217/221 in HUVECs. Moreover, the effect of EGb 761 on MEK 1/2 phosphorylation was reversed by pre-incubation with the phosphatase inhibitor sodium vanadate (Figure 4.33).

Na$_3$VO$_4$				X
EGb 761	X		X	X
FGF		X	X	X
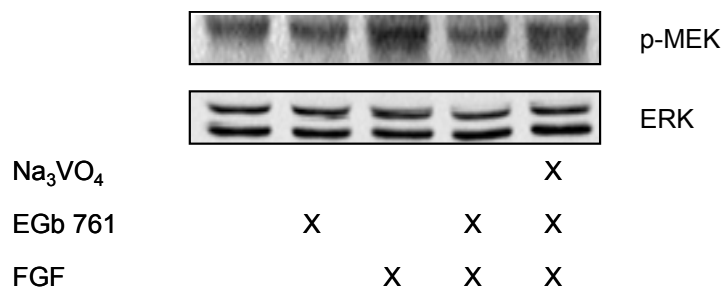
Figure 4.33   *Pre-treatment with sodium vanadate reversed the inhibitory effect of EGb 761 on MEK 1/2 phosphorylation.*
HUVECs were pre-incubated with Na$_3$VO$_4$ (100 µM, 30 min) and afterwards stimulated with EGb 761 (500 µg/ml) and FGF (5 ng/ml, 30 min). Levels of phospho-MEK 1/2 (Ser217/221, upper panel) protein were determined by Western blot analysis. The bottom panel depicts total ERK protein levels as control for equal protein loading.

Furthermore, we observed a reduction of FGF-induced Raf-1 activity as well as a reduction of Raf-1 phosphorylation at Ser338/Tyr341 by EGb 761. Pre-treatment with sodium vanadate blocked the inhibitory effect on Raf-1 activation as well as phosphorylation (Figure 4.34). These data clearly indicate that *Ginkgo biloba* extract inhibits growth factor signaling upstream of the classical Raf-MEK-ERK pathway.

					p-Raf (high intensity)
					p-Raf (low intensity)
					Raf-1 activity (p-MEK)
					ERK
Na$_3$VO$_4$				X	
EGb 761		X		X	X
FGF			X	X	X
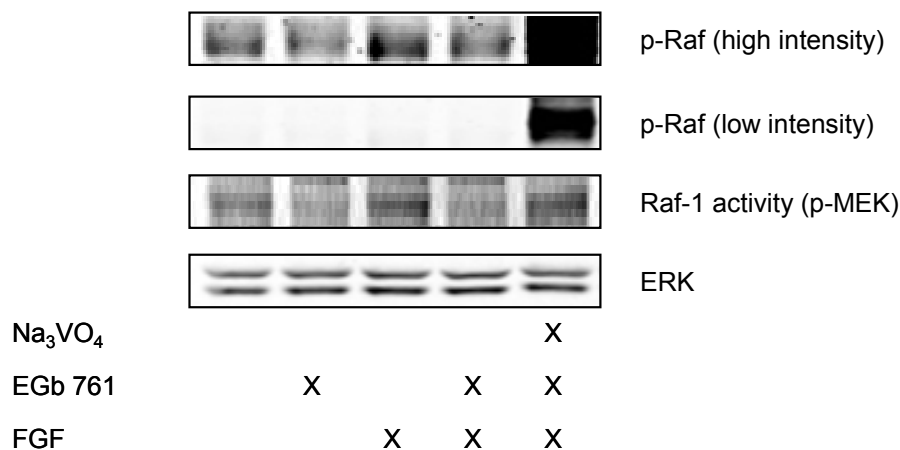
Figure 4.34   *The inhibitory effects of EGb 761 on Raf-1 phosphorylation as well as Raf-1 activity were reversed by pre-incubation with the tyrosine phosphatase inhibitor sodium vanadate.*
HUVECs were pre-incubated with Na$_3$VO$_4$ (100 µM, 30 min) and afterwards stimulated with EGb 761 (500 µg/ml) and FGF (5 ng/ml, 30 min). Representative Western blots are shown for phospho-Raf-1 (Ser338/Tyr341) at both high and low intensity. Additionally, Raf kinase activity (assessed as phospho-MEK 1/2 using Western blot analysis) was determined. Total ERK protein levels served as loading control.

4.2.12   EGb 761 does not influence PMA-induced ERK phosphorylation

In order to confirm an involvement of protein tyrosine phosphatases linked to VEGF and FGF receptors, cells were treated with EGb 761 and phorbol ester phorbol-12 myristate-13 acetate (PMA). PMA leads to growth factor independent activation of the MAPK signaling cascade Raf-MEK-ERK. As expected, EGb 761 did not suppress PMA-induced ERK phosphorylation (Figure 4.35). These results indicate that EGb 761 terminates ERK phosphorylation by activation of one or more tyrosine phosphatases connected with GF receptors, but not by influencing the receptor activities themselves.

				p-ERK
				ERK
PMA			X	X
EGb 761		X		X
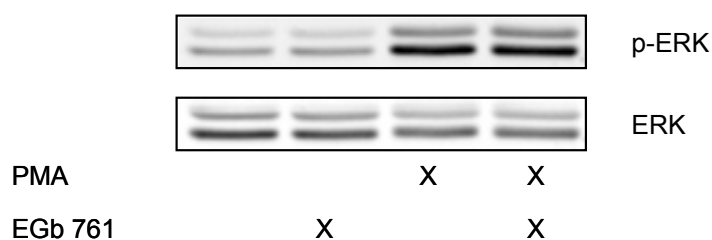
Figure 4.35   *PMA-induced ERK phosphorylation was not diminished by EGb 761.*
HMECs were pre-treated with EGb 761 (500 µg/ml, 30 min) and subsequently exposed to PMA (50 nM, 10 min). Protein levels of phospho-ERK (Thr202/Tyr204, upper panel) and total ERK (lower panel) were determined. All experiments were carried out 3 times with consistent results.

4.2.13   The anti-angiogenic effect of EGb 761 depends on the activation of protein tyrosine phosphatases

To causally link the activation of tyrosine phosphatases to the anti-angiogenic effects of EGb 761, endothelial cell migration was analyzed in the presence of the inhibitor of protein tyrosine phosphatases (PTPs) sodium vanadate (Na_3VO_4).

Endothelial cells were pre-treated with Na_3VO_4 (10 µM, 30 min) before exposure to EGb 761 (100 and 500 µg/ml, respectively) for 16 h. Pre-treatment of endothelial cells with Na_3VO_4 reversed the inhibitory effects of EGb 761 on endothelial cell migration. Figure 4.36 displays representative images, whereas Figure 4.37 shows the quantification of the experiment. In summary, these data provide further evidence that EGb 761 exerts its anti-angiogenic effects *via* an activation of tyrosine phosphatases.

| control | EGb 761 (100 µg/ml) | Na_3VO_4 EGb 761 (100 µg/ml) |

| Na_3VO_4 | EGb 761 (500 µg/ml) | Na_3VO_4 EGb 761 (500 µg/ml) |
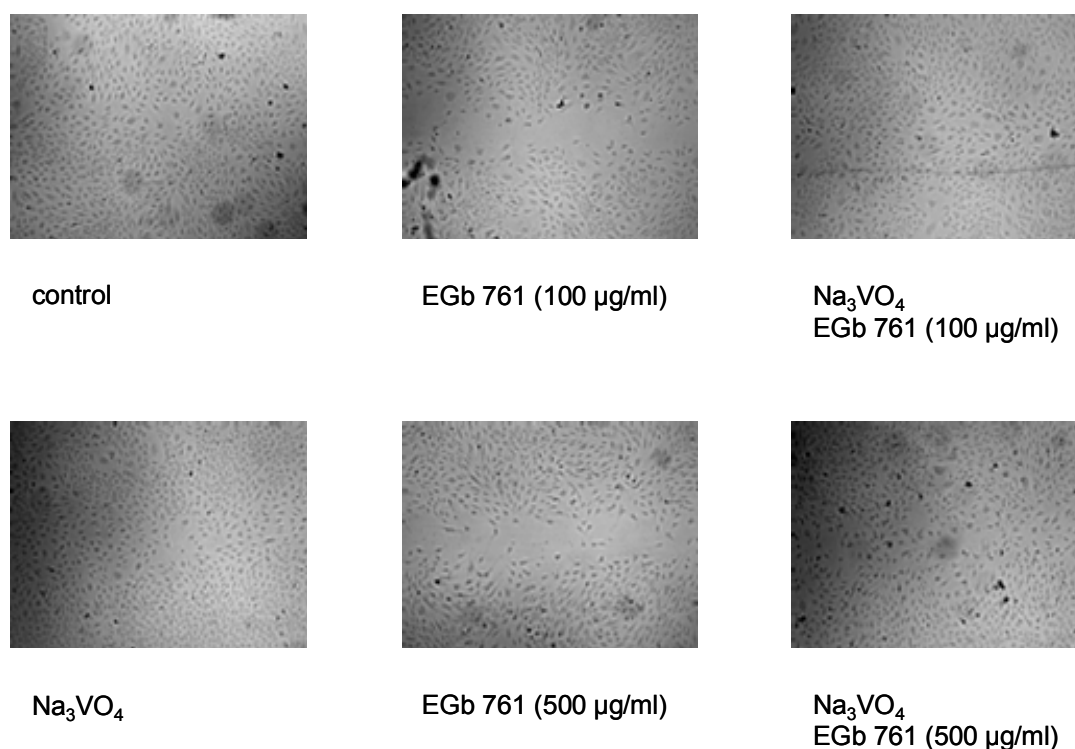
Figure 4.36   *EGb 761 diminishes HUVEC migration by induction of tyrosine phosphatases.*
The wounded monolayers were refed either with EGb 761 (100 and 500 µg/ml, respectively) or Na_3VO_4 (10 µM) alone for 16 h, or were pre-treated with Na_3VO_4 (10 µM, 30 min) before stimulation with EGb 761 for further 16 h. Representative images out of 3 independent experiments are shown.
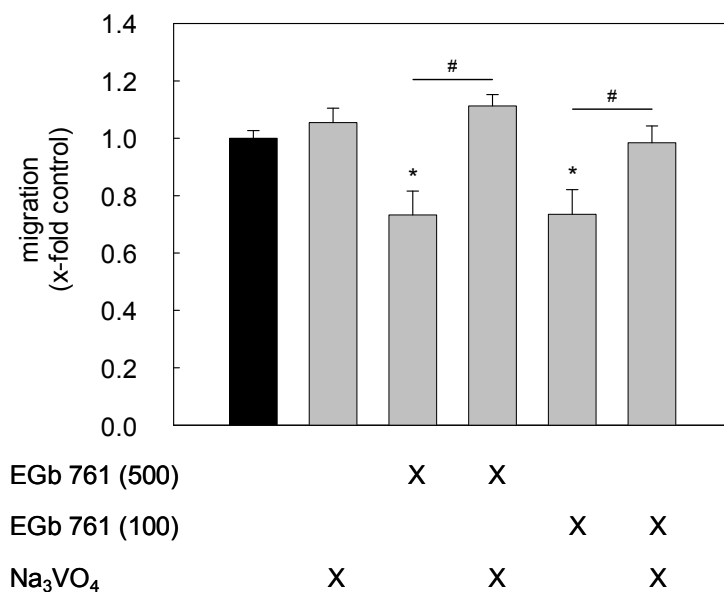
Figure 4.37   *EGb 761 diminishes HUVEC migration by induction of tyrosine phosphatases.*
The wounded monolayers were refed either with EGb 761 (100 and 500 µg/ml, respectively) or
Na$_3$VO$_4$ (10 µM) alone for 16 h, or were pre-treated with Na$_3$VO$_4$ (10 µM, 30 min) before
stimulation with EGb 761 for further 16 h. Values are expressed as mean ± SEM. *p≤0.05 vs.
control, #p≤0.05 vs. EGb 761 (100 and 500 µg/ml, respectively), Kryskal-Wallis One-Way
Analysis of Variance on Ranks followed by Student-Newman-Keuls post-hoc test.

Moreover, the same stimulation scheme was used to analyze the effects of phosphatase
inhibition per se on Raf-1 and ERK phosphorylation. Pre-incubation with sodium vanadate
before exposure to EGb 761 (500 µg/ml, 30 min) revealed a strong increase of both Raf-1 and
ERK phosphorylation (Figure 4.38).
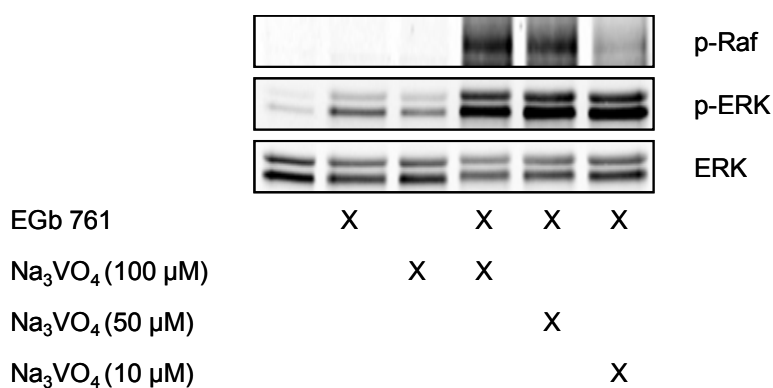
Figure 4.38   *Pre-treatment with sodium vanadate before exposure to EGb 761 increases the*
phosphorylation of ERK, Akt and Raf-1.
HUVECs were pre-treated with different concentrations of Na$_3$VO$_4$ (30 min). Subsequently,
cells were exposed to EGb 761 (500 µg/ml, 30 min). Levels of phospho-ERK
(Thr202/Tyr204), phospho-Akt (Ser473) and phospho-Raf (Ser338/Tyr341) protein were
determined. Total Akt and ERK protein levels served as loading control. One representative
blot out of 3 independent experiments is shown.

4.2.14   Effects of EGb 761 on the phosphatase MKP-1

Since PTPs were identified as the crucial regulators of the anti-angiogenic action as well as the reduced ERK phosphorylation of EGb 761, we were interested which specific phosphatase leads to these inhibitory effects. MKP-1 is a dual specificity MAPK phosphatase, which inactivates ERK by dephosphorylation of the two critical MAPK residues (Thr202/Tyr204) accountable for its activation. MKP-1 mRNA levels, analyzed by Real-time RT-PCR, were up-regulated by EGb 761 (500 µg/ml). Interestingly, MKP-1 protein expression, the main regulatory parameter for MKP-1 activity, was not affected by EGb 761 (Figure 4.39). Hence, MKP-1 is not responsible for the inhibitory effect of EGb 761 on ERK phosphorylation. These findings were attributed by the results that growth factor-induced activation of MEK 1/2 and even Raf-1 were suppressed by *Ginkgo biloba* extract (Figure 4.34).
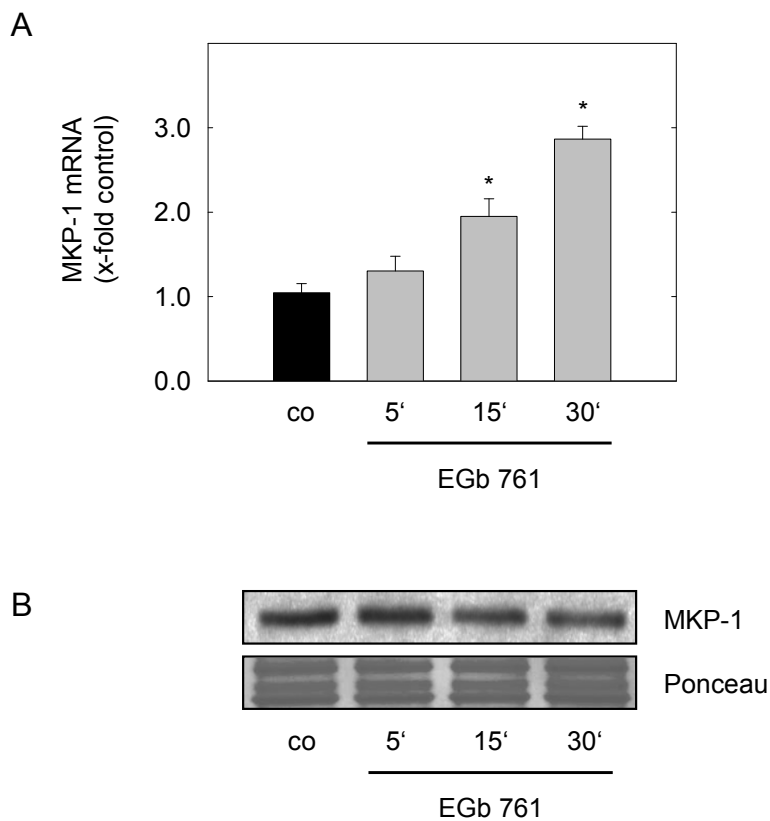
Figure 4.39   *Effects of EGb 761 on MKP-1.*
A, HMECs were either left untreated (co) or were treated with EGb 761 (500 µg/ml) for indicated times. Bars represent mean ± SEM of 3 independent experiments. *$p \leq 0.05$ vs. control, Kryskal-Wallis One-Way Analysis of Variance on Ranks followed by Student-Newman-Keuls post-hoc test. B, HUVECs were either left untreated or were stimulated with EGb 761 (500 µg/ml) for indicated times. Levels of MKP-1 protein (upper panel) were determined. The lower panel depicts the staining with Ponceau as control for equal protein loading. One representative image out of 3 independent experiments is shown.

4.2.15   EGb 761 inhibits endothelial proliferation *via* activation of SHP-1

Another important protein tyrosine phosphatase in FGF and VEGF signaling is the cytoplasmic SHP-1. This phosphatase has been shown to interact with FGF and VEGF receptors and plays a negative regulatory role in the ERK phosphorylation. To analyze a potential involvement of SHP-1 in the inhibitory effects of EGb 761 on ERK phosphorylation, we examined whether *Ginkgo biloba* extract influences SHP-1 activity. Indeed, SHP-1 activity was clearly induced by EGb 761 (500 µg/ml, 30 min) to approximately 1.5-fold (Figure 4.40).
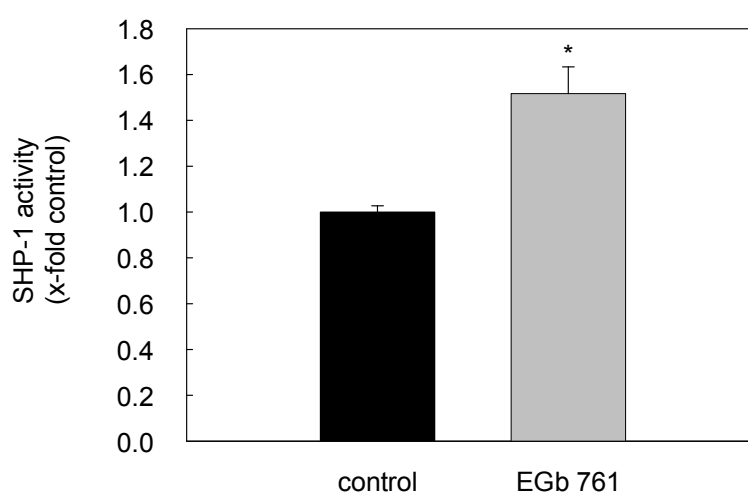
Figure 4.40   *Induction of SHP-1 activity by EGb 761 may lead to the inhibitory effect on endothelial cell proliferation.*
A, HUVECs were either left untreated (control) or were treated with EGb 761 (500 µg/ml) for 30 min. SHP-1 phosphatase activity was determined as described in Material and Methods using pNPP as phosphatase substrate. Bars represent the mean ± SEM of 3 independent experiments. *$p \leq 0.05$ vs. control, Kryskal-Wallis One-Way Analysis of Variance on Ranks followed by Student-Newman-Keuls post-hoc test.

siRNA experiments were performed to verify whether SHP-1 leads to the reduced endothelial proliferation by EGb 761. Indeed, the enhanced growth inhibition in HUVECs transfected with siCONTROL non-targeting siRNA by EGb 761 was clearly, but not completely blocked in cells lacking SHP-1 (Figure 4.41). In detail, we assessed a growth inhibition of 22% in HUVECs transfected with siCONTROL non-targeting siRNA by EGb 761. In contrast, growth inhibition was diminished to 12% in cells lacking the PTP SHP-1. Furthermore, Figure 4.41 shows the success in silencing SHP-1 by siRNA after 24 and 96 h, respectively.
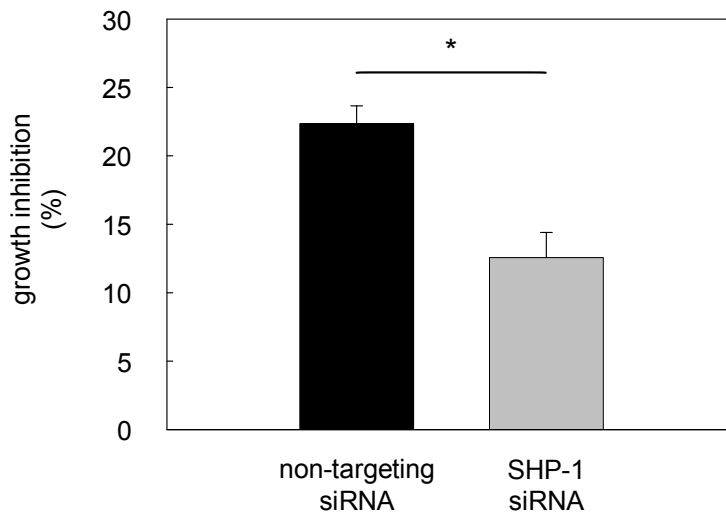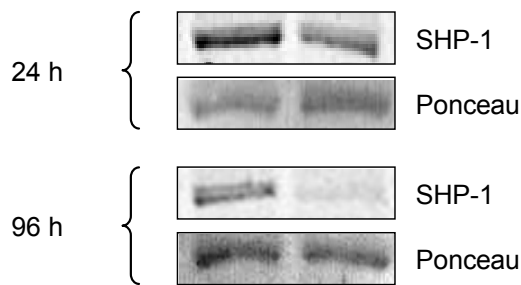
Figure 4.41   *SHP-1 is involved in the reduced proliferation by EGb 761.*
A, HUVECs were transfected with SHP-1 and siCONTROL siRNA. After 24 h Crystal Violet Staining Assaywas performed. HUVECs in a reference plate were stained after 24 h serving as baseline (day 0). HUVECs in the remaining plates were either kept untreated (control) or stimulated with EGb 761 (500 µg/ml, 72 h). Data are presented as mean ± SEM of 3 independent experiments. *p≤0.05 vs. control, Kryskal-Wallis One-Way Analysis of Variance on Ranks followed by Dunn's Method, #p≤0.001 EGb 761 (500 µg/ml) SHP-1 transfected cells vs. non-targeting transfected cells, Student's t-test. B, Transfection control: SHP-1 protein levels in cell lysates from SHP-1 and siCONTROL siRNA were assessed. Equal protein loading was controlled by staining membranes with Ponceau. One representative image out of 3 independent experiments is shown.

Summarizing, our data suggest that SHP-1 activation partly explains the inhibitory effect of EGb 761 on endothelial proliferation and is crucially involved in anti-angiogenic action of *Ginkgo biloba* extract. Thus, we clearly demonstrate that SHP-1 is one but perhaps not the only tyrosine phosphatase that is affected by EGb 761.

5 DISCUSSION

5.1   Endothelial nitric oxide production

5.1.1   EGb 761 and cardiovascular diseases

In recent years, the interest in traditional herbal remedies has grown rapidly in the industrialized world. Moreover, herbal remedies are increasingly recognized as a safe and effective alternative to modern synthetic drugs. *Ginkgo biloba* extract is at the forefront of herbal remedies and has gained great popularity in European countries and the USA over the last decades.[133] The epidemiological and economical importance of this medicinal herb is further supported by the fact that it has maintained a top selling position since 1995 in the USA,[134, 135] a market with sales of herbal medicines of $4 billion per year at that time, and with an annual growth rate of about 25%.[136] The indication for the use of *Ginkgo* extract, which is best documented by clinical trials, is dementia resulting from various origins.[137] In addition, a second field of application for *Ginkgo biloba* is represented by diseases that are connected to dysregulation of vascular tone and endothelial dysfunction, such as Fontaine's Stage II intermittent claudication (peripheral arterial occlusive disease, pAOD),[22, 132, 138] Raynaud's disease,[139] or tinnitus.[23] Furthermore, recent publications revealed an atherosclerosis inhibiting effect of EGb 761 in cardiovascular high-risk patients [140, 141] as well as an improvement of coronary blood flow in patients with coronary artery disease.[142]

Despite its growing popularity and the increasing number of studies supporting the beneficial role of *Ginkgo biloba* extract in the treatment of cardiovascular diseases,[21, 23, 139-142] its clinical use is still underrepresented due to the lack of knowledge about its cellular and molecular mechanisms of action.[143] One potential mode of action of *Ginkgo biloba* extract causing improved vascular perfusion is described by a beneficial effect on pathologically altered hemorheology due to PAF antagonism.[144] However, decrease of blood pressure and increase of perfusion after treatment with *Ginkgo biloba* extracts have also been shown in healthy humans with presumably normal hemorheological status.[145, 146] Taken together, these facts hint towards a second hypothesis that has repeatedly been proposed by the scientific community: the modulation of nitric oxide (NO) generation by *Ginkgo biloba* extracts.

5.1.2   Long-term influence of EGb 761 on transcriptional regulation of eNOS

In principle, there are two ways to increase NO production: induction of endothelial nitric oxide synthase (eNOS) expression and post-translational activation of eNOS.[43, 44, 50] The

former is a more sustained process that would afford protracted elevation of NO levels, while the latter would lead to more acute effects. The latter includes changes in eNOS translocation, phosphorylation, and protein-protein-interactions. Several compounds of biogenic origin can only act *via* one of these ways, while others affect both.[147-149] The present study shows that EGb 761 can enhance production of NO by both aforementioned ways *in vitro* as well as *in vivo* at concentrations (100 µg/ml) that are likely to be achieved in blood through the regular daily intake of 120 to 240 mg, representing normal dosage for effective therapy.[150]

Using both the Luciferase Reporter Gene Assay and Western blot Analysis, we observed an increased eNOS promoter activity and an elevated expression of eNOS protein levels following long-term stimulation for 48 hours with EGb 761 (100 µg/ml or 500 µg/ml, respectively). Interestingly, Cheung *et al.* could not show any influence of *Ginkgo biloba* extract on the expression of endothelial nitric oxide synthase.[151, 152] This study, however, utilized ECV 304 as an endothelial-like cell model and the observation time was relatively short compared to our settings (only 2 or 4 hours). Moreover, the Cheung experiments were performed with a *Ginkgo biloba* extract, which is not considered to be equivalent to the standardized extract EGb 761. Since ECV 304 cells have in the meantime definitely turned out to be of epithelial origin, this discrepancy does not come as a surprise. Furthermore, we investigated the effects of EGb 761 on NO levels measured by [^{14}C]L-arginine/[^{14}C]L-citrulline conversion assay. The observed increase in NO production was dose-dependent and was corroborated by the *in vivo* measurements of Shen *et al.* Using electron spin resonance (ESR) spectroscopic analysis during ischemia-reperfusion injury of rat hearts, they found that low doses of EGb 761 (0, 25, 50, and 100 mg/kg) increased NO production. However, at higher doses (200 mg/kg), EGb 761 appeared to be a scavenger of NO. In addition, an increase of eNOS mRNA after treatment with *Ginkgo biloba* extract has previously been shown in rat aortas;[153] but data on eNOS protein levels were missing in this publication. One crucial problem with increasing eNOS expression seems to be that uncoupling of this enzyme may occur,[154] leading to an increased production of superoxide. This result was only apparent following dramatic upregulation, e.g. by eNOS overexpression (11-fold),[154] while moderate increases (< 3-fold) as demonstrated in our work with *Ginkgo biloba* as well as described for statins and other compounds does not seem to have any of such adverse effects.[147] Along this line, excessive production of NO is balanced by radical scavengers, giving rise to EGb 761 induced cardioprotective properties through the regulation of NO levels.

5.1.3   Short-term influence of EGb 761 on eNOS activation and localization

Along with the long-term influence of EGb 761 on eNOS expression, short-term effects on this enzyme as well as effects on blood pressure regulation were investigated. Interestingly, EGb 761 caused a marked drop in blood pressure *in vivo* within minutes, as well as a significant relaxation of isolated aortic rings that can not be due to altered eNOS expression. Besides, this acute decreased blood pressure, recent studies using either spontaneously hypertensive rats (SHR) or deoxycorticosterone acetate (DOCA)-salt hypertensive rats demonstrated that a long-term administration of *Ginkgo biloba* extract attenuated the increase in blood pressure.[153, 155] Similar observations have previously been made with red wine polyphenols,[156] however the underlying mechanisms of both systems are still unclear. The same applies to *Ginkgo biloba* extract, where acute vasorelaxant effects have been observed.[157] An interesting hypothesis has recently been suggested by Dell'Agli *et al.*, claiming that the vasorelaxant effect of *Ginkgo biloba* could be due to PDE-5 inhibition by biflavones.[158] However, in the special extract used in our experiments, the content of biflavones is below 0.1%, which is equivalent to approximately 5 µM, a concentration that hardly caused PDE-5 inhibition in the work by Dell'Agli *et al*. An alternative mechanism, implying an increase of endogenous endothelial Ca^{2+} levels after *Ginkgo biloba* treatment has been hypothesized.[157] A causal link to vasodilatation or eNOS activation has not been demonstrated yet, nor have further mechanistic insights been gained to date.

In the present study we investigated the role of the phosphoinositide 3-kinases (PI3K)/Akt pathway, since this pathway has been proposed as one of the candidates that are capable of activating eNOS directly by phosphorylation at serine 1177 (in human eNOS, equivalent to Ser1179 in bovine eNOS).[50] Indeed, we provide evidence for a rapid increase of eNOS phosphorylation after treatment with EGb 761 that was paralleled by phosphorylation of Akt at Ser473. Since this phosphorylation site is a substrate for a kinase complex downstream of PI3K (PDK2 or mTOR/rictor), and these responses were abolished by the PI3K inhibitor wortmannin, we propose the following signaling cascade: *Ginkgo* extract causes increase of endothelial Ca^{2+} levels, PI3K is activated, further downstream Akt is phosphorylated and, in turn phosphorylates the enzyme eNOS. The same observations have previously been made with a constituent of green tea, epigallocatechin-3-gallate (EGCG), and the pharmacological active component of ginseng, ginsengoside-Rg1. Both are postulated to rapidly induce NO production from eNOS *via* the non-transcriptional PI3K/Akt pathway.[159, 160] In addition to

phosphorylation, the localization of eNOS is important for its activity.[45] In good accordance, we found an increased level of phosphorylated eNOS (Ser1177) located at the plasma membrane after stimulation with EGb 761 (100 µg/ml). Since translocation of eNOS to the plasma membrane does not depend on phosphorylation,[45] and considering that we found an accumulation of phosphorylated eNOS, but not of total eNOS protein at the plasma membrane, we conclude that this increase results from a translocation of activated Akt to the plasma membrane,[161] and from subsequent local phosphorylation of eNOS at the plasma membrane. This step increases the Ca^{2+} sensitivity of eNOS at a subcellular compartment, where elevated cytoplasmic Ca^{2+} concentrations naturally occur.[47] Interestingly, the higher phosphorylation status of eNOS by EGb 761 did not only occur *in vitro*, but was also seen in rat aortic tissue following EGb 761 application *in vivo*. To the best of our knowledge, this work suggests for the first time that there is an influence of EGb 761 on the PI3K-Akt-eNOS pathway and the phosphorylation of eNOS at the plasma membrane. Activation of the PI3K/Akt pathway is, in addition to its influence on eNOS, a key step for diverse biological effects mediating cell proliferation, cell growth, and cell survival.[56] Therefore, cellular activities brought about by EGb 761-induced Akt activation warrant further investigations.

In conclusion, our study demonstrates that EGb 761 stimulates eNOS protein up-regulation and enzyme activation in endothelial cells, thus leading to an enhanced production of NO. Moreover, our results suggest that EGb 761 exhibits dual effects referring to both the transcriptional and non-transcriptional modulation of endothelial nitric oxide synthase, including protein kinase Akt activation and subsequent eNOS phosphorylation. Keeping in mind the artificial character of our *in vitro* and *in vivo* experiments and their limited transferability to the patient, these basic findings give a first hint to the beneficial cardiovascular effects of EGb 761 as a therapeutic agent in conditions associated with disturbed NO production. Our work supports *Ginkgo biloba* on the growing list of herbal remedies whose modes of actions have now been partially revealed on a molecular level.[162, 163]

5.2 Angiogenesis

5.2.1   The role of *Ginkgo biloba* in cancer treatment

In cancer treatment, the concurrent use of natural health products (NHPs) with conventional chemotherapy and radiation has risen in order to inhibit tumor progression and reduce the risk of metastasis.[164] Consequently, there is an increasing need for understanding the molecular mechanisms and signaling pathways underlying these beneficial effects. The following herbs are traditionally used for anticancer treatment and are anti-angiogenic through multiple interdependent processes that include effects on gene expression, signal processing, and enzyme activities: Artemisia annua (Chinese wormwood), Viscum album (European mistletoe), Resveratrol and Proanthocyanidin (Grape Seed Extract).[165, 166] Another example that was recently published, describes the traditional Chinese preparation, Danggui Longhui Wan, which exhibits anticancer activity with indirubin as active principle.[167]

Among the long list of traditional herbs, the interest in *Ginkgo biloba* extract has grown rapidly in the Western world over the last several decades. Although some studies have reported an anticancer (chemo-preventive) effect of EGb 761 in various *in vitro* and *in vivo* experiments, the actual mechanisms of these effects are still elusive.[13] The extract of *Ginkgo biloba* leaves has been shown to inhibit human breast cancer cell proliferation both *in vitro* and *in vivo*.[168] In recent studies the anti-proliferative effect was extended to glioma, hepatocellular carcinoma, as well as to ovarian and oral cavity cancer cells suggesting a widespread application of EGb 761 for tumor growth control.[164, 169-171] Besides its anti-proliferative properties, *Ginkgo biloba* induces detoxification enzymes such as cytochrom P450 (CYP), glutathione S-transferase and quinine reductase to prevent colon cancer,[172] and exerts anticlastogenic effects on radiation-exposed chromosomes.[173, 174] Furthermore, Ye *et al*. have presented epidemiological data supporting an association between regular use of *Ginkgo biloba* (at least six months continuous) and a decreased risk for ovarian cancer.[164]

In brief, *Ginkgo biloba* extracts are supposed to affect various carcinomas by modulating several pathways. Along this line, restriction of tumor growth through the inhibition of angiogenesis, serves as one major approach for anticancer therapy and is the subject of the current work, providing a rational basis for EGb 761-mediated effects on angiogenic parameters in endothelial cells.

5.2.2   EGb 761 has anti-angiogenic properties

The present study shows for the first time an anti-angiogenic profile of EGb 761 (100 µg/ml and 500 µg/ml, respectively) *in vitro*, by inhibition of endothelial cell proliferation, migration, and tube formation. Regarding the anti-proliferative effect in endothelial cells, we provide valuable insight into the molecular mechanism influenced by EGb 761. We found that *Ginkgo biloba*-treated cells accumulate in S/G$_2$ phase, thereby inhibiting endothelial cell proliferation. Through further investigation we determined that EGb 761 does not induce considerable apoptotic activity on endothelial cells, as it does not affect confluent endothelial cells, and proliferating cells only in the highest concentration of 500 µg/ml. These findings indicate that the reduced number of cells is due to a strong anti-proliferative effect, rather than an induction of apoptosis.

Using the chicken chorioallantoic membrane (CAM) assay, the *in vivo* anti-angiogenic activity of EGb 761 was demonstrated. These findings corroborate the first hints describing that administration of EGb 761 to tumor-bearing mice blocked lymphocyte-induced angiogenesis and intraperitoneal administration of a *Ginkgo biloba* extract inhibited neovascularisation in experimental retinopathy of prematurity.[175, 176] The results of Monte *et al*., restricted to lymphocyte-induced angiogenesis, suggest a mechanism involving the known free radical scavenging activity of *Ginkgo biloba* extract, whereas the results of Juarez *et al*. revealed a decreased content of growth factors in retinal and vitreous tissues of rats or mice. In the present study we propose a new hypothesis that the inhibition of angiogenesis by EGb 761 is mediated *via* ERK inhibition and we provide information supporting the molecular mechanism.

5.2.3   EGb 761 reduces growth factor-induced ERK phosphorylation

The Raf-MEK-ERK pathway which is activated through growth factors including FGF and VEGF is of particular relevance to angiogenesis.[74] This pathway has repeatedly been shown to be essential for proliferation and cell cycle progression.[177] It also protects cells from apoptosis and is involved in extracellular matrix (ECM) degradation, endothelial cell migration as well as differentiation.[63, 178] Accordingly, we found that blockade of ERK activation by U0126, a specific MEK 1/2 inhibitor, attenuates endothelial angiogenesis including proliferation, migration, and tube formation. Furthermore, we have demonstrated that U0126 reversed the number of vascular structures induced by FGF *in vivo*. The results

obtained with U0126 referring to the different angiogenic parameters are comparable with these of EGb 761. Moreover, the results point to the involvement of ERK in the anti-angiogenic properties of EGb 761. The present study shows that EGb 761 (500 µg/ml) reduces ERK phosphorylation induced by the growth factors VEGF and FGF in an endothelial cell model. Our findings are supported by recently published *in vitro* studies showing that *Ginkgo biloba* extract inhibits lipopolysaccharid (LPS)-induced phosphorylation of ERK in vascular smooth muscle cells and macrophages, respectively.[179, 180]

As aforementioned, the activation of ERK is regulated by a three step signaling module, comprised of the upstream MAPK kinase kinase Raf-1 and MAPK kinase MEK 1/2.[64, 65] The pathway can be negatively modulated by various mechanisms at almost every point of the Ras-Raf-MEK-ERK cascade. This inhibition of ERK phosphorylation is achieved either by blockage of the upstream kinases or activation of phosphatases. Activation i.e. phosphorylation of the upstream kinases MEK 1/2 and Raf-1 have been found to be abrogated by EGb 761 after short-term treatment in endothelial cells. Finally the question arose, by which mechanism these upstream kinases are inhibited. As shown in section 5.1 and recently published, EGb 761 activates the signaling cascades of NO/cGMP as well as PI3K/Akt.[26] Both cascades lead to an inhibition of the serine/threonine kinase Raf-1 *via* phosphorylation at Ser259, which keeps the kinase in an auto-inhibited state.[69, 70, 181, 182] Therefore, the involvement of NO/cGMP as well as PI3K/Akt referring the reduced ERK phosphorylation was investigated using specific inhibitors. However, none of these cascades appeared to be involved in the inhibitory effect of EGb 761 on ERK phosphorylation.

Moreover, the present work revealed that EGb 761 clearly enhanced cAMP level. Our finding is supported by recently published *in vivo* studies demonstrating that the concentration of cAMP was augmented by 37.5±9.1% (p<0.0078) in the blood of cardiovascular high-risk patients after a 2-month therapy with *Ginkgo biloba* extract.[141] The vasodilating second messenger cAMP activates the protein kinase A (PKA), which has also been shown to phosphorylate Raf-1 at Ser259, thereby inactivating the Raf-MEK-ERK pathway.[183] The involvement of elevated cAMP/PKA level on the reduced ERK phosphorylation by EGb 761 could be excluded using two specific inhibitors of PKA, the major effector of cAMP.

5.2.4   EGb 761 reduces ERK phosphorylation *via* induction of tyrosine phosphatases

Interestingly, nothing has as yet been investigated regarding the potency of EGb 761 to influence phosphatases. Therefore, it is of special interest that our results show an activation of protein tyrosine phosphatases by EGb 761. On the one hand, protein tyrosine phosphatases (PTPs) were identified as the crucial regulator of the reduced ERK phosphorylation and were causally linked with the anti-angiogenic effect of EGb 761. On the other hand, an involvement of serine/threonine phosphatases on the inhibitory effect of ERK phosphorylation by EGb 761 could be excluded. Furthermore, using a specific phosphatase assay, a diminished activity of the serine/threonine phosphatases PP2A, PP2B, and PP2C by EGb 761 (500 µg/ml) treatment alone or subsequent exposure to EGb 761 and FGF was obtained. Comparing to control experiments, following FGF treatment no increase in activity was detectable for any of the three phosphatases. However, Lao *et al.* working with 10-fold higher concentrations of FGF (50 ng/ml) and human embryonic kidney cells HEK293T revealed a marginal increase in PP2A activity after 30 min and a significant increase after 2 h treatment.[184] The diminished activity of the phosphatase PP2A confirms the inhibitory effect of EGb 761 on ERK phosphorylation since the activity of this phosphatase is required for Raf-1 activation, an upstream kinase of ERK.

Recently, evidence has been given that PTPs function as tumor suppressors and that deregulation of PTP function is associated with tumorigenesis in different types of human cancinoma.[185] Furthermore, individual PTPs exert an antagonistic role in growth factor signaling either by direct dephosphorylation of receptor-tyrosine kinases or by dephosphorylation of a member of the MAP kinase cascade. Regarding the ERK-cascade, the following PTPs have been discussed: MKP-1, LAR, SHP-1, DEP1, PTP1B and HC PTP-A. MKP-1 is a dual specificity MAPK phosphatase, which inactivates ERK by dephosphorylation of the two critical MAPK residues (Thr202/Tyr204) accountable for its activation. MKP-1 is mainly regulated *via* protein expression, which has not been seen to be affected by EGb 761 as determined by Western blot analysis. As we learned that EGb 761 activates phosphatases upstream of the MAPK cascade, we now focused on PTPs which act as direct antagonists of receptor-tyrosine kinases *via* dephosphorylation of tyrosine residues. The hypothesis that EGb 761 terminates ERK phosphorylation by activation of one or more tyrosine phosphatases connected with either VEGF or FGF receptors was confirmed by experiments using PMA as a substrate. PMA leads to a growth factor independent ERK

phosphorylation, which was not inhibited by EGb 761. One example of PTPs, which antagonizes receptor-tyrosine kinases, is the src homology-2 (SH2) domain-containing phosphatase SHP-1, which is a cytoplasmic PTP.

SHP-1 was identified to play a largely negative role by suppressing cellular proliferation and angiogenesis through growth factors including FGF and VEGF *via* direct dephosphorylation of their receptors. Therefore, we hypothesized that EGb 761 acts directly on SHP-1. In a tyrosine phosphatase activity assay, SHP-1 was demonstrated to be rapidly activated by EGb 761 (500 µg/ml) within 30 minutes. Furthermore, by using SHP-1 targeting siRNA we could confirm the role of SHP-1 activation in suppression of endothelial proliferation by *Ginkgo biloba* extract. Thus, SHP-1 has been identified to be one of the target molecules for *Ginkgo biloba* extract conferring its anti-angiogenic activity.

In conclusion, EGb 761 exerts anti-angiogenic effects and activates protein tyrosine phosphatases (SHP-1 among others) resulting in an inhibition of the Raf-MEK-ERK-pathway. These findings provide a rational basis for the chemo-preventive and anticancer effects of the herbal remedy EGb 761. The present study adds *Ginkgo biloba* to the growing list of herbal remedies with a rational, mechanistic molecular background.

6 SUMMARY

6.1   Endothelial nitric oxide production

The standardized *Ginkgo biloba* extract, EGb 761, has been repeatedly proven to be beneficial for the prevention and treatment of cardiovascular diseases. In the present work we revealed the underlying signaling pathway and the molecular basis on which EGb 761 protects endothelial dysfunction both *in vitro* and *in vivo*.

Application of therapeutically feasible doses of EGb 761 for 48 hours caused endothelial nitric oxide (NO) production by increasing endothelial nitric oxide synthase (eNOS) promoter activity, eNOS protein expression, and eNOS activity ($[^{14}C]$L-arginine/$[^{14}C]$L-citrulline conversion) *in vitro*. In addition to these transcriptional effects on eNOS, phosphorylation of the enzyme at a site typical for the protein kinase B/Akt (Ser1177) was acutely enhanced by treatment with EGb 761, as was Akt phosphorylation at Ser473. Furthermore, the *Ginkgo biloba* extract caused an acute relaxation of isolated rat aortic rings and NO-dependent reduction of blood pressure in Sprague-Dawley rats *in vivo*.

In summary, our work provides insights into the mechanism by which EGb 761 exerts beneficial effects on cardiovascular diseases and shows that EGb 761 enhances endothelial NO production by increasing eNOS expression and PI3K/Akt-driven activity of eNOS. These influences on eNOS represent a putative molecular basis for the protective cardiovascular properties of EGb 761.
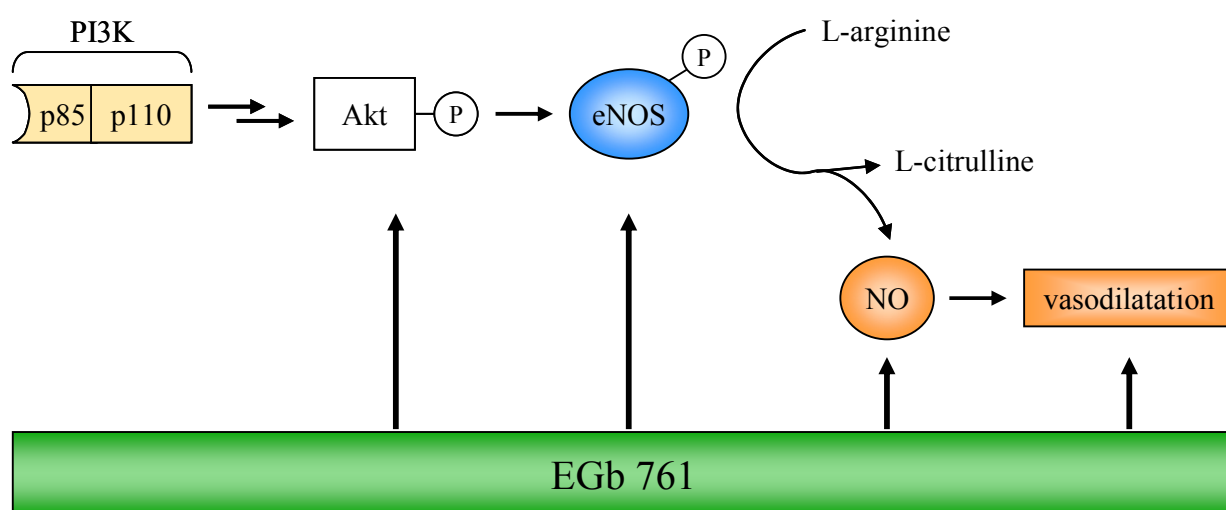
Figure 6.1   *Schematic diagram of the signal transduction pathway of EGb 761 leading to endothelial nitric oxide (NO) production and vasodilation.*

6.2 Angiogenesis

Ginkgo biloba is traditionally used for anticancer treatment. However, as seen with most of the widely used herbal remedies, no profound mechanistic studies providing a rational basis for the respective therapeutic indication exist.

The present study shows an anti-angiogenic profile *in vitro* of the standardized *Ginkgo biloba* extract EGb 761. The extract inhibits endothelial proliferation, migration and tube formation of primary human endothelial cells. Moreover, using the chicken chorioallantoic membrane assay (CAM) *in vivo* anti-angiogenic activity of EGb 761 was demonstrated. During analysis of the underlying molecular mechanisms, a significant inhibition of growth factor-induced ERK phosphorylation by EGb 761 became evident. Interestingly, inhibitory effects of EGb 761 on ERK as well as on upstream kinases MEK 1/2 and Raf-1 could be completely reversed by pre-treatment with sodium vanadate, an inhibitor of tyrosine phosphatases. Sodium vanadate was able to reverse the EGb 761-induced inhibition of endothelial cell migration, an important parameter for angiogenesis. Focusing on tyrosine
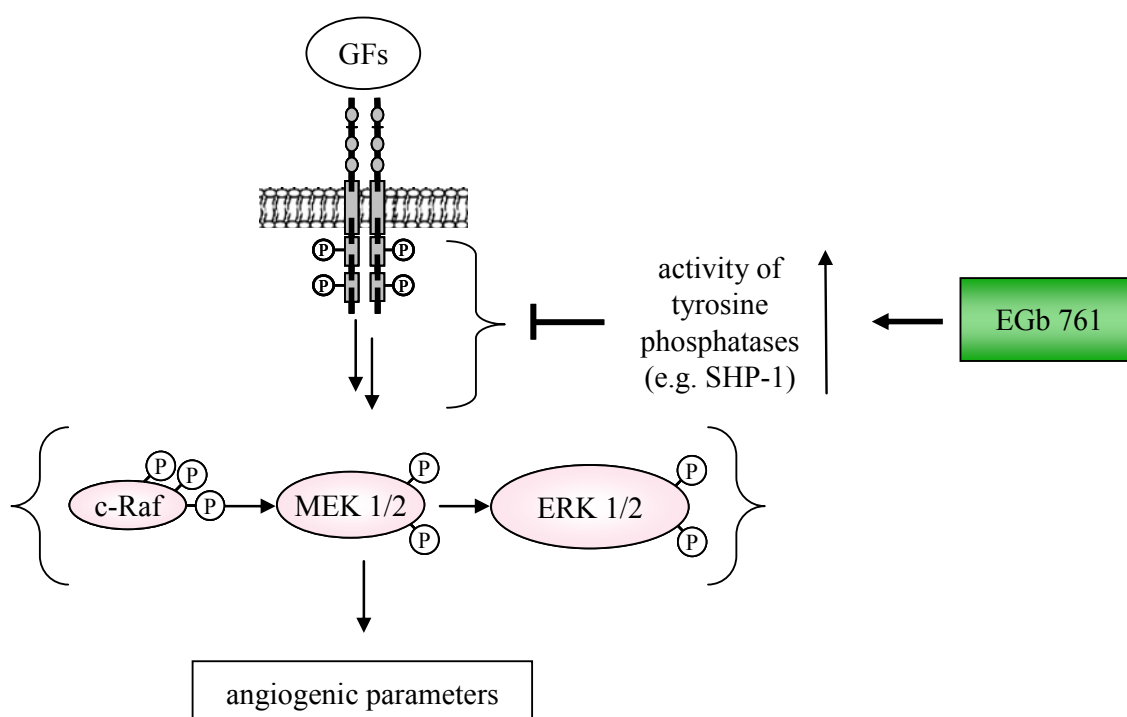
Figure 6.2   *Schematic representation of the molecular mechanism underlying the anti-angiogenic properties of EGb 761.*

phosphatases upstream of the Raf-MEK-ERK cascade, we identified the tyrosine phosphatase SHP-1 as a target of EGb 761. SHP-1 was rapidly activated by EGb 761 and silencing SHP-1 (siRNA experiments) abrogated the EGb 761 evoked reduction of endothelial proliferation.

In summary, our work provides insights into the mechanism by which EGb 761 has anti-angiogenic properties and shows that EGb 761 activates protein tyrosine phosphatases leading to an inhibition of the Raf-MEK-ERK pathway. This work provides a rational basis for the use of the widely consumed herbal remedy *Ginkgo biloba* in anti-angiogenesis based tumor prevention and therapy.

7 REFERENCES

1. Cines DB, Pollak ES, Buck CA, Loscalzo J, Zimmerman GA, McEver RP, Pober JS, Wick TM, Konkle BA, Schwartz BS, Barnathan ES, McCrae KR, Hug BA, Schmidt AM, and Stern DM. Endothelial cells in physiology and in the pathophysiology of vascular disorders. *Blood.* 1998; **91**(10): 3527-3561.

2. Galley HF and Webster NR. Physiology of the endothelium. *Br. J. Anaesth.* 2004; **93**(1): 105-113.

3. Esper RJ, Nordaby RA, Vilarino JO, Paragano A, Cacharron JL, and Machado RA. Endothelial dysfunction: a comprehensive appraisal. *Cardiovasc. Diabetol.* 2006; **5**: 4.

4. Feletou M and Vanhoutte PM. Endothelial Dysfunction: a multifaceted disorder. *Am. J. Physiol Heart Circ. Physiol.* 2006.

5. Feletou M and Vanhoutte PM. Endothelial dysfunction: a multifaceted disorder (The Wiggers Award Lecture). *Am. J. Physiol Heart Circ. Physiol.* 2006; **291**(3): H985-1002.

6. Taddei S, Ghiadoni L, Virdis A, Versari D, and Salvetti A. Mechanisms of endothelial dysfunction: clinical significance and preventive non-pharmacological therapeutic strategies. *Curr. Pharm. Des.* 2003; **9**(29): 2385-2402.

7. Kawashima S and Yokoyama M. Dysfunction of endothelial nitric oxide synthase and atherosclerosis. *Arterioscler. Thromb. Vasc. Biol.* 2004; **24**(6): 998-1005.

8. Li H and Forstermann U. Nitric oxide in the pathogenesis of vascular disease. *J. Pathol.* 2000; **190**(3): 244-254.

9. Förstermann U and Münzel T. Endothelial nitric oxide synthase in vascular disease: from marvel to menace. *Circulation.* 2006; **113**(13): 1708-1714.

10. Aird WC. The role of the endothelium in severe sepsis and multiple organ dysfunction syndrome. *Blood.* 2003; **101**(10): 3765-3777.

11. Aird WC. Endothelium as a therapeutic target in sepsis. *Curr. Drug Targets.* 2007; **8**(4): 501-507.

12. Defeudis FV. *Ginkgo biloba extract (EGb 761): from chemistry to the clinic. Ullstein Medical, Wiesbaden 1998, ISBN 3-86126-173-1.* 1998.

13. Defeudis FV, Papadopoulos V, and Drieu K. Ginkgo biloba extracts and cancer: a research area in its infancy. *Fundam. Clin. Pharmacol.* 2003; **17**(4): 405-417.

14. Jaggy H and Koch E. Chemistry and biology of alkylphenols from Ginkgo biloba L. *Pharmazie.* 1997; **52**(10): 735-738.

15. Defeudis FV. A brief history of EGb 761 and its therapeutic uses. *Pharmacopsychiatry.* 2003; **36 Suppl 1**: S2-S7.

16. Defeudis FV. *Ginkgo biloba extract (EGb 761): Pharmacological activities and clinical applications. Elsevier, Paris 1991, ISBN: 2-906077-21-6.* 2007.

17. Ahlemeyer B and Krieglstein J. Pharmacological studies supporting the therapeutic use of Ginkgo biloba extract for Alzheimer's disease. *Pharmacopsychiatry.* 2003; **36 Suppl 1**: S8-14.

18. Defeudis FV. A brief history of EGb 761 and its therapeutic uses. *Pharmacopsychiatry.* 2003; **36 Suppl 1**: S2-S7.

19. Ernst E and Pittler MH. Ginkgo biloba for Dementia: A Systematic Review of Double-Blind, Placebo-Controlled Trials. *Clin Drug Invest.* 1999; **17**(4): 301-308.

20. Ernst E. Ginkgo biloba in treatment of intermittent claudication. A systematic research based on controlled studies in the literature [In German]. *Fortschr. Med.* 1996; **114**(8): 85-87.

21. Pittler MH and Ernst E. Ginkgo biloba extract for the treatment of intermittent claudication: a meta-analysis of randomized trials. *Am. J. Med.* 2000; **108**(4): 276-281.

22. Horsch S and Walther C. Ginkgo biloba special extract EGb 761 in the treatment of peripheral arterial occlusive disease (PAOD)--a review based on randomized, controlled studies. *Int. J. Clin. Pharmacol. Ther.* 2004; **42**(2): 63-72.

23. Morgenstern C and Biermann E. The efficacy of Ginkgo special extract EGb 761 in patients with tinnitus. *Int. J. Clin. Pharmacol. Ther.* 2002; **40**(5): 188-197.

24. BGA-Kommission E. Monographie: Trockenextrakt (35-67:1) aus Ginkgo-biloba-Blättern, extrahiert mit Aceton-Wasser. *Bundesanzeiger (Banz).* 1994; **133**: 7361.

25. Koch E. Inhibition of platelet activating factor (PAF)-induced aggregation of human thrombocytes by ginkgolides: considerations on possible bleeding complications after oral intake of Ginkgo biloba extracts. *Phytomedicine.* 2005; **12**(1-2): 10-16.

26. Koltermann A, Hartkorn A, Koch E, Furst R, Vollmar AM, and Zahler S. Ginkgo biloba extract EGb((R)) 761 increases endothelial nitric oxide production in vitro and in vivo. *Cell Mol. Life Sci.* 2007; **64**(13): 1715-1722.

27. Defeudis FV and Drieu K. "Stress-Alleviating" and "Vigilance-Enhancing" Actions of Ginkgo biloba Extract (EGb 761). *Drug Development Research.* 2004; **62**: 1-25.

28. Porsolt RD, Martin P, Lenegre A, Fromage S, and Drieu K. Effects of an extract of Ginkgo Biloba (EGB 761) on "learned helplessness" and other models of stress in rodents. *Pharmacol. Biochem. Behav.* 1990; **36**(4): 963-971.

29. Pincemail J, Thirion A, Dupuis M, Braquet P, Drieu K, and Deby C. Ginkgo biloba extract inhibits oxygen species production generated by phorbol myristate acetate stimulated human leukocytes. *Experientia.* 1987; **43**(2): 181-184.

30. Pincemail J, Dupuis M, Nasr C, Hans P, Haag-Berrurier M, Anton R, and Deby C. Superoxide anion scavenging effect and superoxide dismutase activity of Ginkgo biloba extract. *Experientia.* 1989; **45**(8): 708-712.

31. Chandrasekaran K, Mehrabian Z, Spinnewyn B, Chinopoulos C, Drieu K, and Fiskum G. Neuroprotective effects of bilobalide, a component of Ginkgo biloba extract (EGb 761) in global brain ischemia and in excitotoxicity-induced neuronal death. *Pharmacopsychiatry.* 2003; **36 Suppl 1**: S89-S94.

32. Ahlemeyer B and Krieglstein J. Neuroprotective effects of Ginkgo biloba extract. *Cell Mol. Life Sci.* 2003; **60**(9): 1779-1792.

33. Gohil K, Moy RK, Farzin S, Maguire JJ, and Packer L. mRNA expression profile of a human cancer cell line in response to Ginkgo biloba extract: induction of antioxidant response and the Golgi system. *Free Radic. Res.* 2000; **33**(6): 831-849.

34. Furchgott RF and Zawadzki JV. The obligatory role of endothelial cells in the relaxation of arterial smooth muscle by acetylcholine. *Nature.* 1980; **288**(5789): 373-376.

35. Palmer RM, Ferrige AG, and Moncada S. Nitric oxide release accounts for the biological activity of endothelium-derived relaxing factor. *Nature.* 1987; **327**(6122): 524-526.

36. Ignarro LJ, Buga GM, Wood KS, Byrns RE, and Chaudhuri G. Endothelium-derived relaxing factor produced and released from artery and vein is nitric oxide. *Proc. Natl. Acad. Sci. U. S. A.* 1987; **84**(24): 9265-9269.

37. Förstermann U. Endothelial NO synthase as a source of NO and superoxide. *Eur. J. Clin. Pharmacol.* 2006; **62 Suppl 13**: 5-12.

38. Braam B and Verhaar MC. Understanding eNOS for pharmacological modulation of endothelial function: a translational view. *Curr. Pharm. Des.* 2007; **13**(17): 1727-1740.

39. Kawashima S. The two faces of endothelial nitric oxide synthase in the pathophysiology of atherosclerosis. *Endothelium.* 2004; **11**(2): 99-107.

40. Kawashima S and Yokoyama M. Dysfunction of endothelial nitric oxide synthase and atherosclerosis. *Arterioscler. Thromb. Vasc. Biol.* 2004; **24**(6): 998-1005.

41. Alderton WK, Cooper CE, and Knowles RG. Nitric oxide synthases: structure, function and inhibition. *Biochem. J.* 2001; **357**(Pt 3): 593-615.

42. Ghosh DK and Salerno JC. Nitric oxide synthases: domain structure and alignment in enzyme function and control. *Front Biosci.* 2003; **8**: d193-d209.

43. Sessa WC. eNOS at a glance. *J. Cell Sci.* 2004; **117**(Pt 12): 2427-2429.

44. Li H, Wallerath T, and Forstermann U. Physiological mechanisms regulating the expression of endothelial-type NO synthase. *Nitric. Oxide.* 2002; **7**(2): 132-147.

45. Garcia-Cardena G, Oh P, Liu J, Schnitzer JE, and Sessa WC. Targeting of nitric oxide synthase to endothelial cell caveolae via palmitoylation: implications for nitric oxide signaling. *Proc. Natl. Acad. Sci. U. S. A.* 1996; **93**(13): 6448-6453.

46. Mukherjee S, Tessema M, and Wandinger-Ness A. Vesicular trafficking of tyrosine kinase receptors and associated proteins in the regulation of signaling and vascular function. *Circ. Res.* 2006; **98**(6): 743-756.

47. Oess S, Icking A, Fulton D, Govers R, and Müller-Esterl W. Subcellular targeting and trafficking of nitric oxide synthases. *Biochem. J.* 2006; **396**(3): 401-409.

48. Boo YC and Jo H. Flow-dependent regulation of endothelial nitric oxide synthase: role of protein kinases. *Am. J. Physiol Cell Physiol.* 2003; **285**(3): C499-C508.

49. Dudzinski DM, Igarashi J, Greif D, and Michel T. The regulation and pharmacology of endothelial nitric oxide synthase. *Annu. Rev. Pharmacol. Toxicol.* 2006; **46**: 235-276.

50. Fulton D, Gratton JP, and Sessa WC. Post-translational control of endothelial nitric oxide synthase: why isn't calcium/calmodulin enough? *J. Pharmacol. Exp. Ther.* 2001; **299**(3): 818-824.

51. Kone BC. Protein-protein interactions controlling nitric oxide synthases. *Acta Physiol Scand.* 2000; **168**(1): 27-31.

52. Mount PF, Kemp BE, and Power DA. Regulation of endothelial and myocardial NO synthesis by multi-site eNOS phosphorylation. *J. Mol. Cell Cardiol.* 2007; **42**(2): 271-279.

53. Fulton D, Gratton JP, McCabe TJ, Fontana J, Fujio Y, Walsh K, Franke TF, Papapetropoulos A, and Sessa WC. Regulation of endothelium-derived nitric oxide production by the protein kinase Akt. *Nature.* 1999; **399**(6736): 597-601.

54. Shiojima I and Walsh K. Role of Akt signaling in vascular homeostasis and angiogenesis. *Circ. Res.* 2002; **90**(12): 1243-1250.

55. Song G, Ouyang G, and Bao S. The activation of Akt/PKB signaling pathway and cell survival. *J. Cell Mol. Med.* 2005; **9**(1): 59-71.

56. Woodgett JR. Recent advances in the protein kinase B signaling pathway. *Curr. Opin. Cell Biol.* 2005; **17**(2): 150-157.

57. Wipf P and Halter RJ. Chemistry and biology of wortmannin. *Org. Biomol. Chem.* 2005; **3**(11): 2053-2061.

58. Folkman J. Tumor angiogenesis: therapeutic implications. *N. Engl. J. Med.* 1971; **285**(21): 1182-1186.

59. Bergers G and Benjamin LE. Tumorigenesis and the angiogenic switch. *Nat. Rev. Cancer.* 2003; **3**(6): 401-410.

60. Carmeliet P and Jain RK. Angiogenesis in cancer and other diseases. *Nature.* 2000; **407**(6801): 249-257.

61. Carmeliet P. Mechanisms of angiogenesis and arteriogenesis. *Nat. Med.* 2000; **6**(4): 389-395.

62. Madeddu P. Therapeutic angiogenesis and vasculogenesis for tissue regeneration. *Exp. Physiol.* 2005; **90**(3): 315-326.

63. Munoz-Chapuli R, Quesada AR, and Angel MM. Angiogenesis and signal transduction in endothelial cells. *Cell Mol. Life Sci.* 2004; **61**(17): 2224-2243.

64. Chen Z, Gibson TB, Robinson F, Silvestro L, Pearson G, Xu B, Wright A, Vanderbilt C, and Cobb MH. MAP kinases. *Chem. Rev.* 2001; **101**(8): 2449-2476.

65. Qi M and Elion EA. MAP kinase pathways. *J. Cell Sci.* 2005; **118**(Pt 16): 3569-3572.

66. Kolch W. Coordinating ERK/MAPK signalling through scaffolds and inhibitors. *Nat. Rev. Mol. Cell Biol.* 2005; **6**(11): 827-837.

67. Murphy LO and Blenis J. MAPK signal specificity: the right place at the right time. *Trends Biochem. Sci.* 2006; **31**(5): 268-275.

68. Goldsmith ZG and Dhanasekaran DN. G protein regulation of MAPK networks. *Oncogene.* 2007; **26**(22): 3122-3142.

69. Chong H, Vikis HG, and Guan KL. Mechanisms of regulating the Raf kinase family. *Cell Signal.* 2003; **15**(5): 463-469.

70. Wellbrock C, Karasarides M, and Marais R. The RAF proteins take centre stage. *Nat. Rev. Mol. Cell Biol.* 2004; **5**(11): 875-885.

71. Kolch W. Meaningful relationships: the regulation of the Ras/Raf/MEK/ERK pathway by protein interactions. *Biochem. J.* 2000; **351 Pt 2**: 289-305.

72. Raman M, Chen W, and Cobb MH. Differential regulation and properties of MAPKs. *Oncogene.* 2007; **26**(22): 3100-3112.

73. Dhillon AS, Hagan S, Rath O, and Kolch W. MAP kinase signalling pathways in cancer. *Oncogene.* 2007; **26**(22): 3279-3290.

74. Gollob JA, Wilhelm S, Carter C, and Kelley SL. Role of Raf kinase in cancer: therapeutic potential of targeting the Raf/MEK/ERK signal transduction pathway. *Semin. Oncol.* 2006; **33**(4): 392-406.

75. Presta M, Dell'Era P, Mitola S, Moroni E, Ronca R, and Rusnati M. Fibroblast growth factor/fibroblast growth factor receptor system in angiogenesis. *Cytokine Growth Factor Rev.* 2005; **16**(2): 159-178.

76. Fieth C, Kebig A, and Mohr K. Bevacizumab gegen Dickdarmkarzinom. Angiogenese-Hemmung in der Krebstherapie. *Pharm. Unserer Zeit.* 2007; **36**(6): 442-445.

77. Genentech. http://www.gene.com/gene/products/index.jsp. 2007. Ref Type: Internet Communication

78. Ho QT and Kuo CJ. Vascular endothelial growth factor: biology and therapeutic applications. *Int. J. Biochem. Cell Biol.* 2007; **39**(7-8): 1349-1357.

79. Shing Y, Folkman J, Sullivan R, Butterfield C, Murray J, and Klagsbrun M. Heparin affinity: purification of a tumor-derived capillary endothelial cell growth factor. *Science.* 1984; **223**(4642): 1296-1299.

80. Bikfalvi A, Savona C, Perollet C, and Javerzat S. New insights in the biology of fibroblast growth factor-2. *Angiogenesis.* 1998; **1**(2): 155-173.

81. Sorensen V, Nilsen T, and Wiedlocha A. Functional diversity of FGF-2 isoforms by intracellular sorting. *Bioessays.* 2006; **28**(5): 504-514.

82. Yu PJ, Ferrari G, Galloway AC, Mignatti P, and Pintucci G. Basic fibroblast growth factor (FGF-2): the high molecular weight forms come of age. *J. Cell Biochem.* 2007; **100**(5): 1100-1108.

83. Eswarakumar VP, Lax I, and Schlessinger J. Cellular signaling by fibroblast growth factor receptors. *Cytokine Growth Factor Rev.* 2005; **16**(2): 139-149.

84. Dailey L, Ambrosetti D, Mansukhani A, and Basilico C. Mechanisms underlying differential responses to FGF signaling. *Cytokine Growth Factor Rev.* 2005; **16**(2): 233-247.

85. Ho QT and Kuo CJ. Vascular endothelial growth factor: biology and therapeutic applications. *Int. J. Biochem. Cell Biol.* 2007; **39**(7-8): 1349-1357.

86.   Carmeliet P. VEGF as a key mediator of angiogenesis in cancer. *Oncology.* 2005; **69 Suppl 3**: 4-10.

87.   Ferrara N. VEGF as a therapeutic target in cancer. *Oncology.* 2005; **69 Suppl 3**: 11-16.

88.   Shinkaruk S, Bayle M, Lain G, and Deleris G. Vascular endothelial cell growth factor (VEGF), an emerging target for cancer chemotherapy. *Curr. Med. Chem. Anticancer Agents.* 2003; **3**(2): 95-117.

89.   Byrne AM, Bouchier-Hayes DJ, and Harmey JH. Angiogenic and cell survival functions of vascular endothelial growth factor (VEGF). *J. Cell Mol. Med.* 2005; **9**(4): 777-794.

90.   Cebe-Suarez S, Zehnder-Fjallman A, and Ballmer-Hofer K. The role of VEGF receptors in angiogenesis; complex partnerships. *Cell Mol. Life Sci.* 2006; **63**(5): 601-615.

91.   Olsson AK, Dimberg A, Kreuger J, and Claesson-Welsh L. VEGF receptor signalling - in control of vascular function. *Nat. Rev. Mol. Cell Biol.* 2006; **7**(5): 359-371.

92.   Zachary I. VEGF signalling: integration and multi-tasking in endothelial cell biology. *Biochem. Soc. Trans.* 2003; **31**(Pt 6): 1171-1177.

93.   Ferrara N, Gerber HP, and LeCouter J. The biology of VEGF and its receptors. *Nat. Med.* 2003; **9**(6): 669-676.

94.   Yla-Herttuala S, Rissanen TT, Vajanto I, and Hartikainen J. Vascular endothelial growth factors: biology and current status of clinical applications in cardiovascular medicine. *J. Am. Coll. Cardiol.* 2007; **49**(10): 1015-1026.

95.   Takahashi T, Ueno H, and Shibuya M. VEGF activates protein kinase C-dependent, but Ras-independent Raf-MEK-MAP kinase pathway for DNA synthesis in primary endothelial cells. *Oncogene.* 1999; **18**(13): 2221-2230.

96.   Abraham D, Podar K, Pacher M, Kubicek M, Welzel N, Hemmings BA, Dilworth SM, Mischak H, Kolch W, and Baccarini M. Raf-1-associated protein phosphatase 2A as a positive regulator of kinase activation. *J. Biol. Chem.* 2000; **275**(29): 22300-22304.

97.   Janssens V and Goris J. Protein phosphatase 2A: a highly regulated family of serine/threonine phosphatases implicated in cell growth and signalling. *Biochem. J.* 2001; **353**(Pt 3): 417-439.

98.   Millward TA, Zolnierowicz S, and Hemmings BA. Regulation of protein kinase cascades by protein phosphatase 2A. *Trends Biochem. Sci.* 1999; **24**(5): 186-191.

99. Ory S, Zhou M, Conrads TP, Veenstra TD, and Morrison DK. Protein phosphatase 2A positively regulates Ras signaling by dephosphorylating KSR1 and Raf-1 on critical 14-3-3 binding sites. *Curr. Biol.* 2003; **13**(16): 1356-1364.

100. Schonthal AH. Role of serine/threonine protein phosphatase 2A in cancer. *Cancer Lett.* 2001; **170**(1): 1-13.

101. Burridge K, Sastry SK, and Sallee JL. Regulation of cell adhesion by protein-tyrosine phosphatases. I. Cell-matrix adhesion. *J. Biol. Chem.* 2006; **281**(23): 15593-15596.

102. Sallee JL, Wittchen ES, and Burridge K. Regulation of cell adhesion by protein-tyrosine phosphatases: II. Cell-cell adhesion. *J. Biol. Chem.* 2006; **281**(24): 16189-16192.

103. Alonso A, Sasin J, Bottini N, Friedberg I, Friedberg I, Osterman A, Godzik A, Hunter T, Dixon J, and Mustelin T. Protein tyrosine phosphatases in the human genome. *Cell.* 2004; **117**(6): 699-711.

104. Denu JM and Dixon JE. Protein tyrosine phosphatases: mechanisms of catalysis and regulation. *Curr. Opin. Chem. Biol.* 1998; **2**(5): 633-641.

105. Abraham SM and Clark AR. Dual-specificity phosphatase 1: a critical regulator of innate immune responses. *Biochem. Soc. Trans.* 2006; **34**(Pt 6): 1018-1023.

106. Theodosiou A and Ashworth A. MAP kinase phosphatases. *Genome Biol.* 2002; **3**(7): REVIEWS3009.

107. Farooq A and Zhou MM. Structure and regulation of MAPK phosphatases. *Cell Signal.* 2004; **16**(7): 769-779.

108. Neel BG, Gu H, and Pao L. The 'Shp'ing news: SH2 domain-containing tyrosine phosphatases in cell signaling. *Trends Biochem. Sci.* 2003; **28**(6): 284-293.

109. Poole AW and Jones ML. A SHPing tale: perspectives on the regulation of SHP-1 and SHP-2 tyrosine phosphatases by the C-terminal tail. *Cell Signal.* 2005; **17**(11): 1323-1332.

110. Chong ZZ and Maiese K. The Src homology 2 domain tyrosine phosphatases SHP-1 and SHP-2: diversified control of cell growth, inflammation, and injury. *Histol. Histopathol.* 2007; **22**(11): 1251-1267.

111. Cai J, Jiang WG, Ahmed A, and Boulton M. Vascular endothelial growth factor-induced endothelial cell proliferation is regulated by interaction between VEGFR-2, SH-PTP1 and eNOS. *Microvasc. Res.* 2006; **71**(1): 20-31.

112.   Nakagami H, Cui TX, Iwai M, Shiuchi T, Takeda-Matsubara Y, Wu L, and Horiuchi M. Tumor necrosis factor-alpha inhibits growth factor-mediated cell proliferation through SHP-1 activation in endothelial cells. *Arterioscler. Thromb. Vasc. Biol.* 2002; **22**(2): 238-242.

113.   Sugano M, Tsuchida K, Maeda T, and Makino N. SiRNA targeting SHP-1 accelerates angiogenesis in a rat model of hindlimb ischemia. *Atherosclerosis.* 2007; **191**(1): 33-39.

114.   Chong ZZ and Maiese K. The Src homology 2 domain tyrosine phosphatases SHP-1 and SHP-2: diversified control of cell growth, inflammation, and injury. *Histol. Histopathol.* 2007; **22**(11): 1251-1267.

115.   Wu C, Sun M, Liu L, and Zhou GW. The function of the protein tyrosine phosphatase SHP-1 in cancer. *Gene.* 2003; **306**: 1-12.

116.   Ades EW, Candal FJ, Swerlick RA, George VG, Summers S, Bosse DC, and Lawley TJ. HMEC-1: establishment of an immortalized human microvascular endothelial cell line. *J. Invest Dermatol.* 1992; **99**(6): 683-690.

117.   Bouis D, Hospers GA, Meijer C, Molema G, and Mulder NH. Endothelium in vitro: a review of human vascular endothelial cell lines for blood vessel-related research. *Angiogenesis.* 2001; **4**(2): 91-102.

118.   Edgell CJ, McDonald CC, and Graham JB. Permanent cell line expressing human factor VIII-related antigen established by hybridization. *Proc. Natl. Acad. Sci. U. S. A.* 1983; **80**(12): 3734-3737.

119.   Li H, Oehrlein SA, Wallerath T, Ihrig-Biedert I, Wohlfart P, Ulshofer T, Jessen T, Herget T, Forstermann U, and Kleinert H. Activation of protein kinase C alpha and/or epsilon enhances transcription of the human endothelial nitric oxide synthase gene. *Mol. Pharmacol.* 1998; **53**(4): 630-637.

120.   Marin V, Kaplanski G, Gres S, Farnarier C, and Bongrand P. Endothelial cell culture: protocol to obtain and cultivate human umbilical endothelial cells. *J. Immunol. Methods.* 2001; **254**(1-2): 183-190.

121.   Laemmli UK. Cleavage of structural proteins during the assembly of the head of bacteriophage T4. *Nature.* 1970; **227**(5259): 680-685.

122.   Kurien BT and Scofield RH. Protein blotting: a review. *J. Immunol. Methods.* 2003; **274**(1-2): 1-15.

123.   Smith PK, Krohn RI, Hermanson GT, Mallia AK, Gartner FH, Provenzano MD, Fujimoto EK, Goeke NM, Olson BJ, and Klenk DC. Measurement of protein using bicinchoninic acid. *Anal. Biochem.* 1985; **150**(1): 76-85.

124. Bradford MM. A rapid and sensitive method for the quantitation of microgram quantities of protein utilizing the principle of protein-dye binding. *Anal. Biochem.* 1976; **72**: 248-254.

125. Staton CA, Stribbling SM, Tazzyman S, Hughes R, Brown NJ, and Lewis CE. Current methods for assaying angiogenesis in vitro and in vivo. *Int. J. Exp. Pathol.* 2004; **85**(5): 233-248.

126. Auerbach R, Lewis R, Shinners B, Kubai L, and Akhtar N. Angiogenesis assays: a critical overview. *Clin. Chem.* 2003; **49**(1): 32-40.

127. Taraboletti G and Giavazzi R. Modelling approaches for angiogenesis. *Eur. J. Cancer.* 2004; **40**(6): 881-889.

128. Nicoletti I, Migliorati G, Pagliacci MC, Grignani F, and Riccardi C. A rapid and simple method for measuring thymocyte apoptosis by propidium iodide staining and flow cytometry. *J. Immunol. Methods.* 1991; **139**(2): 271-279.

129. Pfaffl MW. A new mathematical model for relative quantification in real-time RT-PCR. *Nucleic Acids Res.* 2001; **29**(9): e45.

130. Morgenstern C and Biermann E. The efficacy of Ginkgo special extract EGb 761 in patients with tinnitus. *Int. J. Clin. Pharmacol. Ther.* 2002; **40**(5): 188-197.

131. Muir AH, Robb R, McLaren M, Daly F, and Belch JJ. The use of Ginkgo biloba in Raynaud's disease: a double-blind placebo-controlled trial. *Vasc. Med.* 2002; **7**(4): 265-267.

132. Pittler MH and Ernst E. Ginkgo biloba extract for the treatment of intermittent claudication: a meta-analysis of randomized trials. *Am. J. Med.* 2000; **108**(4): 276-281.

133. Ernst E. The efficacy of herbal medicine - an overview. *Fundam. Clin. Pharmacol.* 2005; **19**(4): 405-409.

134. Brevoort P. The US botanical market - an overview. *HerbalGram.* 1996; **36**: 49-57.

135. Brevoort P. The booming US botanical market - a new overview. *HerbalGram.* 1998; **44**: 33-46.

136. Muller JL and Clauson K.A. Pharmaceutical considerations of common herbal medicine. *Am. J. Man. Care.* 1997; **3**: 1753-1770.

137. Ernst E and Pittler MH. Ginkgo biloba for dementia: A systematic review of rouble-blind, placebo-controlled trials. *Clin. Drug. Invest.* 1999; **17**: 301-308.

138. Peters H, Kieser M, and Holscher U. Demonstration of the efficacy of ginkgo biloba special extract EGb 761 on intermittent claudication--a placebo-controlled, double-blind multicenter trial. *Vasa.* 1998; **27**(2): 106-110.

139. Muir AH, Robb R, McLaren M, Daly F, and Belch JJ. The use of Ginkgo biloba in Raynaud's disease: a double-blind placebo-controlled trial. *Vasc. Med.* 2002; **7**(4): 265-267.

140. Siegel G, Schafer P, Winkler K, and Malmsten M. Ginkgo biloba (EGb 761) in arteriosclerosis prophylaxis. *Wien. Med. Wochenschr.* 2007; **157**(13-14): 288-294.

141. Rodriguez M, Ringstad L, Schafer P, Just S, Hofer HW, Malmsten M, and Siegel G. Reduction of atherosclerotic nanoplaque formation and size by Ginkgo biloba (EGb 761) in cardiovascular high-risk patients. *Atherosclerosis.* 2007; **192**(2): 438-444.

142. Wu Y, Li S, Cui W, Zu X, Wang F, and Du J. Ginkgo biloba extract improves coronary blood flow in patients with coronary artery disease: role of endothelium-dependent vasodilation. *Planta Med.* 2007; **73**(7): 624-628.

143. Zhou W, Chai H, Lin PH, Lumsden AB, Yao Q, and Chen C. Clinical use and molecular mechanisms of action of extract of Ginkgo biloba leaves in cardiovascular diseases. *Cardiovasc. Drug Rev.* 2004; **22**(4): 309-319.

144. Koch E. Inhibition of platelet activating factor (PAF)-induced aggregation of human thrombocytes by ginkgolides: considerations on possible bleeding complications after oral intake of Ginkgo biloba extracts. *Phytomedicine.* 2005; **12**(1-2): 10-16.

145. Jezova D, Duncko R, Lassanova M, Kriska M, and Moncek F. Reduction of rise in blood pressure and cortisol release during stress by Ginkgo biloba extract (EGb 761) in healthy volunteers. *J. Physiol Pharmacol.* 2002; **53**(3): 337-348.

146. Mehlsen J, Drabaek H, Wiinberg N, and Winther K. Effects of a Ginkgo biloba extract on forearm haemodynamics in healthy volunteers. *Clin. Physiol Funct. Imaging.* 2002; **22**(6): 375-378.

147. Li H, Xia N, Brausch I, Yao Y, and Forstermann U. Flavonoids from artichoke (Cynara scolymus L.) up-regulate endothelial-type nitric-oxide synthase gene expression in human endothelial cells. *J. Pharmacol. Exp. Ther.* 2004; **310**(3): 926-932.

148. Li H, Hergert SM, Schäfer SC, Brausch I, Yao Y, Huang Q, Mang C, Lehr HA, and Förstermann U. Midostaurin upregulates eNOS gene expression and preserves eNOS function in the microcirculation of the mouse. *Nitric. Oxide.* 2005; **12**(4): 231-236.

149. Wallerath T, Li H, Godtel-Ambrust U, Schwarz PM, and Förstermann U. A blend of polyphenolic compounds explains the stimulatory effect of red wine on human endothelial NO synthase. *Nitric. Oxide.* 2005; **12**(2): 97-104.

150. Biber A. Pharmacokinetics of Ginkgo biloba extracts. *Pharmacopsychiatry.* 2003; **36 Suppl 1**: S32-S37.

151. Cheung F, Siow YL, Chen WZ, and O K. Inhibitory effect of Ginkgo biloba extract on the expression of inducible nitric oxide synthase in endothelial cells. *Biochem. Pharmacol.* 1999; **58**(10): 1665-1673.

152. Cheung F, Siow YL, and O K. Inhibition by ginkgolides and bilobalide of the production of nitric oxide in macrophages (THP-1) but not in endothelial cells (HUVEC). *Biochem. Pharmacol.* 2001; **61**(4): 503-510.

153. Sasaki Y, Noguchi T, Yamamoto E, Giddings JC, Ikeda K, Yamori Y, and Yamamoto J. Effects of Ginkgo biloba extract (EGb 761) on cerebral thrombosis and blood pressure in stroke-prone spontaneously hypertensive rats. *Clin. Exp. Pharmacol. Physiol.* 2002; **29**(11): 963-967.

154. Ozaki M, Kawashima S, Yamashita T, Hirase T, Namiki M, Inoue N, Hirata K, Yasui H, Sakurai H, Yoshida Y, Masada M, and Yokoyama M. Overexpression of endothelial nitric oxide synthase accelerates atherosclerotic lesion formation in apoE-deficient mice. *J. Clin. Invest.* 2002; **110**(3): 331-340.

155. Umegaki K, Shinozuka K, Watarai K, Takenaka H, Yoshimura M, Daohua P, and Esashi T. Ginkgo biloba extract attenuates the development of hypertension in deoxycorticosterone acetate-salt hypertensive rats. *Clin. Exp. Pharmacol. Physiol.* 2000; **27**(4): 277-282.

156. Cishek MB, Galloway MT, Karim M, German JB, and Kappagoda CT. Effect of red wine on endothelium-dependent relaxation in rabbits. *Clin. Sci. (Lond).* 1997; **93**(6): 507-511.

157. Kubota Y, Tanaka N, Umegaki K, Takenaka H, Mizuno H, Nakamura K, Shinozuka K, and Kunitomo M. Ginkgo biloba extract-induced relaxation of rat aorta is associated with increase in endothelial intracellular calcium level. *Life Sci.* 2001; **69**(20): 2327-2336.

158. Dell'Agli M, Galli GV, and Bosisio E. Inhibition of cGMP-phosphodiesterase-5 by biflavones of Ginkgo biloba. *Planta Med.* 2006; **72**(5): 468-470.

159. Leung KW, Cheng YK, Mak NK, Chan KK, Fan TP, and Wong RN. Signaling pathway of ginsenoside-Rg1 leading to nitric oxide production in endothelial cells. *FEBS Lett.* 2006; **580**(13): 3211-3216.

160. Lorenz M, Wessler S, Follmann E, Michaelis W, Dusterhoft T, Baumann G, Stangl K, and Stangl V. A constituent of green tea, epigallocatechin-3-gallate, activates endothelial nitric oxide synthase by a phosphatidylinositol-3-OH-kinase-, cAMP-dependent protein kinase-, and Akt-dependent pathway and leads to endothelial-dependent vasorelaxation. *J. Biol. Chem.* 2004; **279**(7): 6190-6195.

161. Osaki M, Oshimura M, and Ito H. PI3K-Akt pathway: its functions and alterations in human cancer. *Apoptosis.* 2004; **9**(6): 667-676.

162. Huang W, Zhang J, and Moore DD. A traditional herbal medicine enhances bilirubin clearance by activating the nuclear receptor CAR. *J. Clin. Invest.* 2004; **113**(1): 137-143.

163. Wallerath T, Deckert G, Ternes T, Anderson H, Li H, Witte K, and Förstermann U. Resveratrol, a polyphenolic phytoalexin present in red wine, enhances expression and activity of endothelial nitric oxide synthase. *Circulation.* 2002; **106**(13): 1652-1658.

164. Ye B, Aponte M, Dai Y, Li L, Ho MC, Vitonis A, Edwards D, Huang TN, and Cramer DW. Ginkgo biloba and ovarian cancer prevention: epidemiological and biological evidence. *Cancer Lett.* 2007; **251**(1): 43-52.

165. Sagar SM, Yance D, and Wong RK. Natural health products that inhibit angiogenesis: a potential source for investigational new agents to treat cancer-Part 1. *Curr. Oncol.* 2006; **13**(1): 14-26.

166. Yance DR, Jr. and Sagar SM. Targeting angiogenesis with integrative cancer therapies. *Integr. Cancer Ther.* 2006; **5**(1): 9-29.

167. Eisenbrand G, Hippe F, Jakobs S, and Muehlbeyer S. Molecular mechanisms of indirubin and its derivatives: novel anticancer molecules with their origin in traditional Chinese phytomedicine. *J. Cancer Res. Clin. Oncol.* 2004; **130**(11): 627-635.

168. Papadopoulos V, Kapsis A, Li H, Amri H, Hardwick M, Culty M, Kasprzyk PG, Carlson M, Moreau JP, and Drieu K. Drug-induced inhibition of the peripheral-type benzodiazepine receptor expression and cell proliferation in human breast cancer cells. *Anticancer Res.* 2000; **20**(5A): 2835-2847.

169. Chao JC and Chu CC. Effects of Ginkgo biloba extract on cell proliferation and cytotoxicity in human hepatocellular carcinoma cells. *World J. Gastroenterol.* 2004; **10**(1): 37-41.

170. Kim KS, Rhee KH, Yoon JH, Lee JG, Lee JH, and Yoo JB. Ginkgo biloba extract (EGb 761) induces apoptosis by the activation of caspase-3 in oral cavity cancer cells. *Oral Oncol.* 2005; **41**(4): 383-389.

171. Li W, Pretner E, Shen L, Drieu K, and Papadopoulos V. Common gene targets of Ginkgo biloba extract (EGb 761) in human tumor cells: relation to cell growth. *Cell Mol. Biol. (Noisy. -le-grand).* 2002; **48**(6): 655-662.

172. Suzuki R, Kohno H, Sugie S, Sasaki K, Yoshimura T, Wada K, and Tanaka T. Preventive effects of extract of leaves of ginkgo (Ginkgo biloba) and its component bilobalide on azoxymethane-induced colonic aberrant crypt foci in rats. *Cancer Lett.* 2004; **210**(2): 159-169.

173. Alaoui-Youssefi A, Lamproglou I, Drieu K, and Emerit I. Anticlastogenic effects of Ginkgo biloba extract (EGb 761) and some of its constituents in irradiated rats. *Mutat. Res.* 1999; **445**(1): 99-104.

174. Emerit I, Oganesian N, Sarkisian T, Arutyunyan R, Pogosian A, Asrian K, Levy A, and Cernjavski L. Clastogenic factors in the plasma of Chernobyl accident recovery workers: anticlastogenic effect of Ginkgo biloba extract. *Radiat. Res.* 1995; **144**(2): 198-205.

175. Juarez CP, Muino JC, Guglielmone H, Sambuelli R, Echenique JR, Hernandez M, and Luna JD. Experimental retinopathy of prematurity: angiostatic inhibition by nimodipine, ginkgo-biloba, and dipyridamole, and response to different growth factors. *Eur. J. Ophthalmol.* 2000; **10**(1): 51-59.

176. Monte M, Davel LE, and de Lustig ES. Inhibition of lymphocyte-induced angiogenesis by free radical scavengers. *Free Radic. Biol. Med.* 1994; **17**(3): 259-266.

177. Chang F, Steelman LS, Shelton JG, Lee JT, Navolanic PM, Blalock WL, Franklin R, and McCubrey JA. Regulation of cell cycle progression and apoptosis by the Ras/Raf/MEK/ERK pathway. *Int. J. Oncol.* 2003; **22**(3): 469-480.

178. Alavi A, Hood JD, Frausto R, Stupack DG, and Cheresh DA. Role of Raf in vascular protection from distinct apoptotic stimuli. *Science.* 2003; **301**(5629): 94-96.

179. Lin FY, Chen YH, Chen YL, Wu TC, Li CY, Chen JW, and Lin SJ. Ginkgo biloba extract inhibits endotoxin-induced human aortic smooth muscle cell proliferation via suppression of toll-like receptor 4 expression and NADPH oxidase activation. *J. Agric. Food Chem.* 2007; **55**(5): 1977-1984.

180. Wadsworth TL, McDonald TL, and Koop DR. Effects of Ginkgo biloba extract (EGb 761) and quercetin on lipopolysaccharide-induced signaling pathways involved in the release of tumor necrosis factor-alpha. *Biochem. Pharmacol.* 2001; **62**(7): 963-974.

181. Suhasini M, Li H, Lohmann SM, Boss GR, and Pilz RB. Cyclic-GMP-dependent protein kinase inhibits the Ras/Mitogen-activated protein kinase pathway. *Mol. Cell Biol.* 1998; **18**(12): 6983-6994.

182. Villalobo A. Nitric oxide and cell proliferation. *FEBS J.* 2006; **273**(11): 2329-2344.

183. Dumaz N and Marais R. Integrating signals between cAMP and the RAS/RAF/MEK/ERK signalling pathways. Based on the anniversary prize of the Gesellschaft fur Biochemie und Molekularbiologie Lecture delivered on 5 July 2003 at the Special FEBS Meeting in Brussels. *FEBS J.* 2005; **272**(14): 3491-3504.

184. Lao DH, Yusoff P, Chandramouli S, Philp RJ, Fong CW, Jackson RA, Saw TY, Yu CY, and Guy GR. Direct binding of PP2A to Sprouty2 and phosphorylation changes are a prerequisite for ERK inhibition downstream of fibroblast growth factor receptor stimulation. *J. Biol. Chem.* 2007; **282**(12): 9117-9126.

185. Ostman A, Hellberg C, and Bohmer FD. Protein-tyrosine phosphatases and cancer. *Nat. Rev. Cancer.* 2006; **6**(4): 307-320.

8 APPENDIX

8.1   mRNA sequences for Real-time RT-PCR analysis

Below the mRNA sequences of the human Dual specificity phosphatase 1 (DUSP1), also denoted as MKP-1, and the Glyceraldehyde-3-phosphate dehydrogenase (GAPDH) are displayed. For both sequences forward as well as reverse primers (light blue) and the TaqMan probes (light gray) are highlighted.

```
DEFINITION:     Dual specificity phosphatase 1 (DUSP1), mRNA.
ACCESSION:      NM_004417
SOURCE:         Homo sapiens (human)

   1 tcgctgcgaa ggacatttgg gctgtgtgtg cgacgcgggt cggaggggca gtcgggggaa
  61 ccgcgaagaa gccgaggagc ccggagcccc gcgtgacgct cctctctcag tccaaaagcg
 121 gcttttggtt cggcgcagag agacccgggg gtctagcttt tcctcgaaaa gcgccgccct
 181 gcccttggcc ccgagaacag acaaagagca ccgcagggcc gatcacgctg ggggcgctga
 241 ggccggccat ggtcatggaa gtgggcaccc tggacgctgg aggcctgcgg gcgctgctgg
 301 gggagcgagc ggcgcaatgc ctgctgctgg actgccgctc cttcttcgct ttcaacgccg
 361 gccacatcgc cggctctgtc aacgtgcgct tcagcaccat cgtgcggcgc cgggccaagg
 421 gcgccatggg cctggagcac atcgtgccca cgccgagct ccgcggccgc ctgctggccg
 481 gcgcctacca cgccgtggtg ttgctggacg agcgcagcgc cgccctggac ggcgccaagc
 541 gcgacggcac cctggccctg cggccggcg cgctctgccg cgaggcgcgc gccgcgcaag
 601 tcttcttcct caaaggagga tacgaagcgt tttcggcttc ctgcccggag ctgtgcagca
 661 aacagtcgac ccccatgggg ctcagccttc ccctgagtac tagcgtccct gacagcgcgg
 721 aatctgggtg cagttcctgc agtaccccac tctacgatca gggtggcccg gtggaaatcc
 781 tgccctttct gtacctgggc agtgcgtatc acgcttcccg caaggacatg ctggatgcct
 841 tgggcataac tgccttgatc aacgtctcag ccaattgtcc caaccatttt gagggtcact
 901 accagtacaa gagcatccct gtggaggaca accacaaggc agacatcagc tcctggttca
 961 acgaggccat tgacttcata gactccatca gaatgctgg aggaagggtg tttgtccact
1021 gccaggcagg catttcccgg tcagccacca tctgccttgc ttaccttatg aggactaatc
1081 gagtcaagct ggacgaggcc tttgagtttg tgaagcagag gcgaagcatc atctctccca
1141 acttcagctt catgggccag ctgctgcagt ttgagtccca ggtgctggct ccgcactgtt
1201 cggcagaggc tgggagcccc gccatggctg tgctcgaccg aggcacctcc accaccaccg
1261 tgttcaactt ccccgtctcc atccctgtcc actccacgaa cagtgcgctg agctaccttc
1321 agagccccat tacgacctct cccagctgct gaaaggccac gggaggtgag gctcttcaca
1381 tcccattggg actccatgct ccttgagagg agaaatgcaa taactctggg aggggctcga
1441 gagggctggt ccttatttat ttaacttcac ccgagttcct ctgggtttct aagcagttat
1501 ggtgatgact tagcgtcaag acatttgctg aactcagcac attcgggacc aatatatagt
1561 gggtacatca agtccatctg acaaaatggg gcagaagaga aaggactcag tgtgtgatcc
1621 ggtttctttt tgctcgcccc tgttttttgt agaatctctt catgcttgac atacctacca
1681 gtattattcc cgacgacaca tatacatatg agaatatacc ttatttattt ttgtgtaggt
1741 gtctgccttc acaaatgtca ttgtctactc ctagaagaac caaatacctc aattttttgtt
1801 tttgagtact gtactatcct gtaaatatat cttaagcagg tttgtttttca gcactgatgg
1861 aaaataccag tgttgggttt tttttagtt gccaacagtt gtatgtttgc tgattatta
1921 tgacctgaaa taatatattt cttcttctaa gaagacattt tgttacataa ggatgacttt
1981 tttatacaat ggaataaatt atggcatttc tattg
```

DEFINITION: Glyceraldehyde-3-phosphate dehydrogenase (GAPDH), mRNA.
ACCESSION: NM_002046
SOURCE: Homo sapiens (human)

```
   1 aaattgagcc cgcagcctcc cgcttcgctc tctgctcctc ctgttcgaca gtcagccgca
  61 tcttcttttg cgtcgccagc cgagccacat cgctcagaca ccatggggaa ggtgaaggtc
 121 ggagtcaacg gatttggtcg tattgggcgc ctggtcacca gggctgcttt taactctggt
 181 aaagtggata ttgttgccat caatgacccc ttcattgacc tcaactacat ggtttacatg
 241 ttccaatatg attccaccca tggcaaattc catggcaccg tcaaggctga aacgggaag
 301 cttgtcatca atggaaatcc catcaccatc ttccaggagc gagatccctc caaaatcaag
 361 tggggcgatg ctggcgctga gtacgtcgtg gagtccactg gcgtcttcac caccatggag
 421 aaggctgggg ctcatttgca ggggggagcc aaaagggtca tcatctctgc cccctctgct
 481 gatgccccca tgttcgtcat gggtgtgaac catgagaagt atgacaacag cctcaagatc
 541 atcagcaatg cctcctgcac caccaactgc ttagcacccc tggccaaggt catccatgac
 601 aactttggta tcgtggaagg actcatgacc acagtccatg ccatcactgc cacccagaag
 661 actgtggatg cccctccgg gaaactgtgg cgtgatggcc gcggggctct ccagaacatc
 721 atccctgcct ctactggcgc tgccaaggct gtgggcaagg tcatccctga gctgaacggg
 781 aagctcactg gcatggcctt ccgtgtcccc actgccaacg tgtcagtggt ggacctgacc
 841 tgccgtctag aaaaacctgc caaatatgat gacatcaaga aggtggtgaa gcaggcgtcg
 901 gagggccccc tcaagggcat cctgggctac actgagcacc aggtggtctc ctctgacttc
 961 aacagcgaca cccactcctc cacctttgac gctggggctg gcattgccct caacgaccac
1021 tttgtcaagc tcatttcctg gtatgacaac gaatttggct acagcaacag ggtggtggac
1081 ctcatggccc acatggcctc caaggagtaa gacccctgga ccaccagccc cagcaagagc
1141 acaagaggaa gagagagacc ctcactgctg gggagtccct gccacactca gtcccccacc
1201 acactgaatc tcccctcctc acagttgcca tgtagacccc ttgaagaggg gaggggccta
1261 gggagccgca ccttgtcatg taccatcaat aaagtaccct gtgctcaacc
```

8.2 Abbreviations

ACh   acetylcholine

Akt   proteinkinase B

APS   ammonium persulfate

ATP   adenosine5'-triphosphate

BSA   bovine serum albumin

CAM   chicken chorioallantoic membrane

cAMP   cyclic adenosine monophosphate

cAMPS-Rp   (R)-adenosine, cyclic 3',5'-(hydrogenphosphorothioate)

CAPS   cyclohexylamino-1-propane sulfonic acid

CCD   charge-coupled device

cDNA   complementary DNA

cGMP   cyclic guanosine monophosphate

CLSM   confocal laser scanning microscopy

DMEM   Dulbecco's Modified Eagle's Medium

DMSO   dimethyl sulfoxide

DNA   deoxyribonucleic acid

DTT   dithiothreitol

ECGM   Endothelial Cell Growth Medium

ECL   enhanced chemoluminescence

ECs   endothelial cells

EDTA   ethylenediaminetetraacetic acid

EGb   Extract of *Ginkgo biloba*

EGTA   ethylene glycol tetraacetic acid

ELISA   enzyme-linked immunosorbent assay

eNOS	endothelial nitric oxide synthase
ERK	extracellular signal-regulated kinase
FACS	fluorescence activated cell sorter
FAM	6-carboxyfluorescein
FBS	fetal bovine serum
FGF	fibroblast growth factor
FL2-H	fluorescent channel 2 height
FSC	forward scatter
GAPDH	glyceraldehyde 3-phosphate dehydrogenase
GF	growth factor
h	hour
HEPES	N-(2-Hydroxyethyl)piperazine-N'-(2-ethanesulfonic acid)
HFS	hypotonic fluorochrome solution
HMEC	human microvascular endothelial cell
HRP	horseradish peroxidase
HSP	heat shock protein
HUVEC	human umbilical vein endothelial cell
IBMX	3-isobutyl-1-methylxanthine
JNK	c-Jun amino-terminal kinases
kDa	kilo Dalton
L-NAME	L-nitro-arginine-methyl ester
LPS	lipopolysaccharide
MAPK	mitogen-activated protein kinase
MAPKK	mitogen-activated protein kinase kinase
MAPKKK	mitogen-activated protein kinase kinase kinase

MEK	MAPK/ERK kinases
MKP-1	mitogen-activated protein kinase phosphatases-1
min	minute
MOPS	3-(N-morpholino)propanesulfonic acid
mRNA	messenger RNA
NO	nitric oxide
NOS	nitric oxide synthase
PAA	polyacrylamide
PAGE	polyacrylamide gel electrophoresis
Pap	papaverine
PBS	phosphate buffered saline
PCR	polymerase chain reaction
PE	phenylephrine
PI	propidium iodide
PI3K	phosphoinositide 3-kinase
PKA	protein kinase A
PKI	protein kinase A inhibitor
PMA	phorbol 12-myristate 13-acetate
PMSF	phenylmethylsulphonyl fluoride
p-NPP	para-Nitrophenyl phosphate
PP	protein serine/threonine phosphatase
PTP	protein tyrosine phosphatase
PVDF	polyvinylidene fluoride
RNA	ribonucleic acid
RNAse	ribonuclease

ROS   reactive oxygen species

sGC   soluble guanylate cyclase

SDS   sodium dodecyl sulfate

SDS-PAGE   sodium dodecyl sulfate polyacrylamide gel electrophoresis

SEM   standard error of the mean value

Ser   serine

SHP-1   src-homology 2 (SH2) domain containing phosphatase

TAMRA   tetramethyl-6-carboxyrhodamine

TBE   tris, borate, EDTA buffer

TE   tris-EDTA buffer

TEMED   N, N, N', N' tetramethylethylene diamine

Thr   threonine

TNF-α tumor necrosis factor-α

Tris   trishydroxymethylaminomethane

Tyr   tyrosine

VEGF   vascular endothelial growth factor

8.3 Alphabetical List of Companies

Agfa-Gevaert AG	Cologne, Germany
Alexis Biochemicals	San Diego, CA, USA
Amaxa	Cologne, Germany
Amersham Biosciences	Freiburg, Germany
Applichem	Darmstadt, Germany
Applied Biosystems	Foster City, CA, USA
B. Braun Biotech International	Melsungen, Germany
BD Biosciences	Heidelberg, Germany
Beckman Coulter	Krefeld, Germany
Berthold Technologies	Bad Wildbad, Germany
BIOCHROME AG	Berlin, Germany
Biomers.net	Ulm, Germany
Bio-Rad	Munich, Germany
Biotrend Chemikalien GmbH	Cologne, Germany
Biozol	Eching, Germany
Cambrex	Verviers, Belgum
Cayman Chemical Company	Michigan, USA
Cell Signalling/New England Biolabs	Frankfurt/Main, Germany
Charles River Wiga GmbH	Sulzfeld, Germany
Dharmacon	Lafayette, CO, USA
Dianova	Hamburg, Germany
Fermentas	St. Leon-Rot, Germany
Fuji	Düsseldorf, Germany
Gibco/Invitrogen	Karlsruhe, Germany

Hugo Sachs   Hugstetten, Germany

ibidi GmbH   Munich, Germany

ICN Biomedicals   Aurora, Ohio, USA

Interdim   Montulocon, France

Kodak   Rochester, USA

Li-Cor Biosciences   Lincoln, NE

Lohmann Tierzucht   Cuxhaven, Germany

Macherey-Nagel   Düren, Germany

Merck   Darmstadt, Germany

Millipore   Bedford, MA, USA

Miltenyi Biotec   Bergisch Gladbach, Germany

Minerva Biolabs   Berlin, Germany

Molecular Probes/Invitrogen   Karlsruhe, Germany

NanoDrop   Wilmington, DE, USA

Olympus   Munich, Germany

PAA Laboratories   Cölbe, Germany

PAN Biotech   Aidenbach, Germany

PeproTech   Rocky Hill, NY, USA

Peqlab Biotechnologie GmbH   Erlangen Germany

Perkin Elmer   Massachusetts, USA

Peske   Aindling-Arnhofen, Germany

Promega   Mannheim, Germany

Provitro   Berlin, Germany

QiagenGmbH   Hilden, Germany

Roche   Mannheim, Germany

Rockland Immunochemicals   Gilbertsville, Pennsylvania, USA

SantaCruz Biotechnology   Heidelber, Germany

S.CO LifeScience   Garching, Germany

Sigma   Taufkirchen, Germany

TECAN   Crailsheim, Germany

TILL Photonics   Gräfelfing, Germany

Tocris   MO, USA

TPP   Trasadingen, Switzerland

Upstate   Lake Placid, NY, USA

Whatman Schleicher & Schüll   Dassel, Germany

Zeiss   Oberkochen, Germany

8.4 Publications

8.4.1 Original Publication

Ginkgo biloba extract EGb 761 increases endothelial nitric oxide production *in vitro* and *in vivo*.

A. Koltermann [a], A. Hartkorn [a], E. Koch [b], R. Fürst [a], A.M. Vollmar [a] and S. Zahler [a]

[a] Department of Pharmacy, Pharmaceutical Biology, University of Munich, Germany

[b] Preclinical Research, Dr. Willmar Schwabe Pharmaceuticals, Karlsruhe, Germany

Cell Mol Life Sci. 2007 Jul;64(13):1715-22.

Ginkgo biloba extract EGb 761 exerts anti-angiogenic properties *via* activation of tyrosine phosphatases

Anja Koltermann [a]; Johanna Liebl [a]; Robert Fürst, PhD [a]; Hermann Ammer, PhD [b]; Angelika M. Vollmar, PhD [a]; Stefan Zahler, PhD [a]

[a] Department of Pharmacy, Pharmaceutical Biology, University of Munich, Germany

[b] Institute of Pharmacology, Toxicology and Pharmacy, University of Munich, Germany

Submitted

8.4.2 Oral Communication

Ginkgo biloba extract (EGb 761) inhibits endothelial cell proliferation *in vitro*.

Frühjahrstagung der Deutschen Gesellschaft für Experimentelle und Klinische Pharmakologie und Toxikologie (DGPT); March 13-15th, 2007, Mainz, Germany.

Ginkgo biloba extract (EGb 761) exerts anti-angiogenic properties *via* activation of tyrosine phosphatases.

Symposium des Graduiertenkollegs (GRK) 438, November 10-11th, 2007, Herrsching, Germany.

8.4.3   Poster presentations

Anti-proliferative effects of the *Ginkgo biloba* extract (EGb 761) on endothelial cells *in vitro*.

Koltermann A, Zahler S., Vollmar AM.

Frühjahrstagung der Deutschen Pharmazeutischen Gesellschaft (PPhG), October 5-8th, 2005, Mainz, Germany.

Ginkgo biloba extract (EGb 761) induces the endothelial nitric oxide system.

Koltermann A, Vollmar AM., Zahler S.

Frühjahrstagung der Deutschen Gesellschaft für Experimentelle und Klinische Pharmakologie und Toxikologie (DGPT), April 4-6th, 2006, Mainz, Germany.

Ginkgo biloba extract (EGb 761) increases endothelial NO production *in vitro* and *in vivo*.

Koltermann A, Hartkorn A, Koch E, Fürst R, Vollmar AM, Zahler S.

Annual Meeting 2006, Gesellschaft für Microzirkulation und Vaskuläre Biologie e.V., October 12-14th, 2006, Munich, Germany.

8.5 Curriculum vitae

<u>Persönliche Angaben</u>

Name:	Anja Koltermann
Geburtsdatum:	17.04.1977
Geburtsort:	Elsterwerda
Familienstand:	ledig

<u>Hochschule:</u>

08/2004 - 12/2007	Dissertation am Lehrstuhl für Pharmazeutische Biologie Department Pharmazie der LMU München Betreuer: Prof. Dr. A.M. Vollmar, PD Dr. S. Zahler
08/2004-11/2007	Mitglied des Graduiertenkolleg GRK 438 „Vaskuläre Biologie in der Medizin"
04/1999 - 05/2003	Studium der Pharmazie an der TU Carolo-Wilhelmina zu Braunschweig
03/2001	Abschluss des Grundstudiums 1. Abschnitt der Pharmazeutischen Prüfung
05/2003	Abschluss des Hauptstudiums 2. Abschnitt der Pharmazeutischen Prüfung
07/2004	3. Abschnitt der Pharmazeutischen Prüfung Erlangung der Approbation zur Apothekerin

Ausbildung und Schule:

1996-1999   Berufsfachschule Dr. Heinemann in Braunschweig

                                  Erlaubnis zur Führung der Berufsbezeichnung:

                                  Pharmazeutisch-technische Assistentin

1991-1996   Elsterschlossgymnasium in Elsterwerda

                                  Abschluss: Allgemeine Hochschulreife

Berufsausbildung und Tätigkeiten

seit 12/2004   promotionsbegleitende Tätigkeit als Apothekerin

                                  Apotheke am Kufsteiner Platz und Arcis-Apotheke in München

06/2003-06/2004   Pharmaziepraktikum

1. Halbjahr: AstraZeneca GmbH in Plankstadt

                                  Unternehmensbereich:

                                  - Qualitätssicherung:

                                  - Pharmafertigung/Verfahrenssicherung

2. Halbjahr: Arcis-Apotheke in München

1999-2002   studiumsbegleitende Tätigkeit als PTA

                                  Arnika-Apotheke in München, Kur-Apotheke bei Bad Harzburg,

                                  Neue Apotheke und Packhof-Apotheke in Braunschweig

09/1998-02/1999   Berufspraktikum

                                  Aesculap-Apotheke in Dresden

8.6 Acknowledgements